THE INTERSTELLAR EXTINCTION OF STARS IN H II REGIONS

Thesis by

Christopher Marlowe Anderson

In Partial Fulfillment of the Requirements

For the Degree of

Doctor of Philosophy

California Institute of Technology

Pasadena, California

1968

(Submitted January 19, 1968)

To Butch

ACKNOWLEDGEMENTS

First, and foremost, I would like to acknowledge the guidance of Dr. Guido Münch who suggested this line of research to me and directed the course of the project through many helpful discussions. Particular credit goes to Dr. J. B. Oke who instructed me in the techniques of spectrophotometric observation. My fellow students have also contributed much to my general understanding of astronomy through countless conversations, and I would like to thank all of them, and particularly Dr. John I. Castor, Dr. Subhash Chandra, and Mr. J. F. Bartlett for their many suggestions.

I gratefully acknowledge the generous allotment of observing time given to me by the Mount Wilson and Palomar Observatories. The aid and patience of the observatory staff and particularly that of the night assistants Gene, Henry, Al, Ray, and Jon was most helpful.

Financial aid during my tenure as a graduate student from National Aeronautics and Space Administration Traineeship, a National Science Foundation Summer Fellowship, a Van Maanen Fellowship as well as from general Institute funds is acknowledged.

Finally, the swift and accurate typing of the manuscript as well as advice in matters both temporal and spiritual rendered by Mrs. Maggie Hayden merits my warmest thanks.

ABSTRACT

Spectrophotometric observations of several stars which appear to be associated with H II regions have been obtained in an attempt to locate other occurences of the reddening anomaly which is seen in the Trapezium stars (θ^1 Orionis) in the Orion Nebula. Several cases of the Orion-like anomaly have been found. The radiation pressure mechanism for the removal of the smallest grains from the nebula has been discussed and has been found to be inoperative because of the drag forces acting upon the grains. It has been shown that the temperature of the grains depends upon the grain size such that the smaller grains might experience more rapid evaporation. The processes of grain-grain fusion and condensation nucleus exhaustion have been investigated as possible causes of the anomalous grain size distribution. Finally, the anomaly has been discussed as if it were a peculiarity in the intrinsic colors of the stars. The large infrared excess observed in these stars could be due to the presence of late-type stellar companions or circumstellar shells.

TABLE OF CONTENTS

I. INTRODUCTION

Trumpler (1930) demonstrated the existence of interstellar extinction by showing that the linear diameters of galactic star clusters deduced from spectroscopic parallaxes became systematically larger with increasing distance from the sun unless a correction for extinction was applied. He also found that the colors of the stars in more distant clusters were systematically redder than the colors of stars of the same spectral type in nearby clusters. In addition to the obvious importance of an extinction producing component of the interstellar medium to distance measurements which depend upon the apparent brightness of "standard candles", the interstellar grains, to which the extinction has been attributed, have more recently been utilized as a primary opacity source in the early phases of star formation (Gaustad, 1963). It has also been suggested that the grains might modify the dynamics of H II regions (Krishna Swamy and O'Dell, 1967, and Mathews, 1967) and that they might act as catalysts in the formation of molecules such as H_2 (Van de Hulst, 1948, and McCrea and McNally, 1960). In all of these contexts a knowledge of the chemical composition and physical structure of the extinction producing medium is desirable.

Unfortunately the means by which the interstellar grains can be observed are not particularly sen-

sitive to the details of the chemical composition and physical structure of the grains. Greenstein (1938) investigated the wavelength of dependence of the extinction and found that a λ^{-1} law described the data reasonably well. In his discussion of the theory of interstellar absorption, Greenstein (1937) concluded that the required amount of extinction could be produced only by a medium of solid particles and remain within the limitation placed upon the total mass by galactic dynamics. He did not make a definitive distinction between dielectric and metallic grain models.

The wavelength dependence of the extinction, which is frequently referred to as the reddening curve, was more precisely determined by the six-color photoelectric photometry of Stebbins and Whitford (1943). By a comparison of the colors of stars of the same spectral type and different degrees of reddening they were able to detect deviations from a λ^{-1} law. The degree of the deviation from, or curvature with respect to the λ^{-1} dependence, was found to be very similar in all the regions of the sky which they studied with the one exception of the stars in the Orion Nebula "Trapezium" group. For the several components of θ^1 Orionis, Stebbins and Whitford (1945) found that the curvature of the reddening law with respect to a λ^{-1} relation was about twice that for most

stars. The color anomaly of the Trapezium stars had first been noted by Baade and Minkowski (1937) who suggested that the anomaly was the result of abnormally large dust grains in the nebula. They further suggested that this peculiar grain population was caused by the action of radiation pressure which, as had been pointed out by Schoenberg and Jung (1933), imparted to the grains an acceleration which was inversely proportional to the radius of the grain. Thus the small grains would be swept from the nebula leaving the mean size of the grains within the nebula greater than the average.

Van de Hulst (1949) made extensive computations of theoretical reddening curves based on the Mie scattering theory. He found that the normal reddening curve of Stebbins and Whitford could be most nearly matched by the theoretical curves for dielectric spheres with a complex index of refraction of the form $1 + \epsilon + i\epsilon \tan \phi$ combined with a grain size distribution which had been derived by Oort and Van de Hulst (1946) from theoretical arguments concerning the nature of the grain formation process and the conditions of interstellar space. In this model ϵ and $\epsilon \tan \phi$ were about 0.25 and 0.03 respectively with slight wavelength dependences imposed upon the real part of the refractive index. For the Trapezium stars, on the other hand, Van de Hulst found that particles about 30 percent larger than average with a slightly larger

imaginary part to the refractive index could best explain the difference between these stars and those of the general field.

Stebbins and Kron (1956) suggested that the color anomaly of the Trapezium stars as well as of θ^2 Orionis and ϕ Persei could be the result of late-type companion stars. This argument is supported by the fact that all of these stars have been reported to be single-line spectroscopic binaries (Struve and Titus, 1944 and Moore and Neubauer, 1948). Recently Krishna Swamy (1965) and Krishna Swamy and O'Dell (1967) have returned to a discussion of the original suggestion of Baade and Minkowski in which the grain size distribution is systematically deficient in small particles. The results of these authors will be discussed below.

If the anomaly which is observed in the Orion Nebula is a result of the abnormal conditions in that H II region as is suggested by the mechanism of Baade and Minkowski, a color anomaly similar to that in Orion might be expected in stars imbedded in other H II regions. A search for anomalies of this type is the primary objective of the present study. If the anomaly is a general characteristic of H II regions and of their associated early-type stars, is the small grain deficient particle size distribution a unique explanation of the phenomenon and

is the radiation pressure mechanism a workable means of instituting the anomaly? Is there any correlation between the occurence of the anomaly and the physical properties of the H II regions? What other situations might lead either to the color anomaly or to the establishment of this particular anomalous grain size distribution? It is a review of these questions to which the discussion of the observations of the present study will be addressed.

II. OBSERVATIONS

II.1 Introduction

In order to investigate the degree to which a reddening anomaly of the type observed in the Orion Nebula is associated with H II regions in general and with their attendant early-type stars, a three-phase observing program was undertaken. These phases were photographic selection of the H II regions of hightest potential interest, spectroscopy of the stars associated with the H II regions as well as of "MK" early-type standard stars and photoelectric spectrophotometry of the H II region stars. An attempt was made to determine nebular line strengths photoelectrically, but it was found that the combination of the high f-ratio of the Cassegrain spectrophotometer and the low surface brightness of all of the nebulae, with the exception of the Orion Nebula, made such observations impractical.

II.2 Photographic Selection

Due to the limited amount of spectrophotometric observing time which could be obtained, it was decided at the outset to limit the search for objects which have reddening curves similar to that in Orion to about ten H II regions with physical properties as nearly similar to those in the Orion Nebula as possible. The original intention

was to attempt to select those H II regions with both high gas density and high dust content so that the contribution to the extinction by the nebular material would be a substantial fraction of the total extinction.

A preliminary list of objects was assembled by selecting from the Sharpless (1959) catalogue of H II regions all those objects for which the brightness index was listed as 3 and which were listed as having angular diameters of 15 arc minutes or more. The brightness index 3 nebulae are essentially those nebulae the images of which are highly blackened on either or both the National Geographic Society Palomar Observatory Sky Survey plates. Since the Sky Survey plates were exposed so as to approach the limiting magnitude of the 48-inch Schmidt telescope, the class of galactic H II regions which have saturated images encompasses a very wide range of surface brightness, the Orion Nebula being the brightest. Thus by the inclusion of only the brightness 3 objects, later photographic inspection would be more likely to discover the objects most nearly like the Orion Nebula. The 15 arc minute limit was set by the number of objects which could be surveyed in the allotted time. From the preliminary list eleven objects were rejected by inspection of the Sky Survey prints. These objects were mostly well known pure reflection nebulae (e.g. Sharpless (S) 1, π Sco) or large

filamentary nebulae lacking well defined condensations with clearly associated early-type stars similar to the Orion Nebula (e.g. S 103, the Network Nebula in Cygnus). The remaining 25 nebulae were surveyed photographically with the 48-inch Schmidt telescope.

Each nebula was photographed with three different plate-filter combinations each of which was selected so as to isolate a different contribution to the nebular radiation. An Eastman 103a-O plate in conjunction with a Schott GG-11 filter was used to isolate the light from the forbidden [O III] lines at λ4959 A and λ5007 A. The GG-11 filter transmits about 90 percent of all light at wavelengths greater than 4900 A and has a very steep cut-off while the "O" emulsion is almost uniformly sensitive out to 4700 A, then drops to about one-tenth its maximum sensitivity by 5100 A. The second combination used was a 103a-D plate with a Corning (C) 3484 filter. This filter has a very steep cut-off at λ5200 A, while the "D" emulsion is almost uniformly sensitive from this wavelength to a wavelength of about 6200 A then falls to one-tenth its maximum sensitivity at λ6500 A. Thus it was hoped that this combination would isolate the continuum radiation between the nebular [O III] lines and H_α, since between these two sets of nebular atomic emission lines there are only very weak nebular lines as may be seen in the list given by Aller, Bowen and Minkowski (1955).

Finally a combination of a 103a-E emulsion and a Schott RG-2 filter was used. The RG-2 filter transmits only those wavelengths greater than about 6200 A while the "E" emulsion has its peak sensitivity at about 6500 A and is down to one-tenth this sensitivity at λ 6800 A. Thus this plate would be exposed mainly to the light of H_α and forbidden [N II] .

After some initial experimentation, standard exposures for each plate-filter combination were adopted. These exposures were 45 minutes, 15 minutes, and 10 minutes for the O, D, and E plates respectively. At least one such set of plates was obtained for each of the 25 nebulae. For some of the brightest and faintest nebulae, one or more plates at considerably shorter or longer exposures were obtained in order to reveal the details which were highly over or under-exposed on the standard plates. In several cases, two or more of the nebulae could be included on a single plate. In all, 80 plates (5 x 7-inches) were obtained on eleven nights between March 1966, and February 1967.

Either before or after exposure in the telescope but prior to development, each plate was processed in a spot sensitometer which placed upon the emulsion a series of eight images of a single illuminated area. Each spot differed in intensity from the adjacent spots by a factor

of the square root of two. The light from the illuminated area was allowed to pass through the same filter as had been (or would be) used with that plate in the telescope. The sensitometric spots for each of the plate-filter combinations were exposed with standardized sets of lamps, lamp voltage, and opal glass diffusing plates so that the total exposures of all plates of a given type would be as nearly uniform and as nearly equal to that in the telescope as possible. In order to avoid pre- or post-exposure by the sky, that portion of the plate which would accept the sensitometric spots was masked off during the exposure in the telescope. All plates were processed for five minutes with constant agitation in D-19 at a temperature within a few degrees of 20°C.

The plates which were obtained during the first two 48-inch observing sessions were studied in an attempt to find some means of determining the "dust content" of the nebulae. Specifically the "D" and "E" plates of NGC 6514, 6523, and 6611 were measured on a densitometer and the ratios of the densities in standard areas on the two plates were compared with the "gas to dust ratio" given by O'Dell, Hubbard, and Peimbert (1966). The sensitometric spots were used to estimate "intensities" within the nebulae and ratios of these intensities were also compared with the "gas-to-dust ratios". No correlation was found in either case and this line of

research was not pursued further for two reasons. First, it was recognized that even if the photographic process were sufficiently precise to detect the expected differences, absolute surface brightness calibration would have been required and was not readily available. Second, it was at once recognized that there were several obvious and more straightforward criteria upon which to base the selection of objects for further study.

The final selection of nebulae for spectrophotometric study was based upon 1) the surface brightness of the nebulae, particularly on the "E" plate, 2) the similarity of the structure of the nebula to that of the Orion Nebula, 3) the availability of stars known to be of early spectral type apparently associated with the nebula, and 4) the presence of dust lanes in and about the nebulosity. Qualitative consideration of these factors lead to the selection of 14 objects for further study. The basis for selection of each individual nebula will be discussed in the next chapter.

The first step in the study of an individual nebula was the selection of the stars for spectrophotometric observation. The table of associated early-type stars in the Sharpless Catalogue of H II regions was used to assemble an initial list. When several stars were listed for a single region, such factors as spectral

type, B-V colors, and association with condensations within the nebula were used to select one or two stars for spectrophotometric study. In some cases a single star or group of stars situated at the apparent center of the nebula could be selected a priori from the photographs. Finally in several cases the very low dispersion objective prism work of Schulte (1956) indicated the presence of very faint, highly reddened stars of early spectral type which were included in the spectrophotometric program. The individual selections are given in Table 1 and will be discussed in Chapter III.

II.3 Photographic Spectroscopy

To aid in the selection of appropriate intrinsic colors with which to compare the observed colors of the program stars, photographic spectra were obtained for most of the H II region stars with particular emphasis on those stars for which well documented spectral types could not be located. Furthermore, a series of plates of spectral type standard stars was obtained.

For this purpose the Newtonian focus, nebular or "B" spectrograph attached to either the Mount Wilson 60-inch or 100-inch telescope was used. All plates were obtained with the 3-inch focal length camera. Twenty-two initial exploratory plates were obtained with the 43 B (300 lines/mm) grating which gave a dispersion of 170 A/mm

TABLE 1

HD/BD	NGC/IC	$\alpha_{1950.0}$	δ	V	Sp	$(\theta_e, \log g)$	E(2.4)	$\mathcal{E}$	$\pm\ \Delta(\Delta_{MOD})$
5005 ABC	281	$00^h49^m50^s$	+56°21'	7.89	06	.126,4.0	.55	.80	.09 (.014)
15570	I1805	02 28 51	+61 09	7.85	07f	.132,4.0	1.11	.86	.05 (.014)
15629	I1805	02 29 21	+61 18	8.34	07	.132,4.0	.98	.72	.04 (.014)
17505	I1848	02 47 07	+60 13	7.06	07	.132,4.0	.91	.70	.04 (.014)
237015	I1848	02 48 43	+60 11	9.39	B1V	.210,4.0	.71	.62	.14 (.117)
37020	1976	05 32 52	-05 24	6.61	B1	.210,4.0	.47	1.02	.09 (.072)
37022	1976	05 32 52	-05 24	5.03	06p	.126,4.0	.53	.92	.04 (.014)
37023	1976	05 32 52	-05 24	6.63	BO.5Vp	.180,4.0	.54	.97	.07 (.038)
42088	2174	06 06 41	+20 30	7.53	06	.126,4.0	.54	.68	.06 (.014)
46150	2244	06 29 16	+04 58	6.80	05	.112,4.0	.65	.74	.05 (.014)
46485	2244	06 31 15	+04 34	8.15	08	.140,4.0	.89	.66	.05 (.014)
164492	6514	17 59 21	-23 02	7.26	08+09	.148,4.0	.47	.90	.06 (.028)
164492a	6514	17 59 21	-23 02	7.68	08	.140,4.0	.46	.90	.05 (.017)
Her 36	6523	18 00 37	-24 21	10.29	06n	.126,4.0	1.16	1.04	.06 (.014)
164906	6523	18 01 22	-22 24	7.45	B1Vnp	———	——	——	—— ——
Annon. A	6618	18 17 43	-16 12	11.09	05	.112,4.0	1.85	.74	.07 (.028)
Annon. C	6618	18 17 43	-16 12	9.82	B1Vp	.210,4.0	1.33	.72	.16 (.114)
200775	7023	21 00 56	+67 58	7.33	B3Vp	.320,4.0	.72	.85	.16 (.150)
215835	7380	22 44 52	+57 48	8.51	05	.112,4.0	.88	.78	.05 (.014)
220057	7635	23 17 51	+60 52	6.89	B3Vp	.250,4.0	.36	.73	.07 (.058)
+60°2522	7635	23 18 26	+60 55	8.57	05	.112,4.0	.99	.74	.05 (.014)

in the second order blue. For actual classification work 58 spectra of program and standard stars were obtained utilizing the 88 B (600 lines/mm) grating which yielded a dispersion of 85 A/mm in the second order blue. The spectroscopic observations were obtained on six half-nights on the 100-inch telescope and three full nights on the 60-inch telescope, between June and December 1966. All plates were obtained from a single box of baked IIa-O plates and were developed for five minutes in D-19. An attempt was made to control the temperature of the developing chemicals to within a few degrees of 20°C, but the success of these measures is somewhat questionable. All spectrograph adjustments (i.e. grating tilt, slit width, and slit length) were kept constant throughout the program. For most of the standard stars, three exposures of different length were made on a single plate in order to have a range of densities to match the spectra of the program stars for which magnitudes and thus proper exposure times were frequently uncertain at the time that spectrographic observations were made.

The set of spectral type standard stars which was used was compiled from the list of Johnson and Morgan (1953) and is given in Table 2. The spectral types of the program stars were determined by direct comparison of the program star spectra with those of the standard stars. The classification criteria listed in the Atlas of Stellar

TABLE 2

SPECTRAL TYPE STANDARDS

HD	Name	1950.0 R.A.	Decl.	Spectral Type
		$6^h29^m16^s$	+4°58'	
46150				O5
-	BD+60°512	2 30 06	+61 11	O6
47839	S Mon	6 38 14	+9 57	O7
46056		6 28 40	+4 52	O8n
46149		6 29 16	+5 04	O8.5
46202		6 29 34	+5 01	O9V
37043	ι Ori	5 32 59	-5 57	O9III
36512	ω Ori	5 29 32	-7 21	BOV
48434		6 40 57	+3 59	BOIII
7252		1 10 49	+60 37	B1V
23180	o Per	3 41 11	+32 08	B1III
3360		0 34 09	+53 38	B2V
886	γ Peg	0 10 38	+14 55	B2IV
30836	π^4 Ori	4 48 33	+5 31	B2III
41753	υ Ori	6 04 44	+14 47	B3V
21483		3 25 45	+30 13	B3III
34759	ρ Aur	5 18 16	+41 45	B5V
34503	τ Ori	5 15 11	-6 54	B5III
23338	19 Tau	3 42 13	+24 19	B6V
23302	17 Tau	3 41 54	+23 58	B6III
87901	α Leo	10 05 44	+12 12	B7V
23288	16 Tau	3 41 49	+24 08	B7IV
23630	η Tau	3 44 30	+23 58	B7III
23324	18 Tau	3 42 10	+24 42	B8V
23850	27 Tau	3 46 11	+23 54	B8III
176437	γ Lyr	18 57 02	+32 37	B9III
172167	α Lyr	18 35 15	+38 44	AOV

Spectra of Morgan, Keenan and Kellman (1943) were used. The adopted spectral types, the more obvious criteria used in each case and other classifications of the program stars are given in Table 3. Several of the program stars were not included in the spectroscopy program since well-established spectral types were already published. These stars are also listed along with the references in Table 3.

II.4 Photoelectric Spectrophotometry

Spectrophotometric observations were obtained on three nights with the 100-inch telescope and 23 nights with the 60-inch telescope of the Mount Wilson Observatory, between April 1966, and July 1967. The instrument used was the Cassegrain photoelectric spectrophotometer (known colloquially as the "scanner") of the Mount Wilson and Palomar Observatories. The optics of this device are of the Ebert-Fastie type (see Code and Liller, 1962) and it was used throughout this study as a slitless monochromator or narrow band pass filter. The 600 line/mm grating yielded a dispersion of 10 A/mm in the second order while an adjustable slit at the focal plane of the spectrometer allowed the band pass to be set at any value between about five and 65 A (second order).

For all the observations herein reported, the light from the spectrometer was recorded by one of two photomultiplier tubes. For wavelengths in the range

Table 3

SPECTRAL CLASSIFICATION DATA

Star	Plate No.*	Spectral Type	Criteria and Remarks	HD-Type	Other Spectral Types ()=reference
HD5005	None	-	-	B2	06(1)
HD15570	℘2868	07f	λ4471: λλ4541, 4200 plus		
"	℘2879	07f	λ4686 in emission	B	05f(1) 05f(2)
HD15629	℘2880	07	λ4471: λ4541	B	05(1) 05(2)
HD17505	℘2870	07	λ4471: λλ4541, 4200	BO	07(1) 07(2)
HDE237015	℘2871	B1V	HeI, λ4009:λ4089	O_e5	
HD37020	None	-	-		B1(3)
HD37022	None	-	-	$O5_e$	06p(4)
HD37023	None	-	-		B0.5Vp(4)
HD42088	None	-	-	$O5_e$	06(2)
HD46150	None	-	-	B2	05(5)
HD46485	None	-	-	B2	08(2)
HD164492a	B2724	08	λλ4471, 4541, 4686, 4200	O_e5	07(1) 07(2)
HD164492bc	B2725	09	λλ4471, 4541, 4686		
Herschel36	B2719	06n	Absence of HeI, weak very wide H	-	07(6)
HD164906	B2722	B1Vnp	λλ4121,4144;v.broad H lines;shell star?	B	B1IVpe(1)
NGC6618A	B2728	05	λλ4200,4541,4686; No! 4471	-	None
NGC6618C	B2726	B1V	λ4009:λ4089	-	None
HD200775	℘2864	B3Vp	HeI and Balmer profiles; shell star?	B5	
HD215835	℘2874	05	λλ4541,4200, No!λ4471	B	06n(1),(2)
HD220057	℘2866	B3V	HeI and Balmer Lines		
"	℘2876	B2V	HeI and Balmer Lines	B5	
BD+60°2522	℘2877	05	λλ4541, 4200, Noλ4471	-	07f(1),(2)

*B indicates 100-inch plate, ℘ indicates 60-inch

(1) Morgan, Code and Whitford 1955
(2) Hiltner 1956
(3) Sharpless 1952
(4) Borgmann 1960
(5) Morgan et al 1965
(6) Woolf 1961

λλ 3390 to 5840 A an RCA 1P21 photomultiplier (S-4 photocathode) was used at a nominal voltage of 775 v.d.c. This tube operated in the second order of the grating and a yellow filter was introduced at λ 4785 and greater in order to eliminate the violet contribution of the third order. Observations in the red and infrared (λλ 5000 to 10800 A) were made in the first order of the grating with an RCA 7102 (S-1 photocathode) photomultiplier operated at a voltage of 1500 v.d.c. For these observations it was necessary to introduce an amber filter at wavelengths of 6370 A and greater to eliminate the blue and violet light of the second order. On four nights an IT&T FW 130 (S-20 photocathode) was used, but electronic difficulties resulting in an excessively large coincidence correction which became apparent upon reduction of this data, made it necessary to discard all of these observations. All tubes were operated at dry ice temperature.

The output from the photomultipliers was recorded by one of two data systems. During the first seven nights of observations, a direct current (d.c.) measuring system was used. In this system the output terminal of the photocell was connected directly to a General Radio Electrometer-Amplifier which was in turn connected to a Brown recording milliammeter. The data for each wavelength point of an observation was thus a deflection and a gain. The use of this type of equipment

necessitated the calibration of the amplifier gain, usually at the beginning and end of each night, by means of reference to a standardized voltaic cell internal to the amplifier according to the procedure outlined in the operation manual of the amplifier. Late in June 1966, pulse-counting apparatus became available (for the 60-inch telescope) and was used for all subsequent observations. In this configuration the photomultiplier output was connected to a preamplifier on the telescope, the signal from which was carried by means of a coaxial cable to a remote station. At this remote position the signal was first amplified and then subjected to pulse height discrimination. In this process those pulses and only those pulses the voltage of which was greater than a certain threshold voltage caused a pulse to be transmitted to the next system, the counter. The counter simply registered the number of pulses received from the discriminator during a preset integration time which was measured by an accurate oscillator internal to the counter. At the end of the selected counting time, the total count was recorded in printed form. The philosophy behind the use of this system rests upon the fact that many of the possible types of interference with the electronics are manifested in the form of the pulses which are very much lower in voltage than those produced by photon-induced electron cascades. Thus,

particularly at Mount Wilson where the ambiant radio frequency flux density is very high, it is possible to discriminate against noise signal and the signal to noise ratio may be materially increased. This was, however, accomplished at the price of two additional calibration procedures. First it was necessary, at the beginning of each observing run, to determine the optimum combination of tube voltage and pulse height discrimination level. This was done by adjusting the voltage, amplifier gain and discriminator threshold until there was a large and consistent difference between the photon pulses and those of the amplifier noise, etc. More important and more difficult was the problem of coincidence correction. The discrimination system was characterized by a finite "dead time" between the receipt of an activating pulse and the relaxation of the system into a state which would accept a second pulse. If a pulse arrived at the discriminator during this dead time, it failed to register. Thus the "coincidence" in time of two photon induced electron cascades registered as a single event. This problem becomes more acute the higher the rate of pulses, so that without correction considerable systematic errors will arize. The coincidence correction which was used for most of the observational reductions was obtained in the Pasadena laboratory by the comparison of actual and predicted count rates for

light levels of known brightness ratio. The adopted correction was 14.8 percent at 10^5 counts/second with a linear relation and zero correction at zero count rate assumed. In practice the coincidence correction was of importance only on the standard star observations and an effort was made to keep the count rate well below 10^5 sec^{-1} by adjustment of the exit slit width.

The mechanical process of obtaining the observations was quite straightforward. At the telescope the star to be observed and a portion of the sky were isolated by means of a circular entrance aperture of the order of ten seconds of arc projected on the sky in diameter (depending somewhat on the seeing conditions and the sky brightness). A reading was then taken, after which the telescope was moved to a clear area of the sky and another reading taken. The difference between the two signals was presumed to be the signal from the star. In the case of stars within H II regions this process of sky subtraction was neither simple or trivial as the nebular background could frequently be seen to be irregular. In these cases an attempt to select a comparison field with an apparent surface brightness similar to that around the star was made. The difficulty in so doing is illustrated by the frequently discordant point at λ 5000 due to the presence of the [OIII] line at λ 5007 in the nebular background. Once such a pair of measurements had been made, the

effective wavelength of the spectrometer was changed and the process repeated in reverse. When the blue sensitive 1P21 was used, a total of 17 wavelength points were observed while with the red sensitive 7102 photomultiplier, 19 points were used. The two lists of wavelengths had five points in common. Normally the wavelength points were observed sequentially from shorter to longer wavelengths and then the sequence was repeated in reverse. Usually the sky comparison field was taken on opposite sides of the star (usually east and west) on the two different measurements of a given wavelength. The observation at each wavelength point was conducted for a sufficiently long time that the individual readings could be defined to within a few percent. Particularly with the pulse counting system at the 60-inch telescope where the counts (but no other data) were recorded at a remote station, it was necessary to adhere to a strict routine in order that the data record could be interpreted.

In addition to the deflection-gain or count data, it was necessary to record certain other data. In general the band pass, the beginning, middle and ending local sidereal time of each stellar observation and notes on the observing conditions such as seeing were recorded. For the d.c. measurements, the records of gain, effective wavelength, and time were recorded on the strip chart record at the telescope. During pulse counting

observations it was necessary to make a separate record of integration times and of any deviations from the routine pattern of wavelengths.

The primary problem involved in spectrophotometric observation is the calibration of the response function of the system. The response function is the product of the effects of deviation from a standard atmospheric extinction correction, several aluminum reflections, several transmission optical elements (prisms, lenses, and filters) and the characteristics of the particular photomultiplier being used. The only practical procedure is the empirical calibration of the system by means of standard stars. The particular set of standard stars used in this study is that given by Oke (1960, 1964) with the Balmer jumps increased by 0.06 magnitudes in accordance with the comments of Mihalas (1966). All of these standard stars are of early spectral types (types B and A) and their calibration is ultimately referred to the star α Lyrae, the fluxes of which are in turn fitted to a model atmosphere calculation with the characteristics $\log g = 4$ and $\theta_e = .525 (T_e = 9600^\circ K)$. An attempt was made to observe at least five or six of these standard stars in the course of a night. Furthermore, whenever possible, the stars were observed at as wide a range of zenith distances as could be obtained. Band passes and integration times were kept large enough to allow

calibration of the system to a precision of one or two percent. Throughout this study only the set of standard wavelength points given by Oke was used. These wavelengths were chosen so as to avoid strong spectral features such as hydrogen lines and also to afford enough points for accurate fitting of slopes to the observations.

All spectrophotometric observations were reduced on an IBM 7094 computer by means of a program devised and kindly loaned to the present investigator by Dr. J. B. Oke. This program required the following input data:

1) Gain calibration and gain identification numbers, two separate calibrations being necessary, the factors of ten gain, G_{10}, and the half magnitude steps, $G_{1/2}$,

2) Coincidence correction, CORR, which is the factor by which the true count rate exceeds the apparent count rate at a given apparent count rate,

3) Extinction coefficients, A_λ, as given by Oke (1965),

4) Standard star calibrations, AB, as described above,

all of which were given as tabular data to be used by the program for all stars. In addition, an identification card for each stellar observation was required and carried the position (right ascension and declination) of the star, the date and the star name. Finally for each measurement the following information was entered:

1) Gain identification number,

2) Band pass, $\Delta\lambda$, in Angstrom units,

3) Effective wavelength, λ ,

4) Integration time ΔT, in seconds,

5) Local sidereal time,

6) Total counts or deflection, N.

Inapplicable quantities, e.g. the coincidence correction for d.c. measurements, were simply omitted or were replaced by a blank card.

From these data the observations were converted to raw magnitudes, OB, by means of the equation:

$$OB = -2.5 \log (I/\Delta\lambda) - A_\lambda \sec z + C \qquad (1)$$

where the appropriate A_λ was found by interpolation in the A_λ table and the quantity sec z was calculated for each measurement from the given star position and local sidereal time. For d.c. measurements the quantity I is given by:

$$I_{dc} = N\, G_{10}\, G_{1/2} \qquad (2)$$

and the constant C was set at 25.000 in order to render OB as a relatively small, positive number. For pulse counting observations:

$$I_{pc} = \frac{N \cdot CORR}{\Delta T} \qquad (3)$$

and C was set at 18.500.

The difference between the individual observed OB's and the corresponding standard star calibrations, AB, was then the measure of the response factor for a given wavelength point. This difference, OB - AB, for each wavelength was then averaged over all those standard star observations which the investigator chose to include in the calibration for a given set of program stars. This was usually all the standard observations for the night on which the program star observation was obtained, however in some instances only those standard observations bracketing the program observation were used. This averaging yielded the quantity (AVOB - AB). The difference between the program star OB and the (AVOB - AB) for the same wavelength was then adopted as the monochromatic magnitude of the program star, also called AB. When a star was observed on more than one night in the same spectral region, precedence was given to the colors rather than to the magnitudes since it was found that there were frequently gray shifts of rather large size in the magnitude. Thus the five overlapping wavelength points of individual night observations were caused to agree on the average, by means of additive "grey" terms which were then applied to all observations of the star on the individual nights. Once such grey shifts as were necessary had been performed, final monochromatic magnitudes were derived as the average of all

observations at a given wavelength weighted by the number of times the wavelength was observed on the individual nights. The adopted monochromatic magnitudes are given in Table 4. These AB's are monochromatic fluxes (units of power per unit area per unit frequency interval) expressed in magnitudes with an additive constant such that the AB for the point at λ 5556 will roughly correspond to the V magnitude.

There are several sources of errors, both random and systematic, which may affect the spectrophotometric observations. Among the sources of random errors, the most easily evaluated is the uncertainty in the measurement due to the statistical nature of photon arrivals. In the pulse counting observations, the evaluation of this source of error is quite straightforward since the individual photon arrivals may be considered to be independent and thus Poisson statistics may be assumed to apply. In this case the standard deviation in a measurement of N events is simply $N^{1/2}$. In the case of direct current measurements the same phenomenon is manifested by a noisy record and the precision with which the mean deflection can be measured can be estimated by repeated reading of signals of various degrees of noisiness. There are other sources of random errors which are more difficult to estimate. Among these are stray light effects. Moving light sources within the dome may cause

Table 4

MONOCHROMATIC MAGNITUDES OF H II REGION STARS

λ^{-1}	HD5005ABC NGC281	HD15570 IC1805*	HD15629 IC1805	HD17505 IC1848	HDE237015 IC1848	HD37020 NGC1976*	HD37022 NGC1976*
2.950 †	7.96	8.76	9.05	7.69	10.20	6.60	5.00
2.900 †	7.95	8.68	9.00	7.66	10.15	6.56	4.98
2.850 †	7.94	8.67	8.99	7.64	10.15	6.60	4.99
2.800 †	7.94	8.65	8.96	7.62	10.12	6.63	4.98
2.750 †	7.93	8.62	8.93	7.58	10.09	6.63	5.01
2.700	7.89	8.55	8.88	7.56	10.02	6.61	4.99
2.589	8.01	8.60	8.95	7.60	9.81	6.63	5.04
2.480	7.89	8.46	8.83	7.48	9.62	6.53	4.98
2.400	7.90	8.43	8.79	7.44	9.61	6.59	5.02
2.350	7.90	8.42	8.76	7.42	9.58	6.59	5.00
2.240	7.90	8.34	8.70	7.37	9.59	6.65	5.06
2.190	7.89	8.29	8.67	7.33	9.56	6.61	5.02
2.090	7.90	8.23	8.64	7.29	9.54	6.61	5.04
2.000	7.90	8.12	8.59	7.23	9.51	6.--*	5.06
1.900	7.90	7.99	8.44	7.17	9.41	6.62	5.04
1.800	7.89	7.85	8.34	7.06	9.39	6.61	5.03
1.712	7.89	7.77	8.27	7.03	9.28	6.62	5.01
1.652	7.93	7.68	8.22	7.00	9.20	6.62	5.05
1.570	7.92	7.64	8.26	7.00	9.36	6.66	5.04
1.471	7.95	7.45	8.18	6.92	9.34	6.57	4.97
1.408	7.95	7.35	8.13	6.91	9.37	6.63	5.07
1.328	7.90	7.26	8.09	6.88	9.38	6.59	5.13
1.274	7.83	7.23	8.08	6.88	9.40	6.68	5.10
1.238	8.01	7.22	8.10	6.84	9.36	6.63	5.11
1.190	7.98	7.12	8.03	6.83	9.43	6.61	5.12
1.136	8.04	7.16	8.13	6.91	9.47	6.66	5.20
1.031	8.14	7.04	8.00	6.87	9.45	6.58	5.22
1.005	8.09	7.02	8.09	6.87	9.52	6.65	5.17
0.976	8.17	7.01	8.02	6.89	9.47	6.63	5.21
0.962	8.18	7.05	8.10	6.93	9.53	6.67	5.21
0.926	8.50	7.01	8.43	7.00	9.21	6.70	5.21

Table 4, Continued

λ^{-1}	HD37023 NGC1976*	HD42088 NGC2174,75	HD46150 NGC2244	HD46485 NGC2244*	HD164492 NGC6514*	HD164492a NGC6514*	Herschel 36 NGC6523*
2.950 †	6.70	7.57	6.96	8.75	7.10	7.73	11.27
2.900 †	6.66	7.50	6.85	8.71	7.14	7.64	11.22
2.850 †	6.69	7.54	6.92	8.66	7.14	7.67	11.18
2.800 †	6.72	7.54	6.94	8.67	7.15	7.64	11.11
2.750 †	6.71	7.53	6.92	8.62	7.19	7.66	11.08
2.700	6.69	7.52	6.88	8.61	7.18	7.67	11.02
2.589	6.70	7.57	6.97	8.62	7.06	7.74	11.12
2.480	6.58	7.52	6.89	8.52	7.16	7.60	10.96
2.400	6.64	7.53	6.90	8.50	7.18	7.60	10.91
2.350	6.63	7.52	6.90	8.48	7.18	7.60	10.90
2.240	6.68	7.56	6.89	8.48	7.22	7.61	10.80
2.190	6.64	7.52	6.87	8.38	7.24	7.62	10.72
2.090	6.63	7.54	6.87	8.35	7.21	7.65	10.65
2.000	6.52	7.53	6.83	8.26	7.24	7.66	10.53
1.900	6.64	7.50	6.80	8.20	7.25	7.65	10.38
1.800	6.63	7.53	6.80	8.15	7.26	7.68	10.29
1.712	6.58	7.51	6.80	8.11	7.27	7.64	10.16
1.652	6.57	7.56	6.77	8.10	7.28	7.68	10.17
1.570	6.59	7.58	6.81	8.00	7.30	7.69	9.92
1.471	6.52	7.58	6.78	8.03	7.34	7.68	9.78
1.408	6.54	7.62	6.76	8.03	7.34	7.73	9.72
1.328	6.56	7.68	6.84	7.89	7.46	7.72	9.63
1.274	6.55	7.70	6.86	7.99	7.40	7.78	9.50
1.238	6.58	7.77	6.87	8.02	7.47	7.84	9.48
1.190	6.52	7.81	6.85	7.97	7.52	7.86	9.32
1.136	6.62	7.83	6.92	8.08	7.54	7.89	9.25
1.031	6.65	7.90	6.91	8.13	7.55	8.00	9.30
1.005	6.64	7.86	7.00	8.08	7.42	7.95	9.05
0.976	6.63	7.99	7.00	8.13	7.56	7.95	8.84
0.962	6.53	7.97	7.04	8.15	7.60	7.98	8.68
0.926	6.52	7.96	6.86	8.02	7.55	8.03	8.53

Table 4, Continued

λ^{-1}	HD164906 NGC6523,30*	Annon. A NGC6618	Annon. C NGC6618	HD200775 NGC7023*	HD215835 NGC7380	HD220057 NGC7635	BD+60°2522 NGC7635
2.950 †	7.63	13.02	11.04	8.20	9.11	7.22	9.20
2.900 †	7.59	12.96	11.17	8.14	9.06	7.20	9.17
2.850 †	7.62	13.06	11.17	8.12	9.04	7.20	9.15
2.800 †	7.61	12.90	11.10	8.06	9.02	7.20	9.15
2.750 †	7.57	12.94	11.04	8.01	9.00	7.18	9.12
2.700	7.66	12.80	10.92	8.06	8.96	7.14	9.07
2.589	7.68	12.72	10.94	7.91	8.94	6.97	9.16
2.480	7.60	12.52	10.74	7.73	8.87	6.83	9.03
2.400	7.57	12.39	10.66	7.65	8.84	6.81	9.01
2.350	7.59	12.32	10.58	7.63	8.82	6.82	9.00
2.240	7.58	12.11	10.48	7.60	8.78	6.87	8.93
2.190	7.56	12.00	10.37	7.55	8.75	6.84	8.90
2.090	7.55	11.85	10.33	7.53	8.72	6.86	8.85
2.000	7.52	11.55	10.12	7.48	8.64	6.88	8.79
1.900	7.50	11.30	10.01	7.38	8.56	6.86	8.66
1.800	7.45	11.09	9.82	7.33	8.51	6.89	8.57
1.712	7.43	10.78	9.68	7.27	8.47	6.90	8.47
1.652	7.50	10.94	9.73	7.22	8.35	6.92	8.47
1.570	7.48	10.58	9.65	7.16	8.36	6.96	8.40
1.471	7.45	10.23	9.50	7.08	8.22	6.97	8.36
1.408	7.44	10.18	9.42	7.03	8.30	7.01	8.32
1.328	7.38	10.06	9.32	6.99	8.33	7.07	8.30
1.274	7.40	10.01	9.27	6.93	8.30	7.10	8.28
1.238	7.37		9.21	6.89	8.33	7.13	8.27
1.190	7.39		9.19	6.90	8.23	7.18	8.22
1.136	7.55		9.08	7.09	8.32	7.21	8.29
1.031	7.60		8.95	6.95	8.32	7.26	8.20
1.005	7.48		8.90	6.97	8.28	7.26	8.30
0.976	7.54		8.90	6.95	8.23	7.31	8.20
0.962	7.55		8.83	6.95	8.27	7.28	8.24
0.926	7.47		8.68	6.86	8.09	7.27	8.27

NOTES ON TABLE 4

λ^{-1}	
2.950 †	0.06 magnitude added to all AB's determined with AB_{64} standards
2.900 †	
2.850 †	
2.800 †	
2.750 †	
HD15570	
IC1805*	Add -0.27 to red tube AB's
HD37020	
NGC1976*	Add -0.094 to red tube AB's Sky subtraction questionable due to λ5007
HD37022	
NGC1976*	Add -.13 to Night 19S AB's
HD37023	
NGC1976*	Add -0.153 to red tube AB's
HD46485	
NGC2244*	Add -0.12 to Night 20S AB's
HD164492	
NGC6514*	Add -0.06 to Night 4S AB's
HD164492a	
NGC6514*	Add -0.35 to Night 25S AB's
Herschel 36	
NGC6523*	Add -0.35 to Night 25S AB's
HD164906	
NGC6523,30*	Add 0.081 to Night 25S AB's
HD200775	
NGC7023*	Add -0.388 to red tube AB's

occasional readings to be too large while momentary bad seeing may cause light to fall outside the entrance aperture, thus making the reading too small. Unevenness in the atmospheric extinction as might be expected in the infrared due to a patchy distribution of water vapor overhead may also effect the observations. As previously mentioned, the unevenness of the sky background, particularly in H II regions, along with the difficulty of exact repositioning of the telescope on the comparison field has been seen to lead to errors. Finally some interference signals may succeed in passing through the discriminator and small variations in the high voltage source could cause variation in the photomultiplier gain and thus cause errors in d.c. readings.

The standard star observations provided a means by which to estimate the influence of these various factors. The standard deviations in the color of the calibration factor AVOB-AB for several wavelength points on each night were calculated and compared with those expected from statistical considerations alone. It was found that on the average the actual standard deviation was about twice the statistically expected value and so this factor was applied to the program stars. Thus the probable error in the difference in AB between λ^{-1} of 2.4 microns^{-1} and 1.8 microns^{-1} was found to have an average overall program stars of $\pm$0.027 magnitudes with

a minimum of ±0.014 and a maximum of ±0.042. In the red region of the spectrum the color of the 1.0 micron^{-1} point with respect to the 1.8 micron^{-1} point was found to have an average probable error of ±0.044 magnitudes with the extreme values being ±0.022 and ±0.085.

The various calibration and correction procedures which were applied to the observations were designed to remove the sources of systematic errors. If, however, any of these corrections are inaccurate, systematic errors may still be present in the observations. To test for the presence of residual errors in the coincidence correction the quantity OB - AB was plotted as a function of count rate for several representative wavelength points in each night's observations. From these plots it was concluded that the adopted coincidence correction was sufficiently accurate to keep its effects on the observations within one percent. Similarly, to check the adequacy of the standard atmospheric extinction correction, the colors of OB - AB were inspected for variations with either zenity distance or time. Oke (1965) has discussed the use of the standard atmospheric extinction correction for narrow band spectrophotometry and had concluded that, except for small grey terms which will not affect colors, this procedure was sufficiently accurate. The findings of the present study corroborate this finding with the exception of one night on which a

slow, systematic drift in the OB - AB color was found. In this case the OB - AB was interpolated between bracketing standard star observations, the individual program stars were assigned more pessimistic error estimates than usual and were also assigned low weight in the averaging of final data. Finally there is the possibility that the calibration of the standard stars is in error. This problem is at present under investigation by various observers (e.g. Schild and Oke) and small additive corrections may soon be available. Since all observations in the present study as well as all those in the study of Whiteoak (1966), with which the present observations are compared, were reduced with the same set of standards, the ability of these observations to discriminate between different types of reddening curves will be unimpared by this source of error. However the reddening curves to be derived in the following chapter should be considered tentative insofar as they are to be used for fitting to particular interstellar grain models until such time as the more nearly definitive calibrations of the spectrophotometric standards is available.

III. REDDENING CURVES

III.1 Introduction

The term "reddening curve" will be used herein to refer to the difference, in magnitudes, between the observed and the assumed intrinsic colors of a given star normalized to a standard difference between two fixed wavelengths. Thus the identification of this reddening curve with the true wavelength dependence of the interstellar extinction depends critically not only upon the accuracy of the stellar photometry and of the calibration of the spectrophotometric system, but also upon the accuracy and appropriateness of the colors chosen to represent the intrinsic colors of the star. It is this choice of representative colors which poses the major problem in the determination of the reddening curve and constitutes the largest single source of potential systematic errors in this representation of the wavelength dependence of the interstellar extinction.

The usual technique used to determine the reddening curve (Stebbins and Whitford, 1943) has been to compare the colors of pairs of stars of the same spectral type, one of which has a higher degree of extinction than the other. Ideally the one star should be completely free of extinction, but for any but the nearest of stars, this is an unattainable condition. This is particaularly true

for the majority of the stars encountered in the present study, which are all very luminous stars of early spectral type, examples of which do not exist within the relatively small volume around the Sun which can be considered to be free of extinction. Furthermore, stars of these types are frequently associated with aggregates of interstellar gas and grains. Since it is the purpose of the present study to search for an effect of just such material which is superimposed upon the more general extinction, the use of comparison objects which might also display the effect is clearly undesirable. Thus a different approach has been taken.

III.2 Derivation of Reddening Curves

The method which was used in the present study was essentially the same as was used by Whiteoak (1966). Rather than utilizing the observed colors of stars with little or no extinction, the intrinsic spectral energy distributions of the stars were simulated by means of the monochromatic fluxes obtained from model atmosphere computations. The particular set of model atmosphere computations used here was that of Mihalas (1965). In these model calculations a high degree of flux constancy was maintained and all sources of opacity known to be of importance in stars of the temperatures dealt with here were included. It was thus felt that these models gave

as accurate a representation of the intrinsic energy distributions as could be obtained. Furthermore, the internal consistency of the model spectra, i.e. the regular progression of Balmer discontinuities and continuum slopes with temperature, lead to confidence that the method could at least differentiate between normal reddening curves and cases of anomalous behavior.

The selection of a model with which to simulate the intrinsic colors of a program star requires the determination of an effective temperature, T_e (or alternatively $\theta_e = 5040\ T_e^{-1}$), and a surface gravity, g. The approach which was used by Whiteoak was to fit the Balmer discontinuities of the models and of the observations. This approach was initially used throughout the present study. However, a number of discrepancies in this procedure became apparent. In several cases the temperature indicated by the Balmer discontinuity and that indicated by the spectral type were highly discordant in the sense that the Balmer discontinuity was smaller and the temperature thus higher than would be expected from the spectral type. Indeed in several cases the Balmer continuum was found to be distinctly in emission. In these cases it was necessary to depend entirely upon the spectral classification of the star and the calibration of the temperature scale of the various early spectral types. The spectral classifications

obtained in the present study as well as those of other workers have been discussed above and are tabulated in Table 3. The temperature calibration of the various spectral types which was used for the selection of models in the present study was based upon the data given by Harris (1963) for spectral types 09.5 and earlier and upon the data given by Johnson (1966) for types BO and later. It was found that, within the accuracy with which the colors of the models could be determined, it was adequate to identify specific spectral types with specific model atmosphere computations. The schedule of these identifications is given in Table 5:

TABLE 5

SPECTRAL TYPE - EFFECTIVE TEMPERATURE SCHEDULE

TYPE	θ_e	TYPE	θ_e
05	.112	09.5	.168
06	.126	B0	.180
07	.132	B1	.210
08	.140	B1.5	.250
08.5	.148	B2	.280
09	.157	B3	.320

In all cases the models for log g = 4.0 were used. This choice is justified for the spectral types earlier than 09 by the fact that the differences in color between the models of various values of log g at a given temperature

were no larger than the errors in the derivation of the colors. For spectral types of 09.5 and later, where significant differences between various values of log g began to appear, the choice of log g = 4.0 was in accordance with the practice of Whiteoak for stars of luminosity class V.

The colors for the model atmosphere spectral energy distributions for each individual standard wavelength point in the spectrophotometric program were derived from the fluxes given by Mihalas by graphical interpolation. These colors, C_m, are given in Table 6, and are defined by the equation:

$$C_m(\lambda^{-1}) = 2.5 \log F_\nu(1.8) - 2.5 \log F_\nu(\lambda^{-1}). \qquad (4)$$

The first step in the derivation of the reddening curves was the conversion of the monochromatic magnitudes, $AB(\lambda^{-1})$, given in Table 4 to monochromatic colors, $C_s(\lambda^{-1})$, according to the equation:

$$C_s(\lambda^{-1}) = AB(\lambda^{-1}) - AB(1.8). \qquad (5)$$

These colors are given in Table 7. Once a model had been selected to represent the intrinsic colors of a program star, the monochromatic color excesses were obtained according to the formula:

$$E(\lambda^{-1}) = C_s(\lambda^{-1}) - C_m(\lambda^{-1}). \qquad (6)$$

Table 6

MIHALAS MODEL COLORS

λ^{-1}	.101,4.0	.112,4.0	.126,4.0	.132,4.0	.140,4.0	.148,4.0
2.950	- .86	- .86	- .83	- .81	- .80	- .78
2.900	.84	.83	.80	.79	.78	.75
2.850	.82	.81	.78	.76	.74	.72
2.800	.79	.78	.75	.73	.72	.70
2.750	.76	.75	.72	.71	.69	.67
2.700	.76	.75	.74	.73	.74	.76
2.589	.69	.68	.67	.66	.67	.69
2.480	.61	.61	.60	.59	.60	.61
2.400	.55	.55	.54	.53	.54	.55
2.350	.51	.51	.50	.48	.50	.51
2.240	.42	.42	.41	.40	.41	.43
2.190	.38	.38	.37	.37	.37	.38
2.090	.29	.29	.29	.28	.29	.29
2.000	.20	.20	.20	.20	.20	.20
1.900	- .10	- .10	- .11	- .10	- .11	- .11
1.800	0.00	0.00	0.00	0.00	0.00	0.00
1.712	+ .09	+ .09	+ .09	+ .09	+ .09	+ .09
1.652	.16	.16	.16	.16	.16	.16
1.570	.26	.26	.25	.25	.25	.25
1.471	.38	.38	.37	.38	.37	.37
1.408	.46	.46	.45	.45	.45	.45
1.328	.57	.57	.56	.56	.56	.57
1.274	.65	.65	.64	.65	.65	.65
1.238	.71	.70	.69	.71	.70	.70
1.190	.80	.79	.78	.77	.76	.77
1.136	.89	.87	.87	.86	.85	.85
1.031	1.08	1.07	1.06	1.05	1.06	1.05
1.005	1.13	1.12	1.11	1.10	1.10	1.10
0.976	1.18	1.18	1.17	1.16	1.16	1.16
0.962	1.21	1.21	1.20	1.19	1.18	1.18
0.926	+1.29	+1.28	+1.26	+1.26	+1.27	+1.26

Table 6, Continued

λ^{-1}	.157,4.0	.168,4.0	.180,4.0	.210,4.0	.25,3.8	.28,4.0	.32,4.0
2.950	- .72	- .66	- .58	- .43	- .21	- .05	+ .16
2.900	.70	.63	.56	.41	.20	.04	.17
2.850	.67	.60	.54	.40	.19	.03	.18
2.800	.65	.58	.52	.38	.18	.01	.18
2.750	.62	.56	.50	.36	.17	.00	+ .19
2.700	.75	.73	.73	.67	.60	.57	- .53
2.589	.68	.67	.66	.61	.55	.52	.48
2.480	.60	.59	.58	.54	.49	.47	.43
2.400	.54	.53	.53	.49	.45	.43	.40
2.350	.50	.49	.49	.45	.42	.40	.37
2.240	.41	.41	.40	.37	.35	.33	.30
2.190	.37	.37	.36	.34	.32	.30	.27
2.090	.29	.28	.28	.26	.25	.23	.21
2.000	.20	.20	.20	.19	.18	.16	.15
1.900	- .10	- .10	- .10	- .10	- .09	- .08	- .08
1.800	0.00	0.00	0.00	0.00	0.00	0.00	0.00
1.712	+ .09	+ .09	+ .09	+ .09	+ .08	+ .08	+ .07
1.652	.16	.16	.15	.15	.14	.14	.13
1.570	.25	.25	.24	.23	.22	.22	.20
1.471	.37	.37	.36	.34	.33	.32	.30
1.408	.45	.45	.43	.41	.39	.38	.36
1.328	.56	.56	.54	.51	.49	.47	.44
1.274	.63	.63	.62	.58	.55	.54	.50
1.238	.70	.69	.67	.62	.60	.59	.55
1.190	.75	.73	.70	.65	.60	.56	.51
1.136	.84	.83	.79	.73	.68	.64	.60
1.031	1.02	1.01	.98	.91	.86	.81	.78
1.005	1.08	1.06	1.03	.97	.90	.86	.82
0.976	1.14	1.12	1.08	1.02	.96	.92	.86
0.962	1.16	1.14	1.11	1.05	.98	.94	.88
0.926	+1.24	+1.23	+1.19	+1.12	+1.06	+1.02	+ .95

Table 7

MONOCHROMATIC COLORS OF H II REGION STARS

λ^{-1}	HD5005ABC NGC281	HD15570 IC1805	HD15629 IC1805	HD17505 IC1848	HDE237015 IC1848	HD37020 NGC1976	HD37022 NGC1976
2.950	+ .07	+ .91	+ .71	+ .63	+ .81	- .01	- .03
2.900	+ .06	+ .83	+ .66	+ .60	+ .76	- .05	- .05
2.850	+ .05	+ .82	+ .65	+ .58	+ .76	- .01	- .04
2.800	+ .05	+ .80	+ .62	+ .56	+ .73	+ .02	- .05
2.750	+ .04	+ .77	+ .59	+ .52	+ .70	+ .02	- .02
2.700	.00	+ .70	+ .54	+ .50	+ .63	.00	- .04
2.589	+ .12	+ .75	+ .61	+ .54	+ .42	+ .02	+ .01
2.480	.00	+ .61	+ .49	+ .42	+ .23	- .08	- .05
2.400	+ .01	+ .58	+ .45	+ .38	+ .22	- .02	- .01
2.350	+ .01	+ .57	+ .42	+ .36	+ .19	- .02	- .03
2.240	+ .01	+ .49	+ .36	+ .31	+ .20	+ .04	+ .03
2.190	.00	+ .44	+ .33	+ .27	+ .17	.00	- .01
2.090	+ .01	+ .38	+ .30	+ .23	+ .15	.00	+ .01
2.000	+ .01	+ .27	+ .25	+ .17	+ .12	----	+ .03
1.900	+ .01	+ .14	+ .10	+ .11	+ .02	+ .01	+ .01
1.800	0.00	0.00	0.00	0.00	0.00	0.00	0.00
1.712	.00	- .08	- .07	- .03	- .11	+ .01	- .02
1.652	+ .04	- .17	- .12	- .06	- .19	+ .01	+ .02
1.570	+ .03	- .21	- .08	- .06	- .03	+ .05	+ .01
1.471	+ .06	- .40	- .16	- .14	- .05	- .04	- .06
1.408	+ .06	- .50	- .21	- .15	- .02	+ .02	+ .04
1.328	+ .01	- .59	- .25	- .18	- .01	- .02	+ .10
1.274	- .06	- .62	- .26	- .18	+ .01	+ .07	+ .07
1.238	+ .12	- .63	- .24	- .22	- .03	+ .02	+ .08
1.190	+ .09	- .73	- .31	- .23	+ .04	.00	+ .09
1.136	+ .15	- .69	- .21	- .15	+ .08	+ .05	+ .17
1.031	+ .25	- .81	- .34	- .19	+ .06	- .03	+ .19
1.005	+ .20	- .83	- .25	- .19	+ .13	+ .04	+ .14
0.976	+ .28	- .84	- .32	- .17	+ .08	+ .02	+ .18
0.962	+ .29	- .80	- .24	- .13	+ .14	+ .06	+ .18
0.926	+ .61	- .84	+ .09	- .06	- .18	+ .09	+ .18

Table 7, Continued

λ^{-1}	HD37023 NGC1976	HD42088 NGC2174,75	HD46150 NGC2244	HD46485 NGC2244	HD164492 NGC6514	HD164492a NGC6514	Herschel 36 NGC6523
2.950	+ .07	+ .04	+ .16	+ .60	- .16	+ .05	+ .98
2.900	+ .03	- .03	+ .05	+ .56	- .12	- .04	+ .93
2.850	+ .06	+ .01	+ .12	+ .51	- .12	- .01	+ .89
2.800	+ .09	+ .01	+ .14	+ .52	- .11	- .04	+ .82
2.750	+ .08	.00	+ .12	+ .47	- .07	- .02	+ .79
2.700	+ .06	- .01	+ .08	+ .46	- .08	- .01	+ .73
2.589	+ .07	+ .04	+ .17	+ .47	- .20	+ .06	+ .83
2.480	- .05	- .01	+ .09	+ .37	- .10	- .08	+ .67
2.400	+ .01	.00	+ .10	+ .35	- .08	- .08	+ .62
2.350	.00	- .01	+ .10	+ .33	- .08	- .08	+ .61
2.240	+ .05	+ .03	+ .09	+ .33	- .04	- .07	+ .51
2.190	+ .01	- .01	+ .07	+ .23	- .02	- .06	+ .43
2.090	.00	+ .01	+ .07	+ .20	- .05	- .03	+ .36
2.000	- .11	.00	+ .03	+ .11	- .02	- .02	+ .24
1.900	.01	- .03	.00	+ .05	- .01	- .03	+ .09
1.800	0.00	0.00	0.00	0.00	0.00	0.00	0.00
1.712	- .05	- .02	.00	- .04	+ .01	- .04	- .13
1.652	- .06	+ .03	- .03	- .05	+ .02	.00	- .12
1.570	- .04	+ .05	+ .01	- .15	+ .04	+ .01	- .37
1.471	- .11	+ .05	- .02	- .12	+ .08	.00	- .51
1.408	- .09	+ .09	- .04	- .12	+ .08	+ .05	- .57
1.328	- .07	+ .15	+ .04	- .26	+ .20	+ .04	- .66
1.274	- .08	+ .17	+ .06	- .16	+ .14	+ .10	- .79
1.238	- .05	+ .24	+ .07	- .13	+ .21	+ .16	- .81
1.190	- .11	+ .28	+ .05	- .18	+ .26	+ .18	- .97
1.136	- .01	+ .30	+ .12	- .07	+ .28	+ .21	-1.04
1.031	+ .02	+ .37	+ .11	- .02	+ .29	+ .32	- .99
1.005	+ .01	+ .33	+ .20	- .07	+ .16	+ .27	-1.24
0.976	.00	+ .46	+ .20	- .02	+ .30	+ .27	-1.45
0.962	- .10	+ .44	+ .24	.00	+ .34	+ .30	-1.61
0.926	- .11	+ .43	+ .06	- .13	+ .29	+ .35	-1.76

Table 7, Continued

λ^{-1}	HD164906 NGC6523,30	Annon.A NGC6618	Annon.C NGC6618	HD200775 NGC7023	HD215835 NGC7380	HD220057 NGC7635	BD+60°2522 NGC7635
2.950	+ .18	+1.93	+1.22	+ .87	+ .60	+ .33	+ .63
2.900	+ .14	+1.87	+1.35	+ .81	+ .55	+ .31	+ .60
2.850	+ .17	+1.97	+1.35	+ .79	+ .53	+ .31	+ .58
2.800	+ .16	+1.81	+1.28	+ .73	+ .51	+ .31	+ .58
2.750	+ .12	+1.85	+1.22	+ .68	+ .49	+ .29	+ .55
2.700	+ .21	+1.71	+1.10	+ .73	+ .45	+ .25	+ .50
2.589	+ .23	+1.63	+1.12	+ .58	+ .43	+ .08	+ .59
2.480	+ .15	+1.43	+ .92	+ .50	+ .36	- .06	+ .46
2.400	+ .12	+1.30	+ .84	+ .32	+ .33	- .09	+ .44
2.350	+ .14	+1.23	+ .76	+ .30	+ .31	- .07	+ .43
2.240	+ .13	+1.02	+ .66	+ .27	+ .27	- .02	+ .36
2.190	+ .11	+ .91	+ .55	+ .22	+ .24	- .06	+ .33
2.090	+ .10	+ .76	+ .51	+ .20	+ .21	- .03	+ .28
2.000	+ .07	+ .46	+ .30	+ .15	+ .13	- .01	+ .22
1.900	+ .05	+ .21	+ .19	+ .05	+ .05	- .03	+ .09
1.800	0.00	0.00	0.00	0.00	0.00	0.00	0.00
1.712	- .02	- .31	- .14	- .06	- .04	+ .01	- .10
1.652	+ .05	- .15	- .09	- .11	- .16	+ .03	- .10
1.570	+ .03	- .51	- .17	- .17	- .15	+ .07	- .17
1.471	.00	- .86	- .32	- .25	- .29	+ .08	- .21
1.408	- .01	- .91	- .40	- .30	- .21	+ .12	- .25
1.328	- .07	-1.03	- .50	- .34	- .18	+ .18	- .27
1.274	- .05	-1.08	- .55	- .40	- .21	+ .21	- .29
1.238	- .08		- .61	- .44	- .18	+ .24	- .30
1.190	- .06		- .63	- .43	- .28	+ .29	- .35
1.136	+ .10		- .74	- .24	- .19	+ .32	- .28
1.031	+ .15		- .87	- .38	- .19	+ .37	- .37
1.005	+ .03		- .92	- .36	- .23	+ .37	- .27
0.976	+ .09		- .92	- .38	- .28	+ .42	- .37
0.962	+ .10		- .99	- .38	- .24	+ .39	- .33
0.926	+ .02		-1.14	- .47	- .42	+ .38	- .30

These monochromatic color excesses are listed in Table 8. Finally, the monochromatic color excesses were normalized to a color excess of 0.50 magnitudes at $\lambda^{-1} = 2.4$:

$$\mathcal{E}(\lambda^{-1}) = \frac{E(\lambda^{-1})}{2E(2.4)} \quad . \tag{7}$$

The monochromatic reddening curves, $\mathcal{E}(\lambda^{-1})$, are listed in Table 9.

The choice of the λ 5556, or $\lambda^{-1} = 1.8$, as the point with respect to which to refer the colors was dictated by the fact that among the points common to the two photomultiplier ranges it was the only one which was high enough on both response curves to yield consistently high precision neasurements. The selection of the 2.4 (λ 4167) point for the normalization was motivated by the facts that this point is near the maximum sensitivity of the spectrophotometric system in the blue, is in a spectral region well removed from the strong atomic absorption lines and showed a consistently small scatter with respect to a smooth curve through it and the adjacent points. Furthermore the minimum monochromatic color excesses observed at this point were very near the convenient figure of 0.50 magnitudes so that this mode of normalization would not tend to scale up scatter or systematic errors.

In addition to the errors in the spectrophoto-

Table 8

MONOCHROMATIC COLOR EXCESSES OF H II REGION STARS

λ^{-1}	HD5005ABC (.126,4.0)	HD15570 (.132,4.0)	HD15629 (.132,4.0)	HD17505 (.132,4.0)	HDE237015 (.21,4.0)	HD37030 (.21,4.0)	HD37022 (.126,4.0)
2.950	+ .90	+1.72	+1.52	+1.44	+1.24	+ .42	+ .80
2.900	.86	1.62	1.45	1.39	1.17	.36	.75
2.850	.83	1.58	1.41	1.34	1.16	.39	.74
2.800	.80	1.53	1.35	1.29	1.11	.40	.70
2.750	.76	1.48	1.30	1.23	1.06	.38	.70
2.700	.74	1.43	1.27	1.23	1.30	.67	.70
2.589	.79	1.41	1.27	1.20	1.03	.63	.68
2.480	.60	1.20	1.08	1.01	.77	.46	.55
2.400	.55	1.11	.98	.91	.71	.47	.53
2.350	.51	1.05	.90	.84	.64	.43	.47
2.240	.42	.89	.76	.71	.57	.41	.44
2.190	.37	.81	.70	.64	.51	.34	.36
2.090	.30	.66	.58	.51	.41	.26	.30
2.000	.21	.47	.45	.37	.31	----	.23
1.900	+ .12	+ .24	+ .20	+ .21	+ .12	+ .11	+ .12
1.800	0.00	0.00	0.00	0.00	0.00	0.00	0.00
1.712	- .09	- .17	- .16	- .12	- .20	- .08	- .11
1.652	.12	.33	.28	.22	.34	.14	.14
1.570	.22	.46	.33	.31	.26	.18	.24
1.471	.31	.78	.54	.52	.39	.38	.43
1.408	.39	.95	.66	.60	.43	.39	.41
1.328	.55	1.15	.81	.74	.52	.53	.46
1.274	.70	1.27	.91	.83	.57	.51	.57
1.238	.57	1.34	.95	.93	.65	.60	.61
1.190	.69	1.50	1.08	1.00	.61	.65	.69
1.136	.72	1.55	1.07	1.01	.65	.68	.70
1.031	.81	1.86	1.39	1.24	.85	.94	.87
1.005	.91	1.93	1.35	1.29	.84	.93	.97
0.976	.89	2.00	1.48	1.33	.94	1.00	.99
0.962	.91	1.99	1.43	1.32	.91	.99	1.02
0.926	- .65	-2.10	-1.17	-1.32	- .94	-1.03	-1.08

Table 8, Continued

λ^{-1}	HD37023 (.18,4.0)	HD42088 (.126,4.0)	HD46150 (.112,4.0)	HD46485 (.140,4.0)	HD164492 (.148,4.0)	HD164492 (.140,4.0)
2.950	+ .65	+ 87	+1.02	+1.40	+ .62	+ .85
2.900	.59	.77	.88	1.34	.63	.74
2.850	.60	.79	.93	1.25	.60	.73
2.800	.61	.76	.92	1.24	.59	.68
2.750	.58	.72	.87	1.16	.60	.67
2.700	.79	.73	.83	1.20	.66	.73
2.589	.73	.71	.85	1.14	.49	.73
2.480	.53	.59	.70	.97	.51	.52
2.400	.54	.54	.65	.89	.47	.46
2.350	.49	.49	.61	.83	.43	.42
2.240	.45	.44	.51	.74	.39	.34
2.190	.37	.36	.45	.60	.36	.31
2.090	.28	.30	.36	.49	.24	.26
2.000	.09	.20	.23	.31	.18	.18
1.900	+ .11	+ .08	+ .10	+ .16	+ .10	+ .08
1.800	0.00	0.00	0.00	0.00	0.00	0.00
1.712	- .14	- .11	- .09	- .13	- .08	- .13
1.652	.21	.13	.19	.21	.14	.16
1.570	.28	.20	.25	.40	.21	.24
1.471	.47	.32	.40	.49	.29	.37
1.408	.52	.36	.50	.57	.37	.40
1.328	.61	.41	.53	.82	.37	.52
1.274	.70	.47	.59	.81	.51	.55
1.238	.72	.45	.63	.83	.49	.54
1.190	.81	.50	.74	.94	.51	.58
1.136	.80	.57	.75	.92	.57	.64
1.031	.96	.69	.96	1.08	.76	.74
1.005	1.02	.78	.92	1.17	.94	.83
0.976	1.08	.71	.98	1.18	.86	.89
0.962	1.21	.76	.97	1.18	.84	.88
0.926	-1.30	.83	-1.22	-1.40	- .97	- .92

Table 8, Continued

λ^{-1}	Herschel36 (.126,4.0)	NGC6618A (.112,4.0)	NGC6618C (.21,4.0)	HD200775 (.32,4.0)	HD215835 (.112,4.0)	HD200775 (.25,3.8)	BD+60°2522 (.112,4.0)
2.950	+1.81	+2.79	+1.65		+1.46	+ .54	+1.49
2.900	1.73	2.70	1.76		1.38	.51	1.43
2.850	1.67	2.78	1.75		1.34	.50	1.39
2.800	1.57	2.59	1.66		1.29	.49	1.36
2.750	1.51	2.60	1.58		1.24	.46	1.30
2.700	1.47	2.46	1.77	+1.26	+1.20	.85	1.25
2.589	1.50	2.31	1.73	1.06	1.11	.63	1.27
2.480	1.27	2.04	1.46	.93	.97	.43	1.07
2.400	1.16	1.85	1.33	.72	.88	.36	.99
2.350	1.11	1.74	1.21	.67	.82	.35	.94
2.240	.92	1.44	1.03	.57	.69	.33	.78
2.190	.80	1.29	.89	.49	.62	.26	.71
2.090	.65	1.05	.77	.41	.50	.22	.57
2.000	.44	.66	.49	.30	.33	.17	.42
1.900	+ .20	+ .31	+ .29	+ .13	+ .15	+ .06	+ .19
1.800	0.00	0.00	0.00	0.00	0.00	0.00	0.00
1.712	- .22	- .40	- .23	- .13	- .13	- .07	- .19
1.652	.28	.31	.24	.24	.32	.11	.26
1.570	.62	.77	.40	.37	.41	.15	.43
1.471	.88	1.24	.66	.55	.67	.25	.59
1.408	1.02	1.37	.81	- .66	.67	.27	.71
1.328	1.22	1.60	1.01		.75	.31	.84
1.274	1.43	-1.73	1.13		.86	.34	.94
1.238	1.50		1.23		.88	.36	1.00
1.190	1.75		1.28		1.07	.31	1.14
1.136	1.91		1.47	- .84	1.06	.36	1.15
1.031	2.05		1.78	1.16	1.26	.49	1.44
1.005	2.35		1.89	1.18	1.35	.53	1.39
0.976	2.62		1.94	1.24	1.46	.54	1.55
0.962	2.81		2.04	1.26	1.45	.59	1.54
0.926	-3.02		-2.26	1.42	-1.70	- .68	-1.58

Table 9

NORMALIZED MONOCHROMATIC REDDENING CURVES OF H II REGION STARS

λ^{-1}	HD5005ABC NGC281	HD15570 IC1805	HD15629 IC1805	HD17505 IC1848	HDE237015 IC1848	HD37020 NGC1976	HD37022 NGC1976
2.950	+ .82	+ .77	+ .78	+ .79	+ .87	+ .45	+ .75
2.900	.78	.73	.74	.76	.82	.38	.71
2.850	.75	.71	.72	.74	.82	.41	.70
2.800	.73	.69	.69	.71	.78	.43	.66
2.750	.69	.67	.66	.68	.75	.40	.66
2.700	.67	.64	.65	.68	.92	.71	.66
2.589	.72	.64	.65	.66	.72	.67	.64
2.480	.55	.54	.55	.55	.54	.49	.52
2.400	.50	.50	.50	.50	.50	.50	.50
2.350	.46	.47	.46	.46	.45	.46	.44
2.240	.38	.40	.39	.39	.40	.44	.42
2.190	.34	.36	.36	.35	.36	.36	.34
2.090	.27	.30	.30	.28	.29	.28	.28
2.000	.19	.21	.23	.20	.22	.00	.22
1.900	+ .11	+ .11	+ .10	+ .12	+ .08	+ .12	+ .11
1.800	0.00	0.00	0.00	0.00	0.00	0.00	0.00
1.712	- .08	- .07	- .08	- .07	- .14	- .09	- .10
1.652	.11	.15	.14	.12	.24	.15	.13
1.570	.20	.21	.17	.17	.18	.19	.23
1.471	.28	.35	.28	.29	.27	.40	.41
1.408	.35	.43	.34	.33	.30	.41	.39
1.328	.50	.52	.41	.41	.37	.56	.43
1.274	.64	.57	.46	.46	.40	.54	.54
1.238	.52	.60	.48	.51	.46	.64	.58
1.190	.63	.68	.55	.55	.43	.69	.65
1.136	.65	.70	.55	.55	.46	.72	.66
1.031	.74	.84	.71	.68	.60	1.00	.82
1.005	.83	.87	.69	.71	.59	.99	.91
0.976	.81	.90	.76	.73	.66	1.06	.93
0.962	.83	.89	.73	.73	.64	1.05	.96
0.926	- .59	- .95	- .60	- .73	- .66	-1.10	-1.02

Table 9, Continued

λ^{-1}	HD37023 NGC1976	HD42088 NGC2174,75	HD46150 NGC2244	HD46485 NGC2244	HD164492 NGC6514	HD164492a NGC6514	Herschel36 NGC6523
2.950	+ .60	+ .81	+ .78	+ .78	+ .66	+ .92	+ .78
2.900	.55	.71	.68	.75	.67	.80	.75
2.850	.56	.73	.72	.70	.64	.79	.72
2.800	.56	.70	.71	.70	.63	.74	.68
2.750	.54	.67	.67	.65	.64	.73	.65
2.700	.73	.68	.64	.67	.70	.79	.63
2.589	.67	.66	.65	.64	.52	.79	.65
2.480	.49	.55	.54	.54	.54	.57	.55
2.400	.50	.50	.50	.50	.50	.50	.50
2.350	.45	.45	.47	.47	.46	.46	.48
2.240	.41	.41	.39	.42	.41	.37	.40
2.190	.34	.33	.35	.34	.38	.34	.34
2.090	.26	.28	.28	.28	.26	.28	.28
2.000	.08	.19	.18	.17	.19	.20	.19
1.900	+ .10	+ .07	+ .08	+ .09	+ .11	+ .09	+ .09
1.800	0.00	0.00	0.00	0.00	0.00	0.00	0.00
1.712	- .13	- .10	- .07	- .07	- .09	- .14	- .09
1.652	.19	.12	.15	.12	.15	.17	.12
1.570	.26	.19	.19	.22	.22	.26	.27
1.471	.43	.30	.31	.28	.31	.40	.38
1.408	.48	.33	.38	.32	.39	.43	.44
1.328	.56	.38	.41	.46	.39	.56	.53
1.274	.65	.44	.45	.46	.54	.60	.62
1.238	.67	.42	.48	.47	.52	.59	.65
1.190	.75	.46	.57	.53	.54	.63	.75
1.136	.74	.53	.58	.52	.61	.70	.82
1.031	.89	.64	.74	.61	.81	.80	.88
1.005	.94	.72	.71	.66	1.00	.90	1.01
0.976	1.00	.66	.75	.66	.91	.97	1.13
0.962	1.12	.70	.75	.66	.89	.96	1.21
0.926	-1.20	- .77	- .94	- .79	-1.03	-1.00	-1.30

Table 9, Continued

λ^{-1}	Annon.A NGC6618	Annon.C NGC6618	HD200775 NGC7023	HD215835 NGC7380	HD220057 NGC7635	BD+60°2522 NGC7635
2.950	+ .75	+ .62		+ .83	+ .75	+ .75
2.900	.73	.66		.78	.71	.72
2.850	.75	.66		.76	.69	.70
2.800	.70	.62		.73	.68	.69
2.750	.70	.59		.70	.64	.66
2.700	.66	.66	+ .87	.68	1.18	.63
2.589	.62	.65	.74	.63	.87	.64
2.480	.55	.54	.65	.55	.60	.54
2.400	.50	.50	.50	.50	.50	.50
2.350	.47	.45	.47	.47	.49	.47
2.240	.39	.39	.40	.39	.46	.39
2.190	.35	.33	.34	.35	.36	.36
2.090	.28	.29	.28	.28	.31	.29
2.000	.18	.18	.21	.19	.24	.21
1.900	+ .08	+ .11	+ .09	+ .09	+ .08	+ .09
1.800	0.00	0.00	0.00	0.00	0.00	0.00
1.712	- .11	- .09	- .09	- .07	- .10	- .10
1.652	.08	.09	.17	.18	.15	.13
1.570	.21	.15	.26	.23	.21	.22
1.471	.34	.25	.38	.38	.35	.30
1.408	.37	.30	- .46	.38	.38	.36
1.328	.43	.38		.43	.43	.42
1.274	- .47	.42		.49	.47	.47
1.238		.46		.50	.50	.50
1.190		.48		.61	.43	.58
1.136		.55	- .58	.60	.50	.58
1.031		.67	.81	.72	.68	.72
1.005		.71	.82	.77	.74	.70
0.976		.73	.86	.83	.75	.78
0.962		.77	.87	.82	.82	.78
0.926		- .85	- .98	- .97	- .94	- .80

metry which have been discussed previously, error may arise in the determination of the two-color excesses of equation (7) from the errors in the model colors. These errors are of two types, errors in the determination of the model colors, and errors in the selection of models with which to represent intrinsic colors. This latter error, once made, is systematic in nature while the others are purely random. However, since the uncertainty occurs in the choice of the model which could be in error in either direction, this error was included as if it were purely random. To estimate the cumulative effects of the various sources of error, the following procedure was followed. Independent determinations of several model colors on different occasions indicated that the precision of the graphical interpolation process was about 0.01 magnitudes and this value was adopted as a minimum error in the model colors. To estimate the effects of incorrect model choice, the variation in the colors at λ^{-1} points 2.4 and 1.005 between the chosen model and those adjacent to it in temperature were determined from Table 5. In those cases where the model choice was based upon data from the present study which was corroborated by other studies, this difference between adjacent models was adopted as the probable error in the model determination. When the selection was

based solely upon the spectral types found in this study or when those spectral types were considerably different from those of other investigators, twice the normal value was assumed as the probable error. Finally, the net effect of all the various sources of error upon the normalized extinction $\mathcal{E}$ (1.005) was computed for each star according to the formulae given by Beers (1962). These cumulative errors are listed in the final column of Table 1 and are indicated by the error bars on the various figures. The numbers in parentheses in Table 1 are the contribution to the error of the uncertainty in the model choice. The cumulative errors range from ± 0.04 to ± 0.17 magnitudes with an average of ± 0.077. The model choice errors range from ± 0.014 to ± 0.165 with an average value of ± 0.047.

III.3 Individual Objects

In this section the individual objects will be discussed. Commented upon will be the reasons for selection of the nebulae and the stars therein, the spectroscopic and spectrophotometric observations of each star, the choice of a representative model for each star and the characteristics of the reddening curves obtained.

NGC 281

Although this nebula is of rather low surface brightness, it was chosen for study because of its

symmetry about the exciting stars and because of the numerous dust lanes and patches which mark its surface. Furthermore, the appearance of the D-plate (continuum) seemed to suggest a distribution of exposure which was unlike that on the O- and E-plates somewhat like the situation reported for IC 405 by Herbig (1958). This might indicate the existence of considerable dust and thus reddening interior to the nebula.

The Sharpless catalogue lists only one star for this nebula, HD 5005. This object is, however, a multiple system and is number 719 in the catalogue of double stars of Aitken (1932) which lists five components. The Henry Draper spectral type is given as B2, but the more recent work of Morgan, Code and Whitford (1955) indicates a spectral type of 06 which was adopted for this study. During spectrophotometric observations it was impossible to isolate the O-star because of the closeness of two of the components (B and C in the Aitken catalogue). However, these two stars were both more than a magnitude fainter than the primary and thus an entrance aperture large enough to insure their consistent inclusion was used. Numerical experiments in the construction of composite models were conducted and it was found that stars of the magnitude differences involved here did not cause detectable changes in the colors of the primary. Thus the schedule of Table 5 was followed in the selection of

the representative model colors.

The apparent spectral energy distribution of HD 5005 is shown in Figure 1. The observed Balmer discontinuity is quite small as would be expected from the early spectral type; indeed both temperature selection criteria indicate the same effective temperature. The monochromatic reddening curve is shown in Figure 2. In this figure (as in all the monochromatic reddening curves to follow) the normalized extinction curve is compared with the extinction curves for the Orion Nebula (dashed curve) and for the average of 28 stars in Cygnus, Cepheus, Perseus, and Monoceros (solid curve) as given by Whiteoak (1966). As can be seen, the most critical region for the distinction of the normal and anomalous reddening curves is in the infrared near a wavelength of one micron. At λ^{-1} 1.005 the field and Orion Nebula curves are defined to within an estimated probable error of $\pm$0.03 magnitudes. The reddening curve for NGC 281 seems to be distinctly different from that of the field stars but not so anomalous as that in the Orion Nebula. As a quantative indication of the degree of the extinction anomaly we shall adopt the normalized color excess at the point λ^{-1} 1.000 as found from a smoothed curve drawn through the points in the vicinity of one micron by inspection. In the case of HD 5005 this extinction criterion, $\mathcal{E}$ (1.0), is -0.80$\pm$0.09 whereas the similar numbers for the field

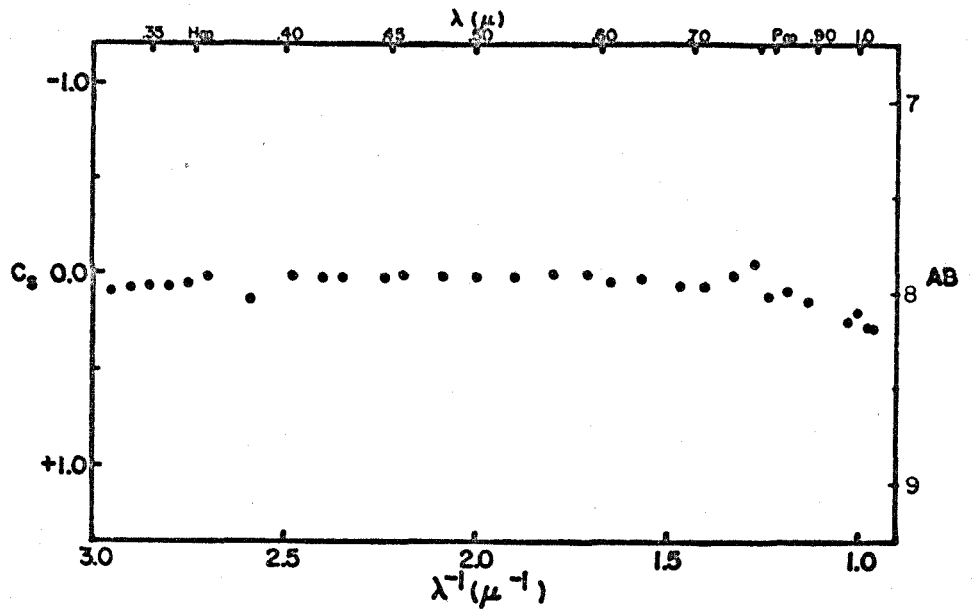

Fig. 1. Monochromatic colors, C_s, and magnitudes, AB, as a function of frequency (in units of reciprocal microns) for the star HD 5005 in NGC 281.

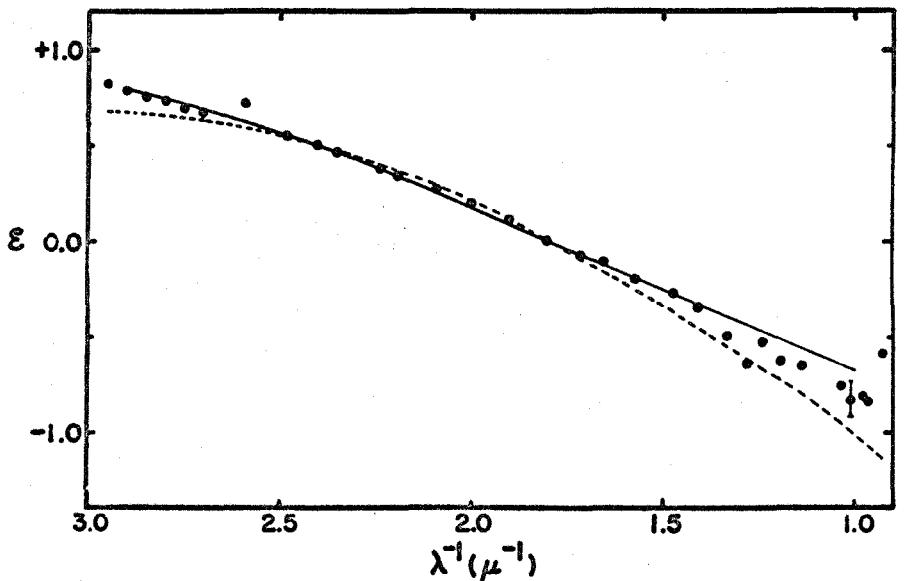

Fig. 2. The monochromatic reddening curve for HD 5005 in NGC 281 (filled circles). Also shown are the reddening curves for the field (solid line) and for the Orion Trapezium (dashed line) according to Whiteoak (1966).

and for the Orion Nebula are -0.67 and -1.01 respectively.

IC 1805

This very complicated nebular structure was chosen largely because of the abundance of early-type stars which are associated with it. The Sharpless catalogue lists eight associated early-type stars for this object. From this list two were chosen; HD 15629 was chosen because it seemed to be most nearly associated with a condensation in that region of the very large nebulosity. HD 15570, on the other hand, was chosen because it did not seem to be directly associated with such a condensation. This latter star was classified in the present study as 07f upon the basis of the strengths of the He I and He II lines of which λ4686 was clearly in emission. Previous authors (Morgan, Code and Whitford, 1955 and Hiltner, 1956) classified this star as 05f. Since the difference in colors for the two spectral types were negligible, the type from the present study was used. HD 15629 was also classified as 07 in the present study and as 05 in the previously mentioned studies. The results of the spectrophotometric observations are shown in Figures 3 and 5. The monochromatic reddening curves as shown in Figures 4 and 6. Both of these stars have very small Balmer discontinuities and both have rather large color excesses. The normalized extinction for

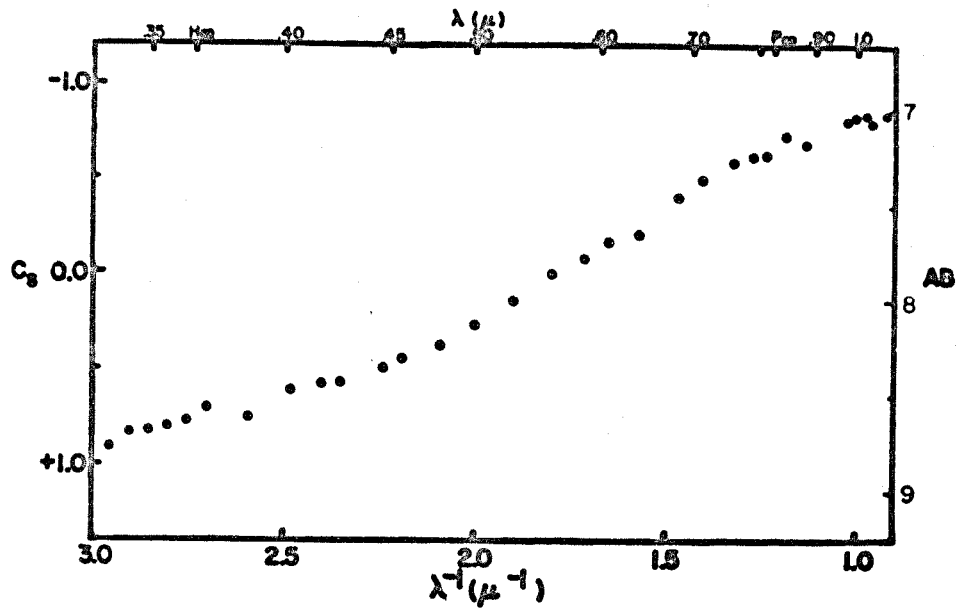

Fig. 3. Monochromatic colors, C_s, and magnitudes, AB, for HD 15570 in IC 1805.

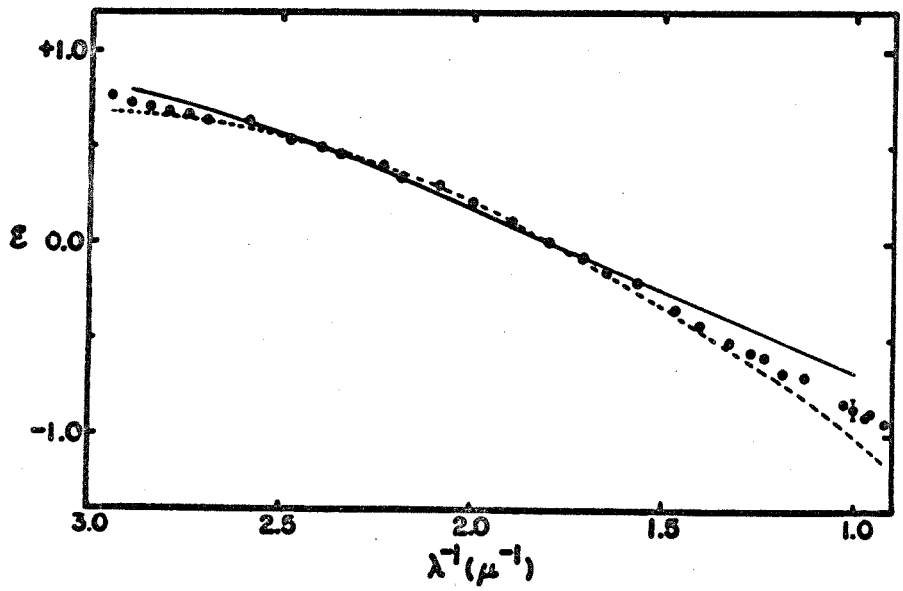

Fig. 4. The monochromatic reddening curve for HD 15570 in IC 1805.

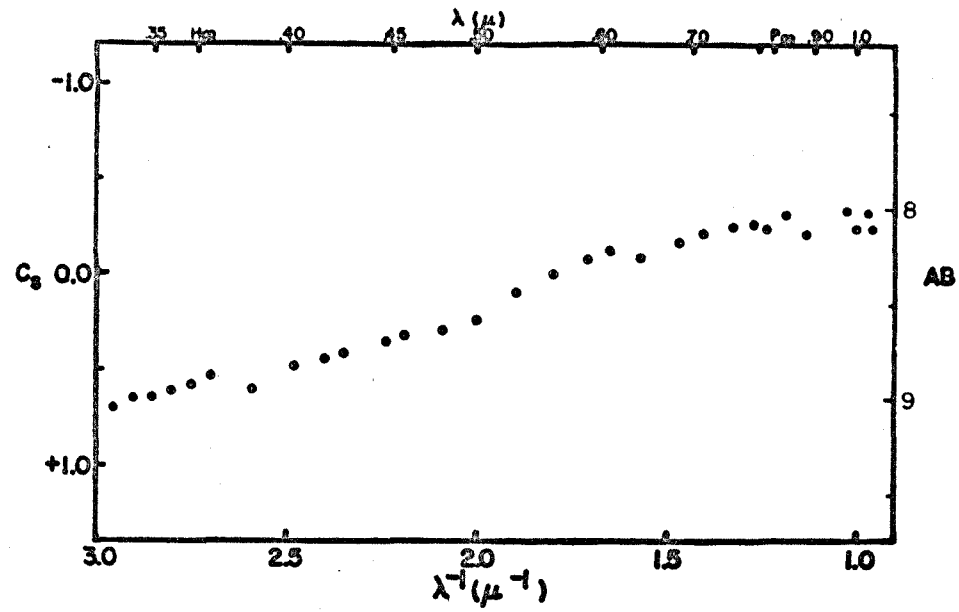

Fig. 5. Monochromatic colors, C_s, and magnitudes, AB, for HD 15629 in IC 1805.

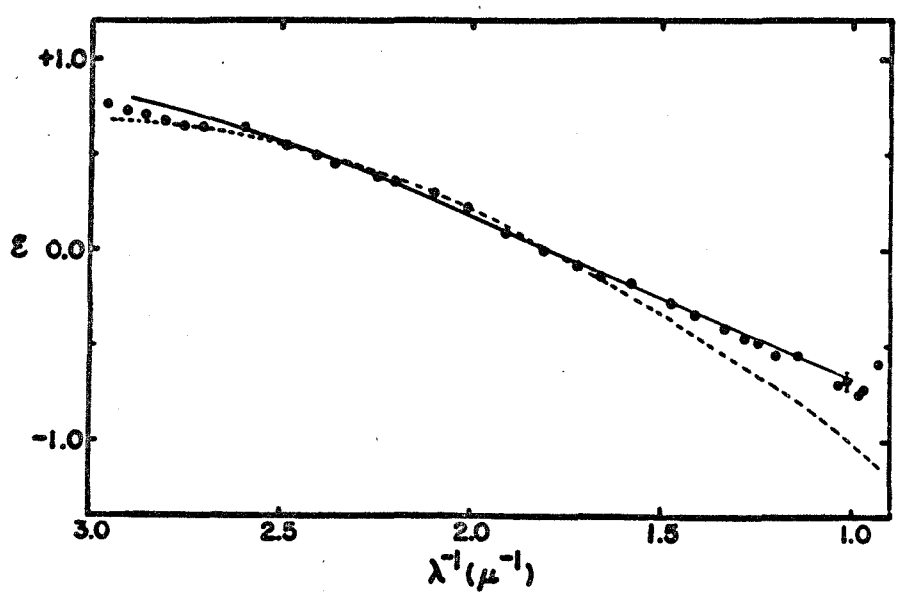

Fig. 6. The monochromatic reddening curve for HD 15629 in IC 1805.

HD 15570 seems to be very much like that of HD 5005 in that its $\mathcal{E}$ (1.0) is -0.86±0.05 while the star HD 15629, with $\mathcal{E}$ (1.0) of -0.72±0.04, seems to be more nearly like the field in its reddening curve. In connection with these stars it is interesting to note that the star which was picked because it was not associated with nebular condensations has a larger color excess and more nearly Orion-like reddening curve than the star which was chosen for just such an association.

IC 1848

Like IC 1805, this nebula has a rather low surface brightness and a very complex structure. It was also chosen because of the large number of associated early-type stars of which nine are listed by Sharpless. Of these, two were chosen for spectrophotometric observation. HD 17505 is the brightest star in the cluster of stars within the nebula and is situated near the center of a condensation which can best be seen on the blue Sky Survey plate. This star was classified as 07 in the present study, which is in agreement with several other classifications. Also observed was HDE 237015 which appears to be in a region of somewhat less concentrated nebulosity than HD 17505. HDS 237015 was classified as B1V which implies a temperature in very good agreement with that deduced from the Balmer discontinuity. The spectrophotometric data for these two stars are shown in Figures 7 and 9, and the

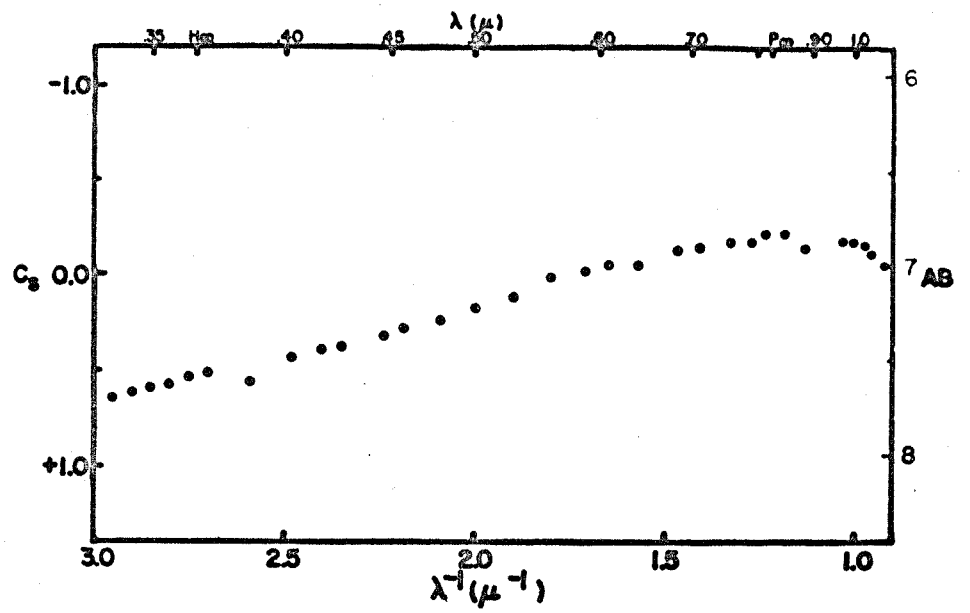

Fig. 7. Monochromatic colors, C_s, and magnitudes, AB, for HD 17505 in IC 1848.

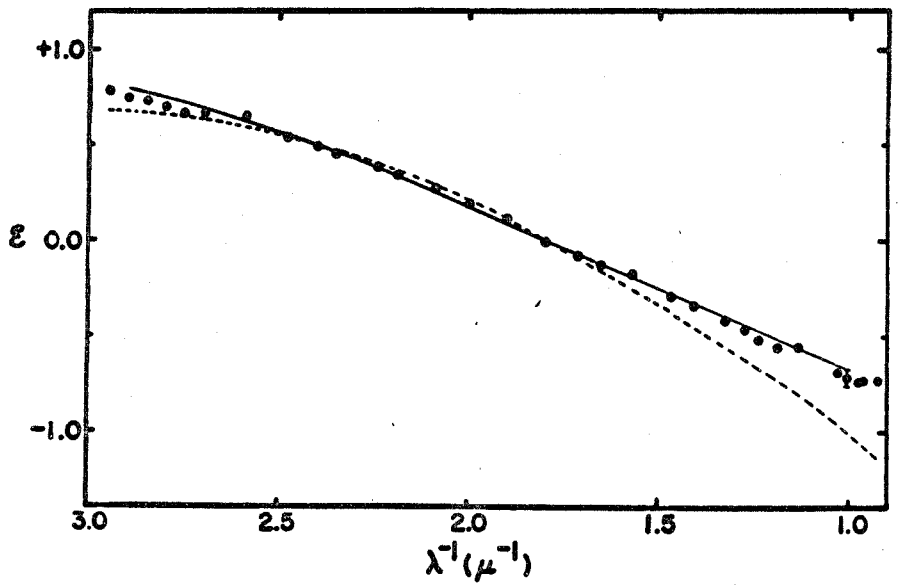

Fig. 8. The monochromatic reddening curve for HD 17505 in IC 1848.

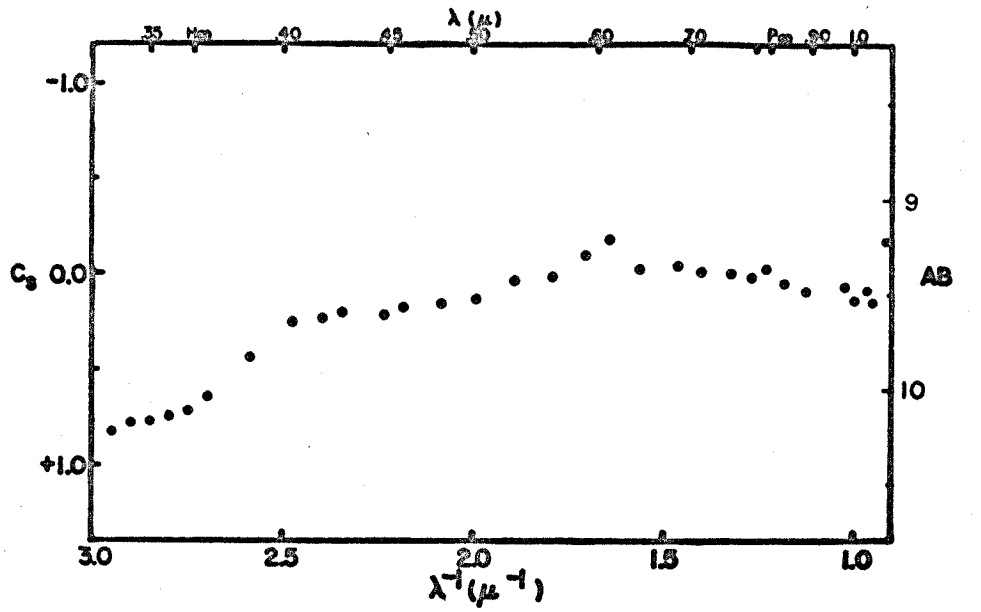

Fig. 9. Monochromatic colors, C_s, and magnitudes, AB, for HDE 237015 in IC 1848.

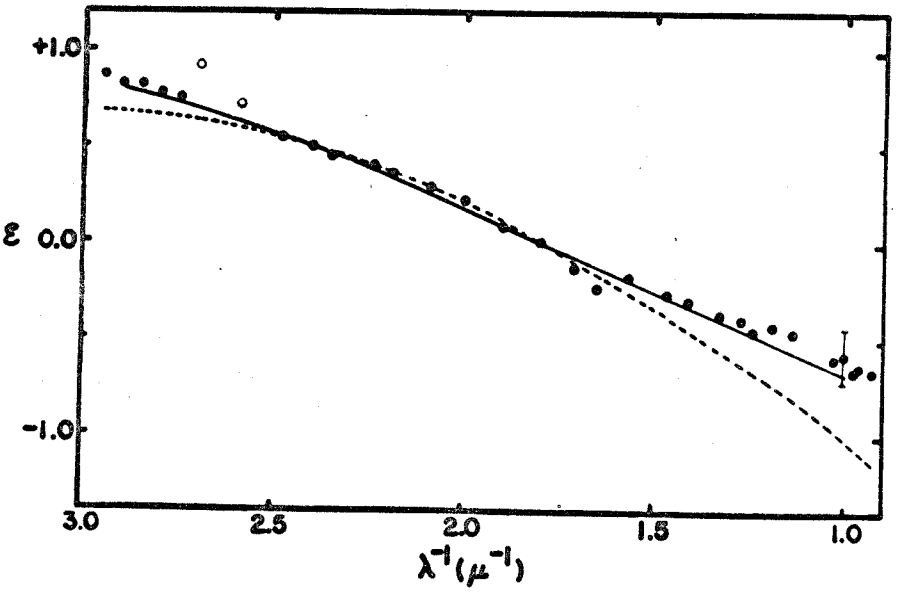

Fig. 10. The monochromatic reddening curve for HDE 237015 in IC 1848.

normalized reddening curves are given in Figures 8 and 10. Both of these stars seem to be quite field-like in their reddening curves and have normalized one micron extinctions of -0.70 ± 0.04 and -0.62 ± 0.14 for HD 17505 and HDE 237015 respectively.

NGC 1976

The Orion Nebula was reobserved in order to check the agreement of the reddening curves of the present study with those found by Whiteoak (1966). Of the stars in the Trapezium spectrophotometric observations were obtained for HD 37020 (θ^1Ori A), HD 37022 (θ^1Ori C), and HD 37023 (θ^1Ori D). The spectral types of these objects are B1 (Sharpless, 1952), O6p and BO.5Vp (Borgmann, 1960) respectively. The results of the spectrophotometry of these stars are shown in Figures 11, 13 and 15 while the monochromatic normalized reddening curves are given in Figures 12, 14 and 16. As can be seen from these latter figures the agreement of the reddening curves of the present study with those of Whiteoak is quite good. The one-micron normalized extinction found in this investigation had an average of -0.97 ± 0.07 against the previously quoted value of -1.01 from the Whiteoak data. This result is taken as an indication that the present system of monochromatic reddening curves is essentially the same as that used by Whiteoak and thus the comparison of the reddening curves herein derived with those of

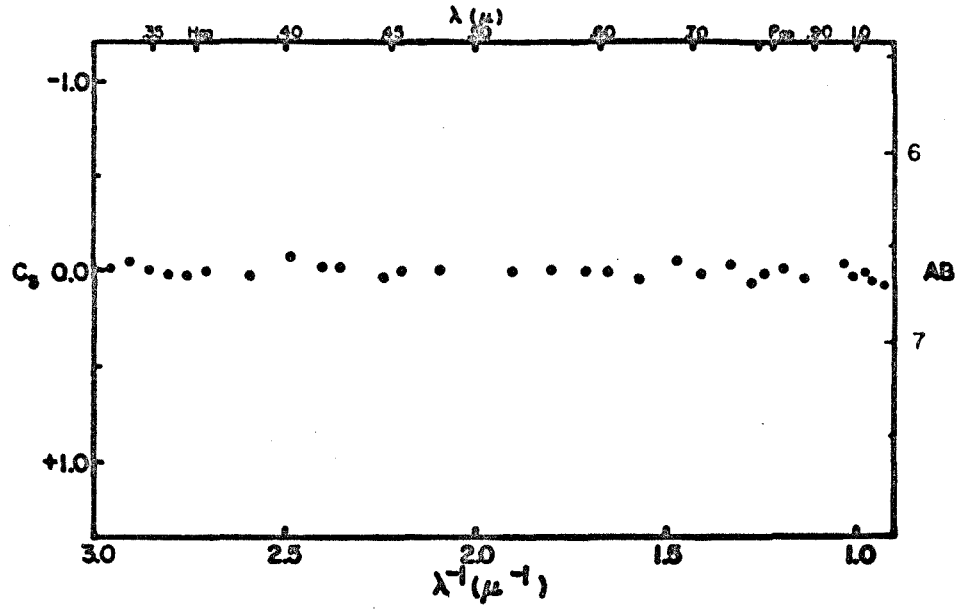

Fig. 11. Monochromatic colors, C_s, and magnitudes, AB, for HD 37020 in NGC 1976 (the Orion Nebula).

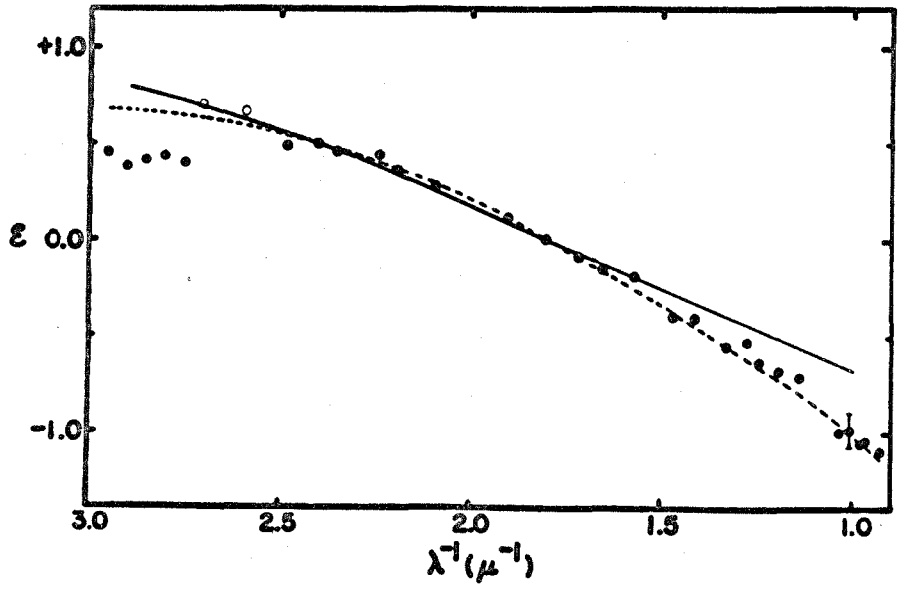

Fig. 12. The monochromatic reddening curve for HD 37020 in NGC 1976.

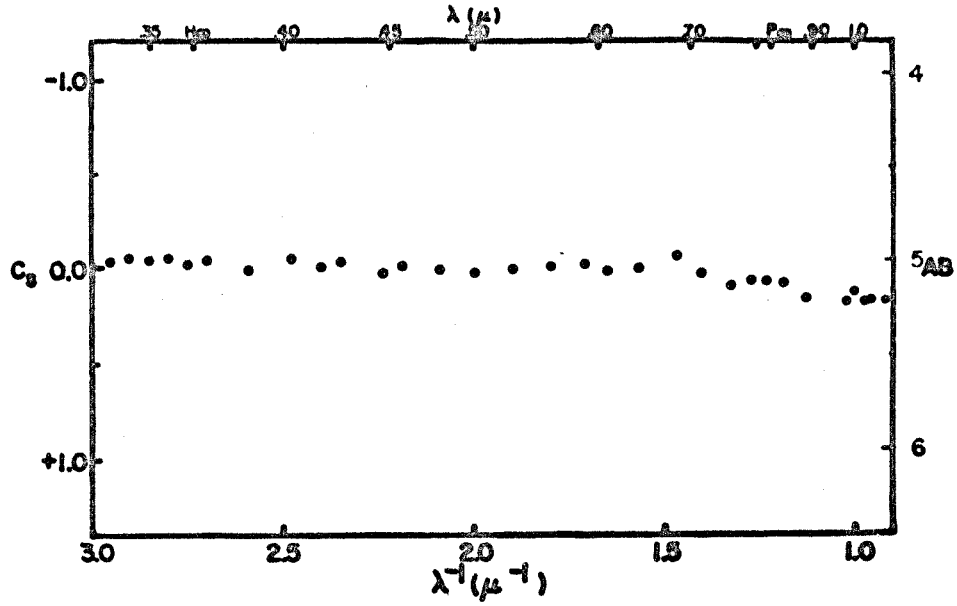

Fig. 13. Monochromatic colors, C_s, and magnitudes, AB, for HD 37022 in NGC 1976.

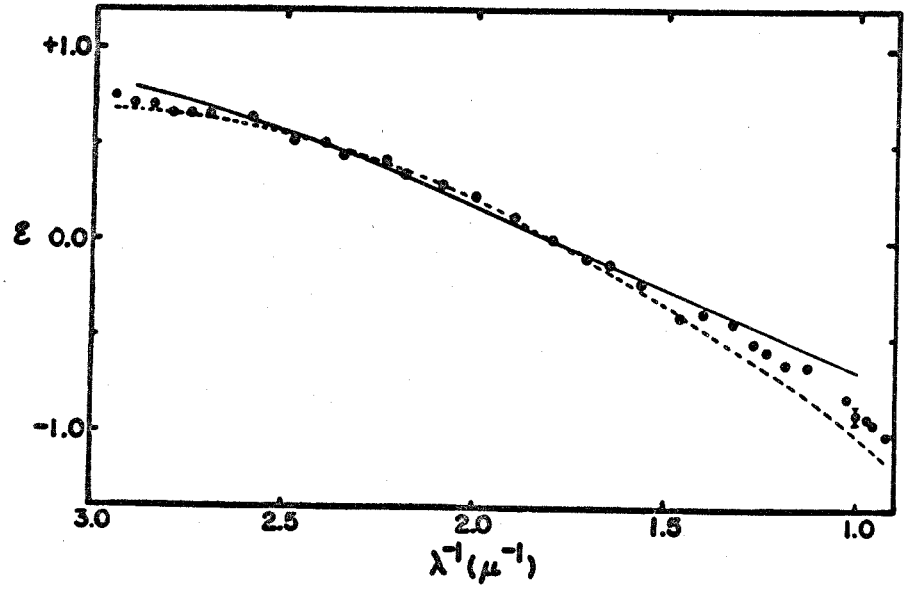

Fig. 14. The monochromatic reddening curve for HD 37022 in NGC 1976.

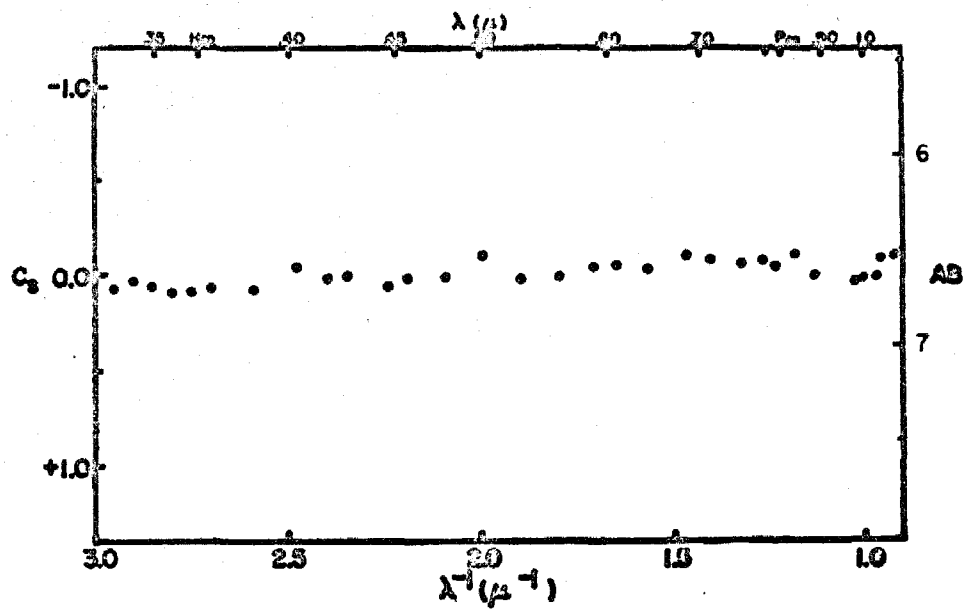

Fig. 15. Monochromatic colors, C_s, and magnitudes, AB, for HD 37023 in NGC 1976.

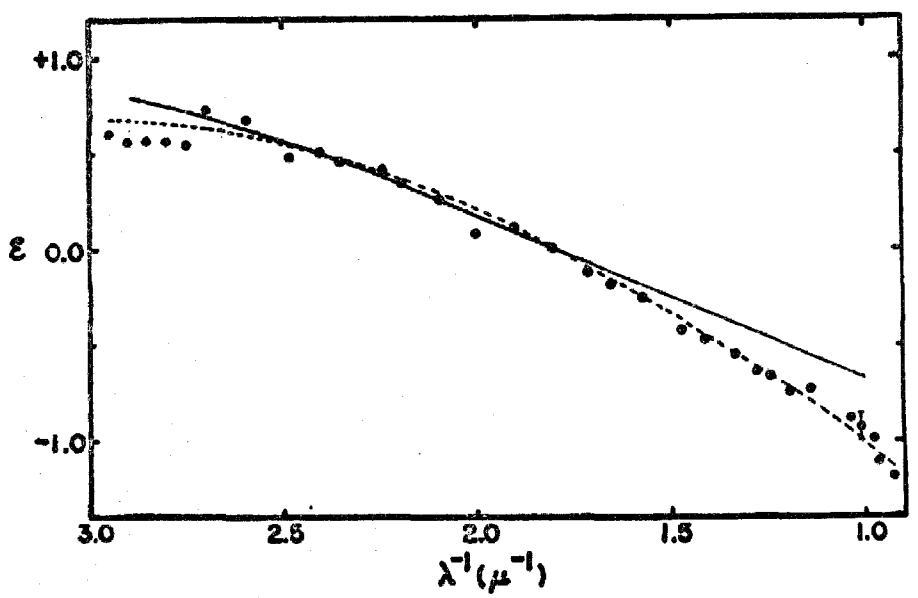

Fig. 16. The monochromatic reddening curve for HD 37023 in NGC 1976.

Whiteoak is a valid procedure for the determination of the degree of reddening anomaly found in the various nebulae.

NGC 2174, 75

This nebular complex is of medium surface brightness and has a relatively high degree of symmetry about the primary exciting star, HD 42088. The distribution of exposure on the continuum sensitive D-plate was noticeably different from that on the O- and E-plates which was taken as an indication of the presence of considerable dust within the nebula. Furthermore there is the report of Terzian (1965) that there is a density minimum near the center of the nebula which may be produced by the action of radiation pressure upon dust grains according to the scheme outlined by Mathews (1967). Of particular interest was the area immediately around the star BD +20°1288 which appeared much brighter on the D-plate than on the other two plates. Furthermore the color excess of this latter star is considerably greater than that of the former, $E(2.4) = 0.92$ for BD +20°1288 as opposed to 0.54 for HD 42088. Unfortunately infrared observations were not obtained for this star due to its faintness and the low sensitivity of the S-1 photomultiplier. The blue observations which were obtained are given in Appendix A. The spectrophotometric data

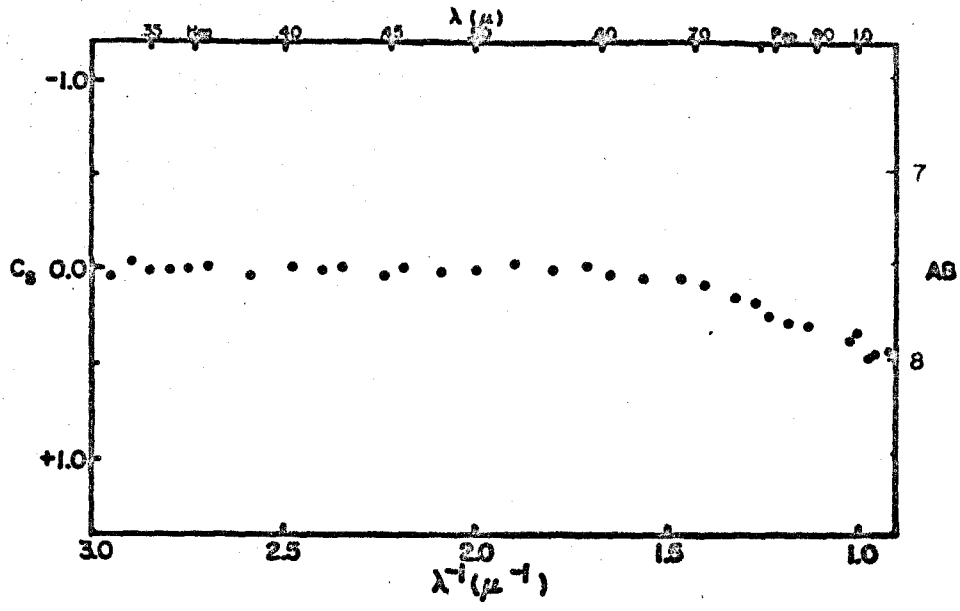

Fig. 17. Monochromatic colors, C_s, and magnitudes AB, for HD 42088 in NGC 2174, 75.

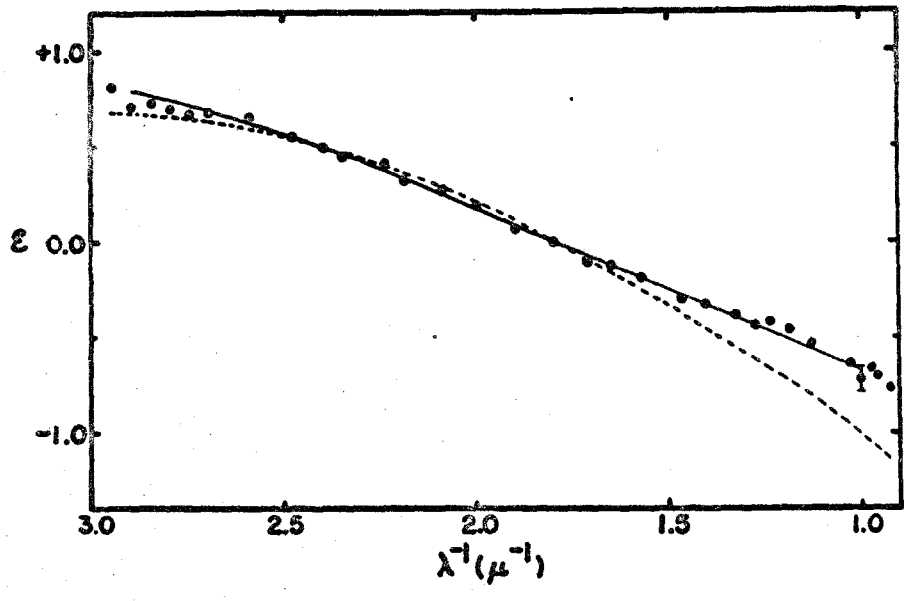

Fig. 18. The monochromatic reddening curve for HD 42088 in NGC 2174, 75.

for HD 42088 is given in Figure 17. This star was classified as 06 by Hiltner (1956) and the resultant normalized monochromatic reddening curve is shown in Figure 18. This curve is in good agreement with the field reddening curve and has a normalized one-micron extinction of -0.68±0.06.

NGC 2244

The Rosette Nebula is a medium surface brightness nebula with a high degree of symmetry about the cluster of very early type stars at its center, many of which are standards of these early spectral types. This nebula was of particular interest because of the suggestion of Mathews (1967) that the central "hole" could be produced by the action of radiation pressure upon the interstellar grains. Two stars in this nebula were observed photometrically. HD 46150 is one of the brightest stars in the central region of the nebula and has been classified as 05 by Morgan et al (1965). In the eastern side of the annulus of the Rosette is the star HD 46485 which has been classified by Hiltner (1956) as 08. The photoelectric data are shown in Figures 19 and 21, and the monochromatic reddening curves are given in Figures 20 and 22. The reddening curves of both of these stars appear to be quite normal or field-like. The values of the one micron normalized color excess are -0.74±0.05 and -0.66±0.05 for HD 46150 and HD 46485 respectively. This result is

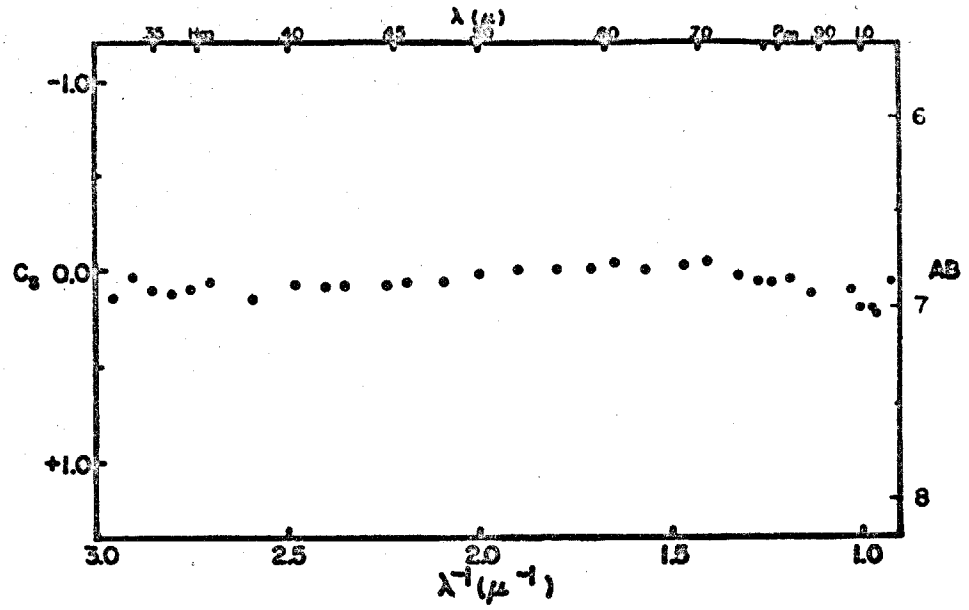

Fig. 19. Monochromatic colors, C_s, and magnitudes, AB, for HD 46150 in NGC 2244.

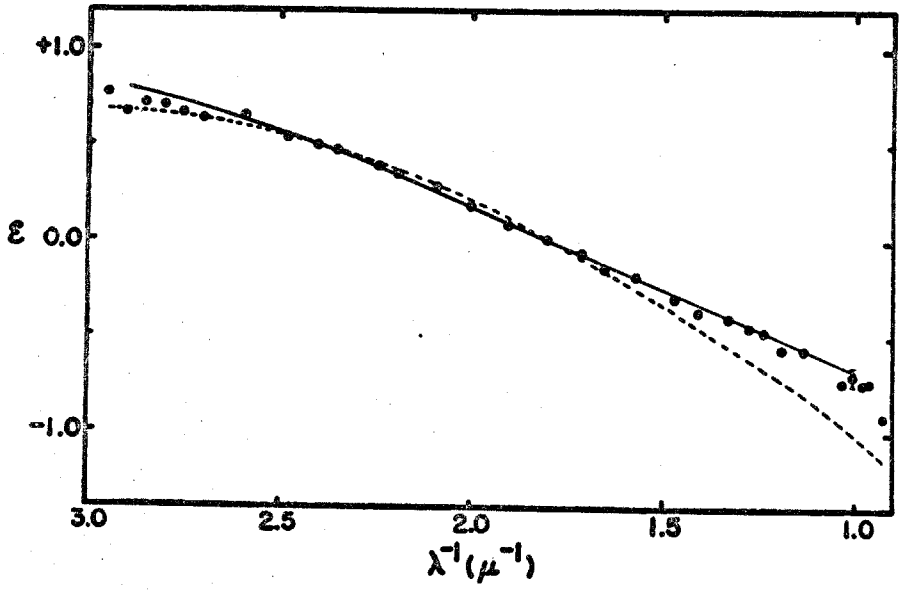

Fig. 20. The monochromatic reddening curve for HD 46150 in NGC 2244.

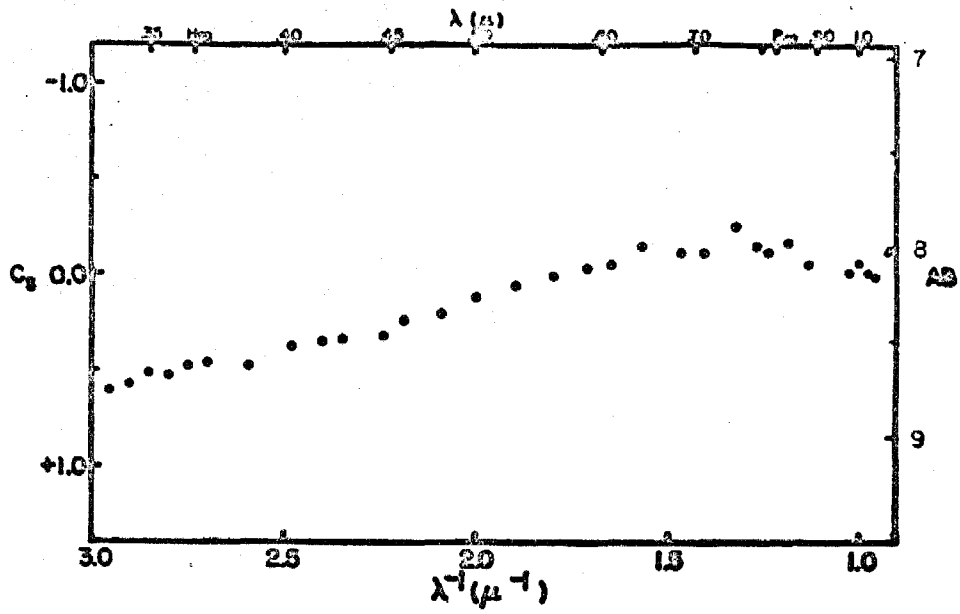

Fig. 21. Monochromatic colors, C_s, and magnitudes AB, for HD 46485 in NGC 2244.

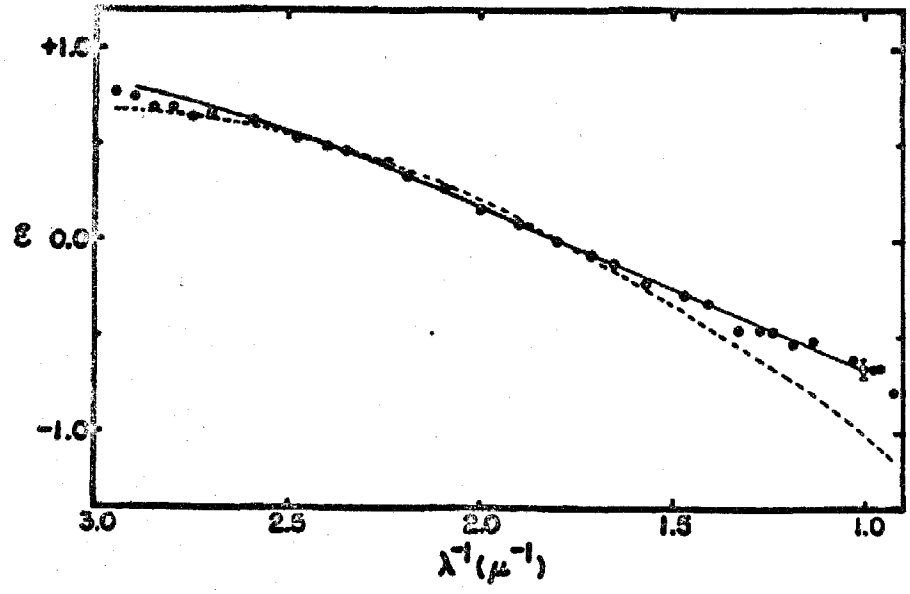

Fig. 22. The monochromatic reddening curve for HD 46485 in NGC 2244.

interesting in light of the recent result of Johnson (1965). By means of the variable extinction method, Johnson has obtained a ratio of total to selective extinction of 6, similar to that which he finds for the Orion region. If both of these results are correct, then the anomalous behaviour of the Rosette region is of an entirely different type than that of the Orion Nebula. The Johnson result is, it should be noted, based upon a very small range of extinction ($\Delta E_{B-V} \approx 0^m.2$) over the face of the nebula and a rather large amount of scatter (Δ V-M_V = $1^m.1$ at E_{B-V} = 0.4) in the apparent distance modulus is evident in Figure 6 of the Johnson paper. Thus the anomality of the reddening in this region should be considered highly questionable in the light of the results of the present study. With respect to the previously mentioned suggestion of Mathews, it is interesting to note that the color excess of the star HD 47485, which is in the periphery of the nebular annulus, is 14 percent greater than the color excess of the star HD 46150, which is situated at the center of the nebula. This observation is consistent with the idea that the dust has been swept from the central region of the nebula and has swept along the gas by virtue of the charge on the dust grains which couples the plasma to the dust. The relevance of this observation depends upon

the position of HD 46485 within the nebula and should thus be taken only as a consistency check and not as proof of the validity of the Mathews process.

NGC 6514

The Trifid Nebula, M20, is one of the highest surface brightness objects which was observed. Its image was highly exposed on all of the standard plates taken in the present study. The nebula is quite symmetrical about the central stars and there are numerous dust lanes across the surface in addition to a region of general extinction surrounding the nebula. This latter region is taken by O'Dell, Hubbard, and Peimbert (1966) to be an indication of the fact that this nebula is an ionization bounded H II region. They further deduced that this nebula has a low "gas to dust ratio" by means of a comparison of the fluxes in the nebular continuum and in the nebular H_β line. The central star of this system is HD 164492. This star is actually a multiple system designated ADS 10991 in the Aitken Double Star Catalogue which lists seven components, two of which (ADS 10991 A and ADS 10991 C) contribute about 90 percent of the light of the system. Because of the proximity of several of the components of the system, spectrophotometric observations of the individual stars could be obtained only in the best of seeing conditions. Indeed, a complete set of such observations was obtained for only

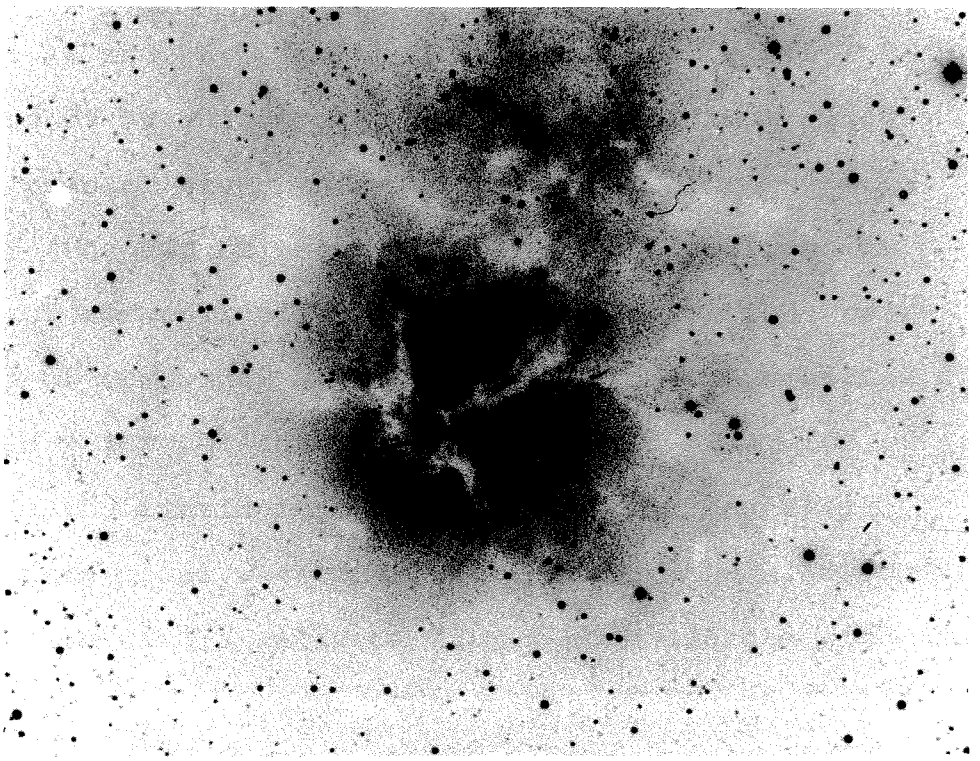

Fig. 23. NGC 6514, the Trifid Nebula (M 20), a 45-minute exposure with the 48-inch Schmidt telescope on a 103aO plate with a GG-11 filter. The central stars, HD164492 (ADS 10991 A through G) are contained within the very intense central condensation (arrow). North is at the top; east is at the left.

the brightest of the individual stars, ADS 10991 A. In addition to these data, a complete set of spectrophotometric data was obtained for the combined light of the five innermost components (components A, B, C, D, and E). The spectrophotometric results are shown in Figures 24 and 26. The spectral type of HD 164492 is given as 07 by Morgan et al (1955) and Hiltner (1956). In the present study the spectral types of components A and B (the two brightest stars) were classified as 08 and 09 respectively. The model used for the observations of component A was selected from the schedule of Table 5 for the spectral type 08. In order to simulate the intrinsic colors of the combined stars, a composite model was constructed from the θ_e .140 and .157 models with a ratio of fluxes commensurate with the magnitudes of the stars. The colors of the resultant model at the extreme wavelength points were found to differ insignificantly from the colors of the $\theta_e = 0.148$ model and thus this latter model was ultimately used to derive the color excesses of the combined light of the central stars of NGC 6514.

In spite of the obvious dust lanes and general obscuration in the vicinity of the nebula, the color excesses of the stars therein were found to be comparatively small. The normalized monochromatic reddening curves for

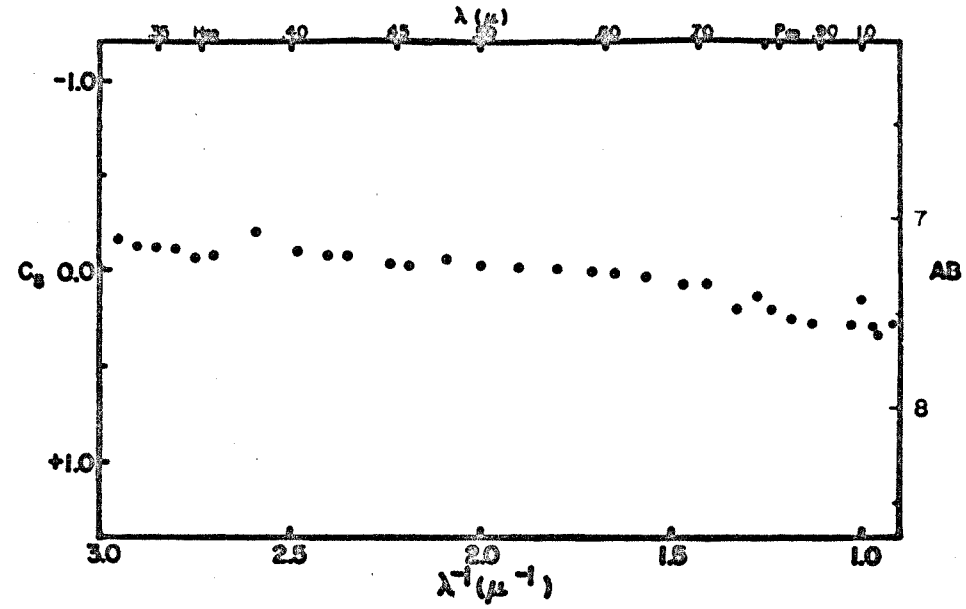

Fig. 24. Monochromatic colors, C_s, and magnitudes, AB, of the combined components of HD 164492 in NGC 6514.

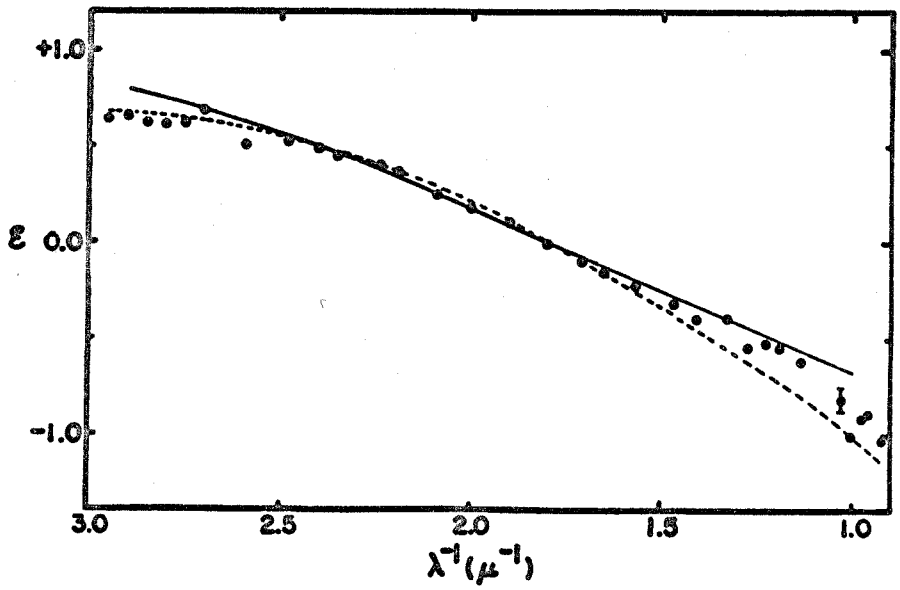

Fig. 25. The monochromatic reddening curve for the combined components of HD 164492 in NGC 6514.

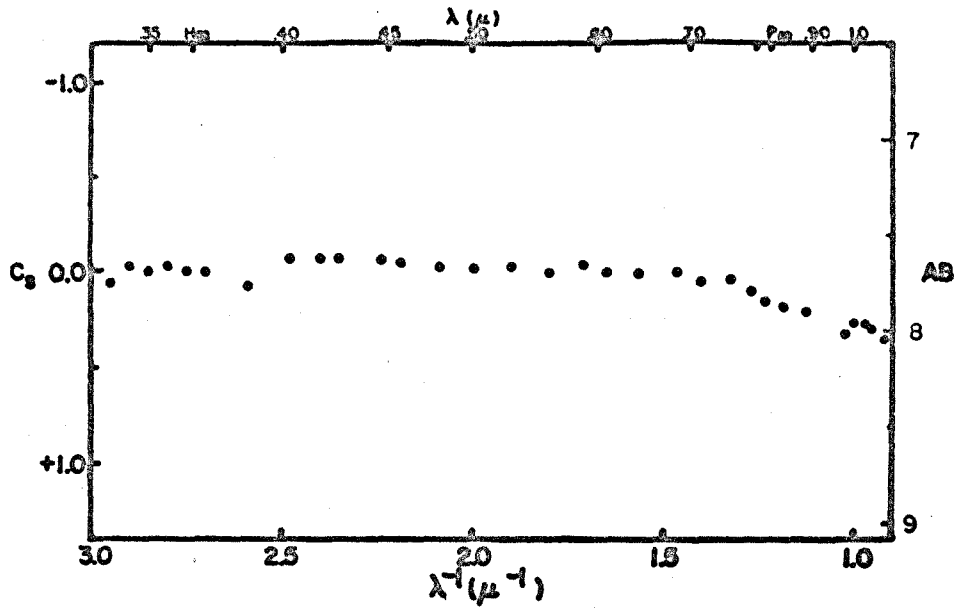

Fig. 26. Monochromatic colors, C_s, and magnitudes, AB, of the brightest component of HD 164492 (ADS 10991 A) in NGC 6514.

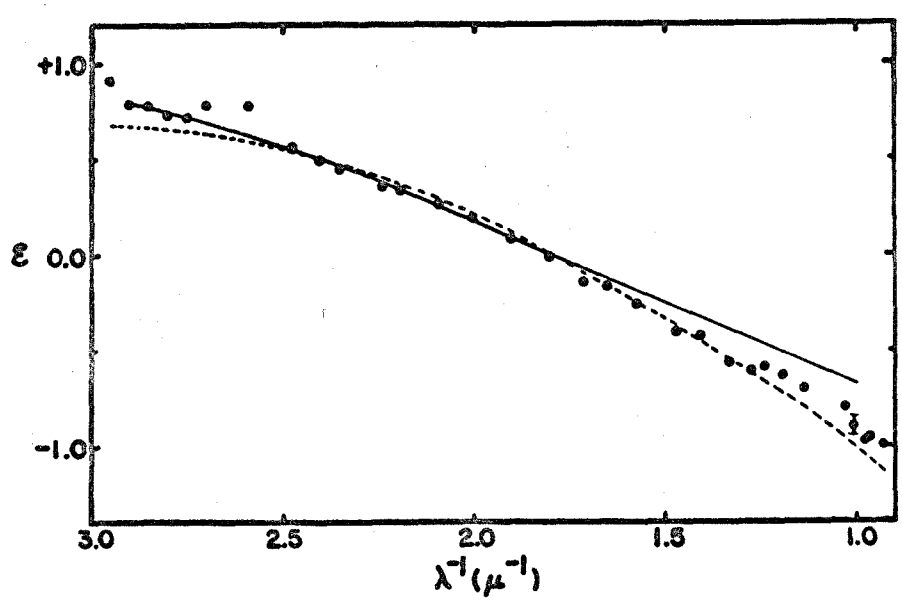

Fig. 27. The monochromatic reddening curve for the brightest component of HD 164492 (ADS 10991 A) in NGC 6514.

the two sets of observations are shown in Figures 25 and 27. In both cases a marked anomaly is apparent although it does not appear to be as strong as that in the Orion Nebula. The normalized one-micron extinction in each case is -0.90 with estimated probable errors of ±0.06 and ±0.05 for the combined and single star observations respectively.

NGC 6523

The Lagoon Nebula, M 8, is a very high surface brightness nebula particularly in the vicinity of the so-called "hour glass". The nebula is very large in extent and contains the very young star cluster NGC 6530 (see Walker, 1957). There is a strong degree of concentration in the vicinity of the hour glass where there are also numerous obscuration patches. This central configuration has been discussed by numerous authors such as Woolf (1961). In the immediate vicinity of the hour glass there is a star which is designated as Herschel 36 and which was identified as a star of early spectral type and high interstellar reddening in the low dispersion, objective prism work of Schulte (1956). This rather faint star was selected for spectrophotometric observation and its faintness required considerable expenditure of observing time such that coverage of other stars within the nebula was mininal. Several of the brighter stars given in the

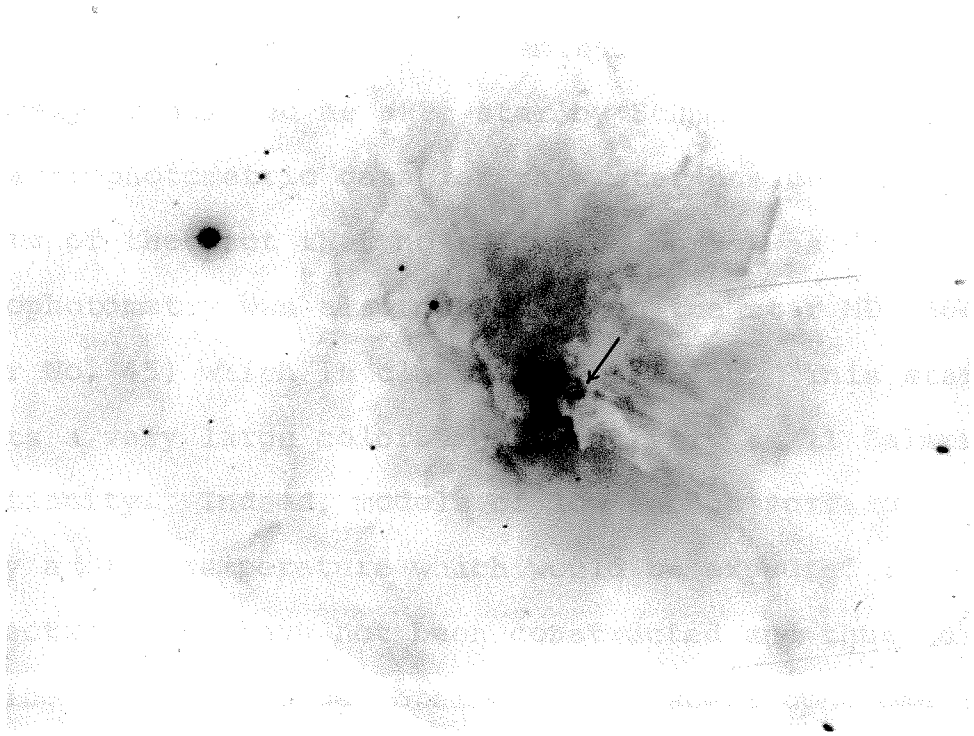

Fig. 28. The central region of NGC 6523, the Lagoon Nebula (M 8), a 90-second exposure with the 200-inch Hale telescope on a 103a-E plate with an Hα interference filter. The star Herschel 36 is indicated by the arrow. North is at the top; east is at the left.

lists of Walker were observed but the spectrophotometric observations could not be used for the derivation of reddening curves because spectral peculiarities made the selection of appropriate models impossible. The star HD 164906 (Walker No. 65) was found to exhibit both the Balmer and Paschen continuua in emission and has been positively identified as a Be star by Schmidt-Kaler (1967). The spectrophotometric data for this star has been given in spite of the fact that no reddening curve was derived. Spectrophotometry was also performed on the star HD 164865 (Walker No. 45) which is classified as B9Iab. This star exhibits a very large color excess and very small Balmer discontinuity. Indeed, models of low enough surface gravity at the temperature which would be expected from the spectral type have not been constructed and thus no reddening curve could be obtained. The spectrophotometric data for this star are given in Appendix A. Finally, the faint, later type members of the cluster were avoided because of the large amount of observing time required to observe them and because of the sensitivity of the intrinsic colors to the model selection.

The spectrophotometric observations of Herschel 36 are shown in Figure 29. In the present study the spectral type of this object was found to be O6n whereas Woolf (1961) gives it the type O7. The former classification was used for the selection of an intrinsic

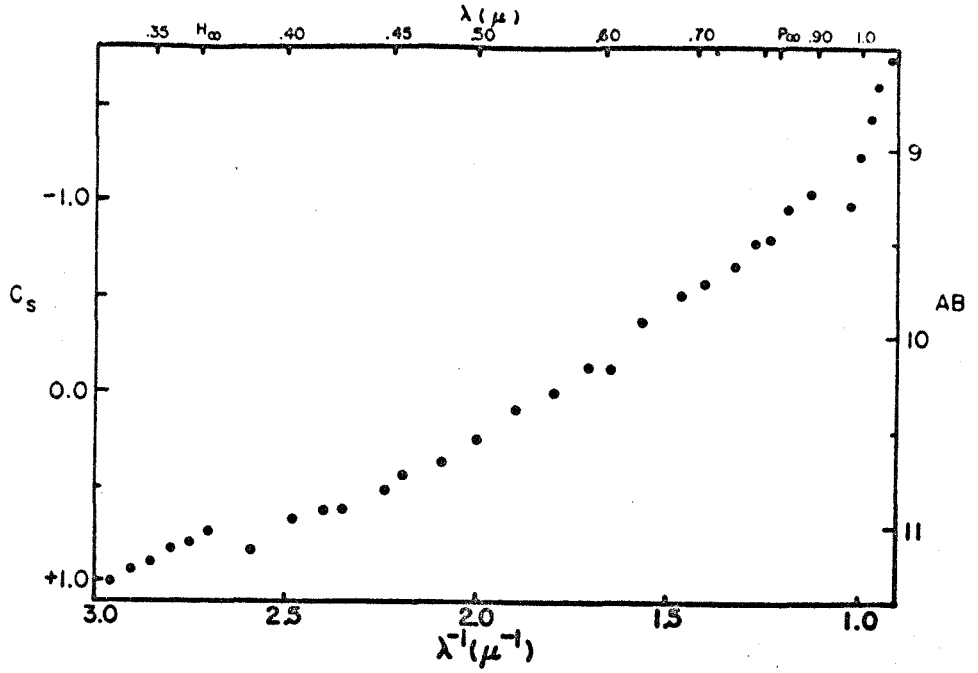

Fig. 29. Monochromatic colors, C_S, and magnitudes, AB, for Herschel 36 in NGC 6523.

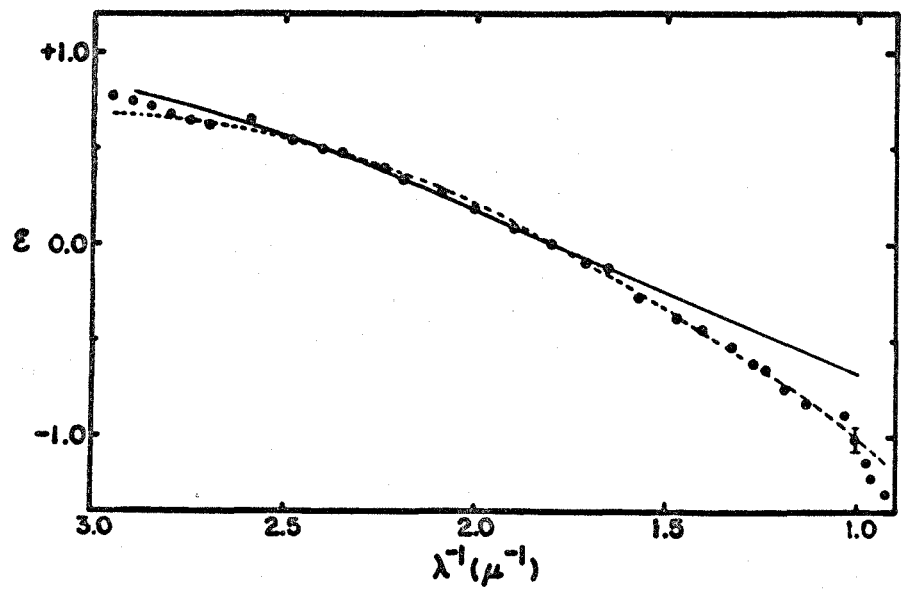

Fig. 30. The monochromatic reddening curve for Herschel 36 in NGC 6523.

spectral energy distribution. The resultant wavelength dependence of the interstellar extinction is shown in Figure 30. As can be seen from the figure, the curve for this highly reddened object displays an anomaly which is perhaps slightly stronger than that in the Orion Nebula. In this case the one-micron normalized extinction is -1.04 ± 0.06. This result is in agreement with the data given by Johnson (1967).

The association of the star Herschel 36 with the nebula NGC 6523 and the cluster NGC 6530 might well be questioned. If we utilize a total to selective extinction ratio of 3.0 and approximate the V magnitude and B-V color excess by means of AB (1.8) and E (2.240) respectively, we find that at the distance of NGC 6530 given by Pottasch (1965), 1100 parsecs, the absolute visual magnitude of Herschel 36 would be -2.7 which is rather low for its spectral type of O6 and might suggest that the star is in the background. If, however, we assume the total to selective extinction ratio of 6 which is associated with the Orion Nebula reddening anomaly, the absolute magnitude would be -5.4. The ratio which is given for this nebula by Johnson is 7.8 which would lead to $M_V = -7.1$. Either of these latter two ratios yield absolute magnitudes which are more nearly appropriate to the spectral type, place the star at a distance not incompatible with its association with the nebula, and lead

to the assumption of a total to selective extinction ratio which is different from that of the field as would be expected from the details of the extinction curve. It should be mentioned that the distance of 1100 parsecs was obtained from members of the cluster NGC 6530 on the basis of a total to selective extinction ratio of 3.0 after Morgan, Harris, and Johnson (1953). This normal ratio is consistent with the extinction curves for stars in the cluster other than Herschel 36 and HD 164906 as observed by Johnson (1967a). Thus it would seem that the peculiar extinction curve is a phenomenon which is localized in the vicinity of the very early type star.

NGC 6618

This nebula, M 17, like the previous two is of comparatively high surface brightness, but unlike them does not show the high degree of concentration about a single early-type star. It's inclusion in the program was chiefly motivated by the identification by Schulte (1956) of several stars of early spectral type and high reddening. An identification chart for these objects is given in Figure 31. Complete spectrophotometry was obtained for stars A and C, although the faintness of star A and the rapidly decreasing sensitivity of the red photomultiplier limited these observations to wavelengths less than 8000 A. These two stars were assigned spectral types of O5 and B1Vp. The spectrophotometric data are

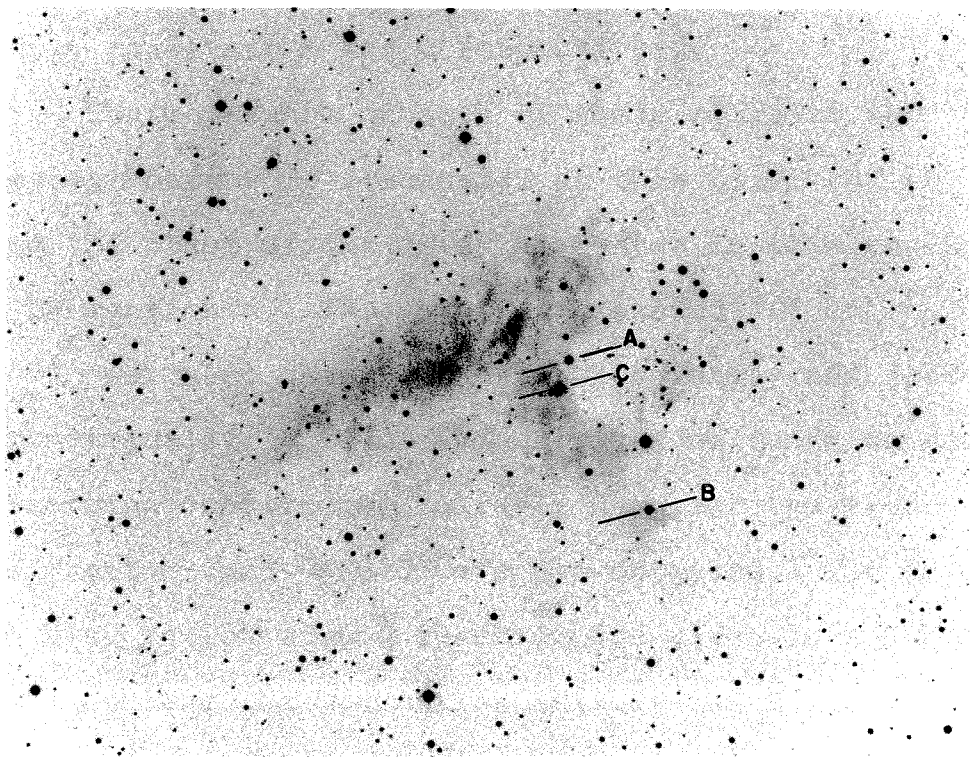

Fig. 31. NGC 6618, the Omega Nebula (M 17), a three-minute exposure with the 48-inch Schmidt telescope on a 103a-D plate with a C-3484 filter. The three faint stars which are observed spectrophotometrically are indicated. North is at the top; east is at the left.

displayed in Figures 32 and 34 and the resultant reddening curves in Figures 33 and 35. The normalized monochromatic reddening curves for both of these objects appear to be very nearly normal or field-like and yield normalized one-micron extinctions of -0.74 ± 0.07 and -0.72 ± 0.16 for stars A and C respectively.

The relevance of each of these stars to the H II region bears some discussion at this point and to this end the observations of a third star in this region should be mentioned. This star, designated "B" on Figure 31 was also observed spectroscopically and spectrophotometrically, but due to equipment malfunction and poor observing conditions, reliable data for the wavelengths greater than λ 5840 were not obtained. The data for the blue region of the spectrum are given in Appendix A. If we utilize the quantities AB(1.8) and E(2.240) as estimates of the visual magnitude, V, and the color excess, E_{B-V}, respectively and further assume a total to selective extinction ratio of 3.0, we may deduce distances for each of the stars. The spectral types of the stars have been found to be O5, O6 and B1V for stars A, B and C respectively to which we may assign absolute magnitudes of -6, -5.7, and -3.3 respectively after the data given by Arp (1958). We would then find distances of 3400 psc., 3100 psc., and 1100 psc. for stars A, B, and C respectively. Both the small distance and the

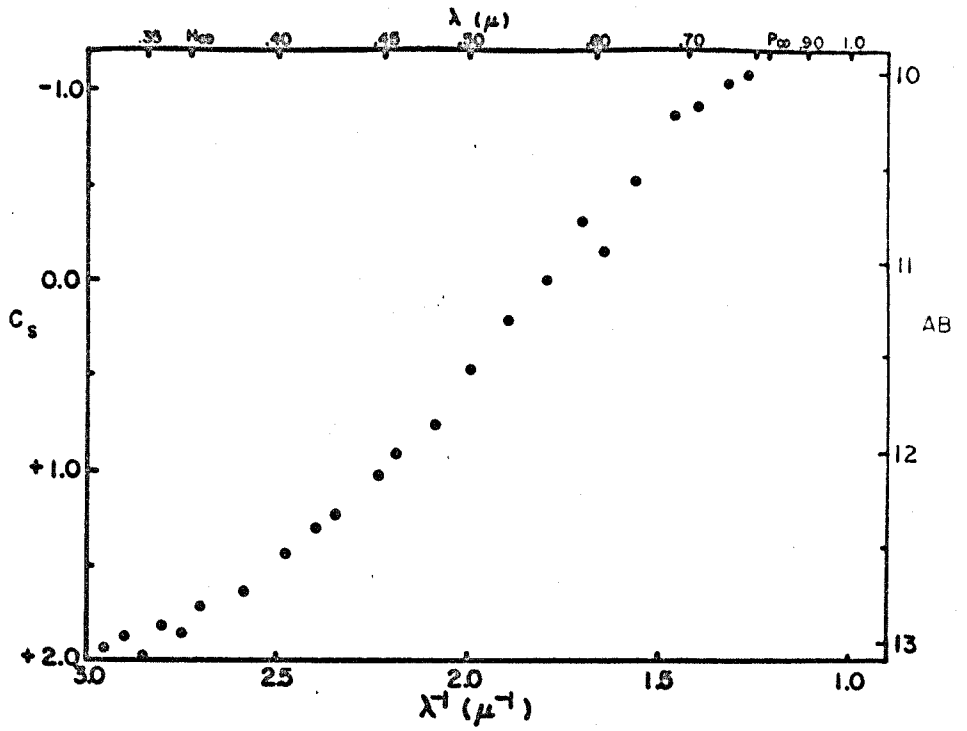

Fig. 32. Monochromatic colors, C_s, and magnitudes, AB, for Star A in NGC 6618.

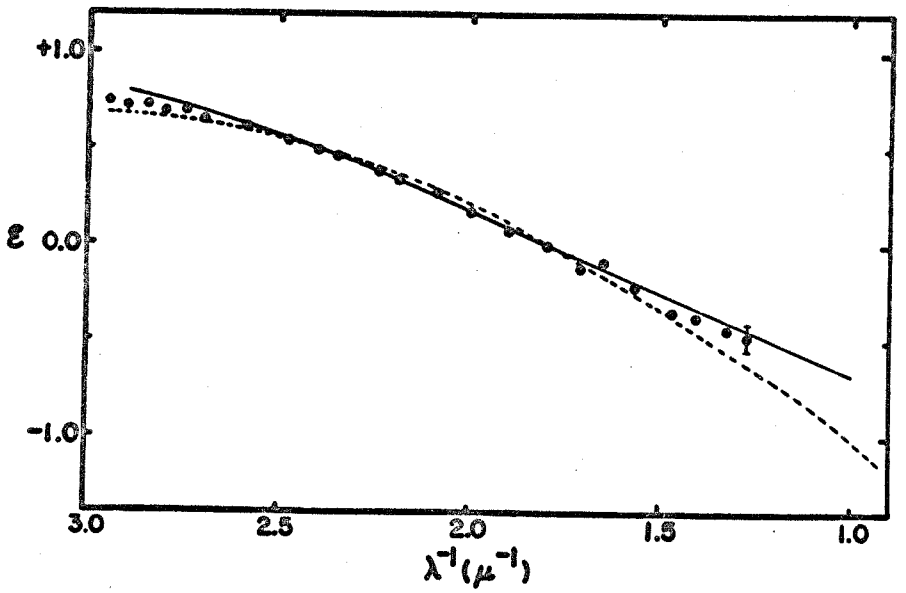

Fig. 33. The monochromatic reddening curve for Star A in NGC 6618.

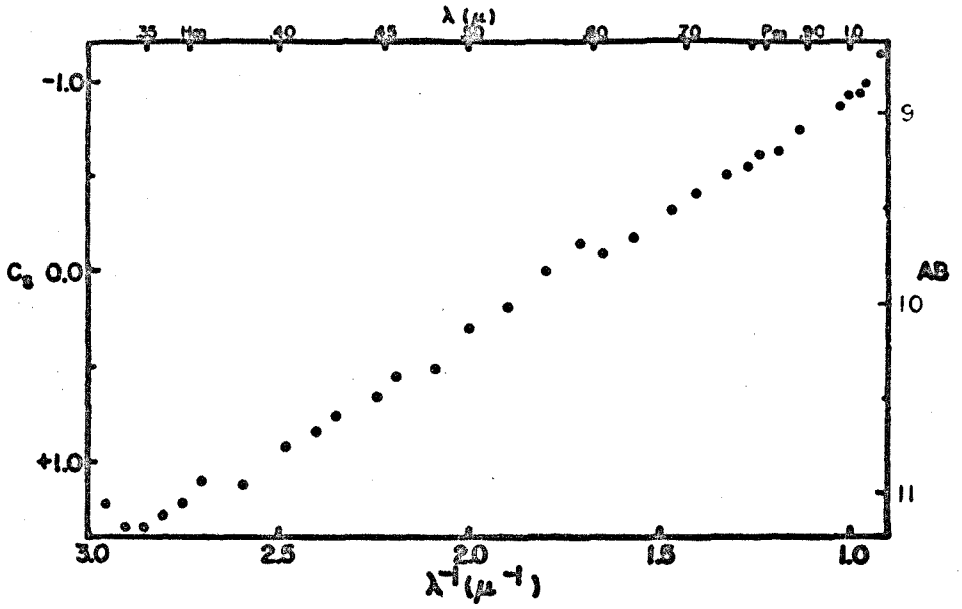

Fig. 34. Monochromatic colors, C_S, and magnitudes, AB, for Star C in NGC 6618.

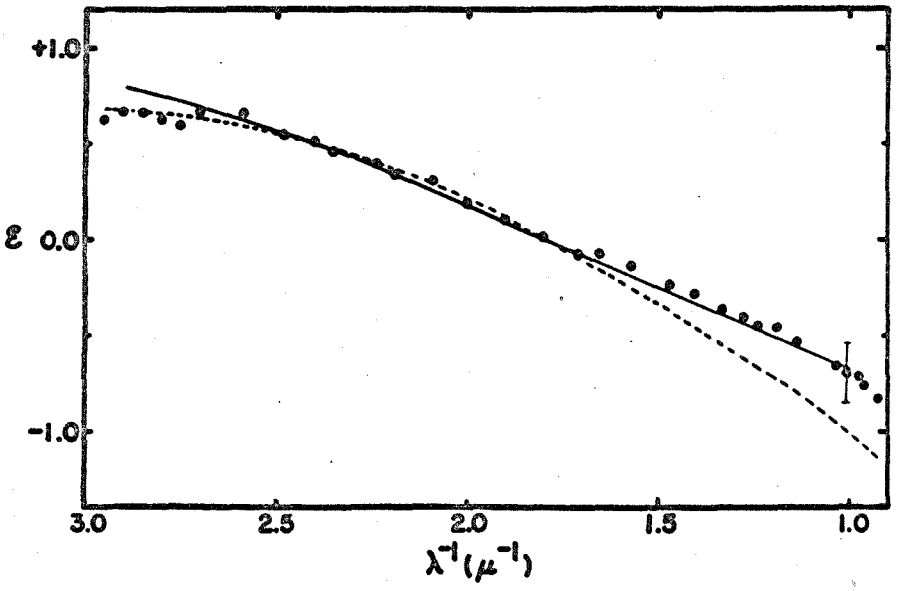

Fig. 35. The monochromatic reddening curve for Star C in NGC 6618.

lower color excess would tend to indicate that star C is well in the foreground with respect to the other two stars, and since the spectrophotometry of star A was not completed out to the one-micron region, the identification of the reddening curve for this star (and of the nebula if indeed this star is truly associated with it) as normal should be considered tentative. Unfortunately no reliable distance for the nebula has been located in the literature, but the earlier spectral types of stars A and B would argue in favor of their association with the cloud of gas and dust.

NGC 7023

This object is a reflection nebula of exceptionally high surface brightness and was included in the program so as to have one representative of this type of nebulosity. The nebula is in the center of an area of heavy obscuration which is almost one degree in diameter. Within this area there is but one star, HD 200775, of any consequence. Spectrophotometry of this star was conducted (Figure 36) and it was found to exhibit strong emission in the Balmer and Paschen continuua. Spectroscopically this star was classified as B3Vp and exhibits strong, broad emission at H_β .

In spite of the pecularity of this object, an attempt was made to obtain a partial extinction curve

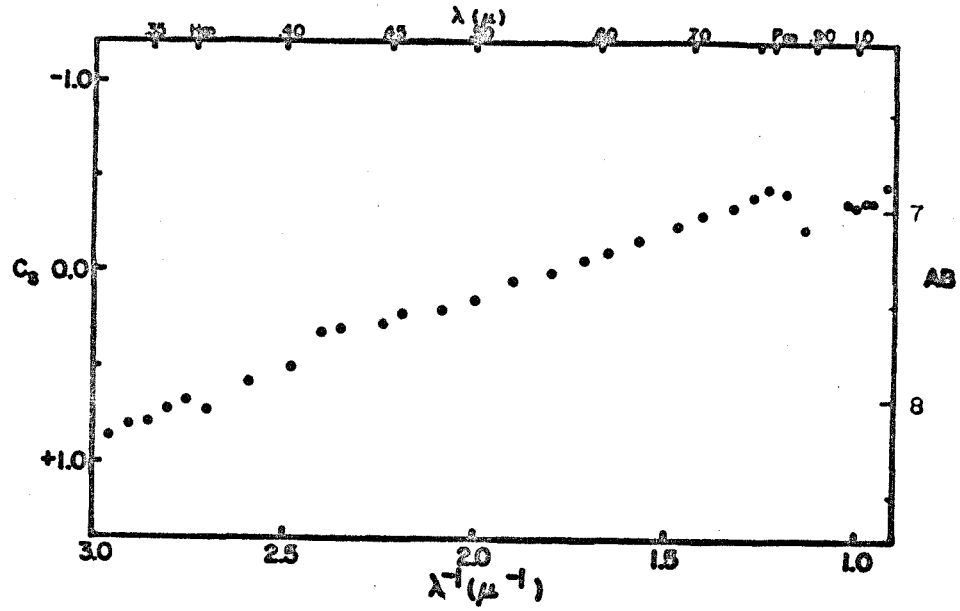

Fig. 36. Monochromatic colors, C_s, and magnitudes, AB, for HD 200775 in NGC 7023.

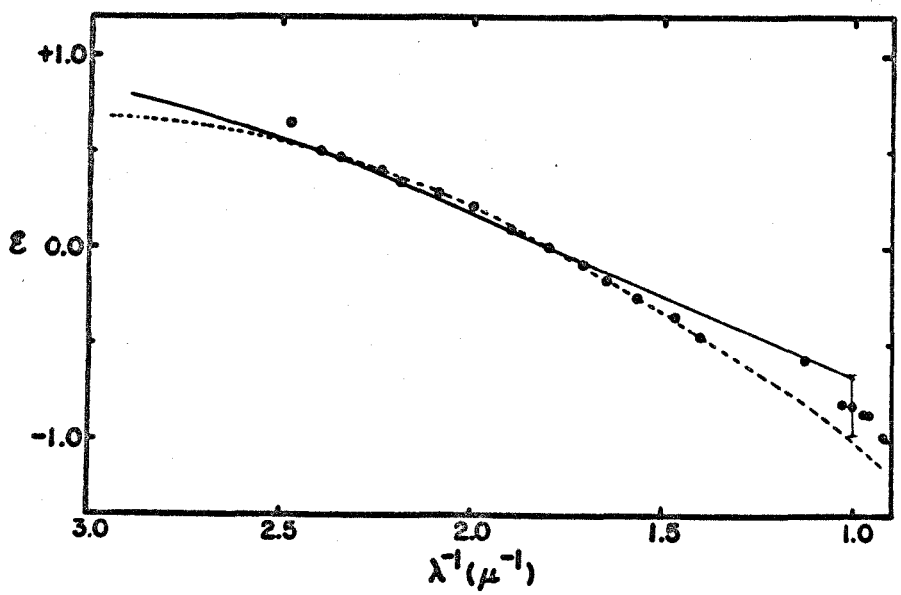

Fig. 37. The monochromatic reddening curve for HD 200775 in NGC 7023.

utilizing the B3 model from the schedule of Table 5. The resultant reddening curve (Figure 37) is seen to be slightly anomalous. The normalized one-micron extinction is -0.85 ± 0.16 and the large error is primarily due to the uncertainty in the model selection. In view of the abnormal spectrum of this star, the identification of this as a case of anomalous reddening should be considered suspect.

NGC 7380

This object is of rather low surface brightness and has a somewhat complicated structure. The three associated stars listed by Sharpless seem to be well to the west of the main body of the nebulosity in an area which is not particularly affected by obscuration. There are several lanes of obscuration which cross the face of the main body of the nebulosity which, along with the availability of early type stars, motivated the selection of the nebula. Of the three stars mentioned by Sharpless the one nearest the main body of the nebula, HD 215835, was selected for spectrophotometric study. As in the case of NGC 2175, there is a small, high continuum brightness condensation further to the east than the star HD 215835 and within this condensation there is a very faint star, which, unfortunately is too faint to observe spectrophotometrically.

The spectral type of HD 215835 was found to be

05 in the present study which is in reasonable agreement with previous determinations (e.g. 06n according to Morgan, Code and Whitford, 1955). The spectrophotometric data are shown in Figure 38 and the resultant reddening curve is displayed in Figure 39. This curve exhibits a rather weak degree of anomaly with respect to the Whiteoak field-reddening curve. The normalized one-micron extinction was found to be -0.78 ± 0.05.

NGC 7635

This medium surface brightness nebula displays a most curious physical structure. Near the star BD $+60^{\circ}2522$ there appears an intense arc-like structure which on very long exposures can be seen to make a complete ring. Portions of this ring shown up quite well on the continuum plate whereas some other portions of the nebula which are relatively bright on the red plate fail to appear on the continuum exposure. This fact was taken as an indication that there may be considerable quantities of dust within the nebula and it was thus included in the program. Stellar observations for both of the stars which are listed by Sharpless were obtained. The star HD 220057 was found to have a spectral type of B3V. If we utilize AB(1.8) = 6.9 and E(2.240) = 0.33 to simulate the V magnitude and the E_{B-V} respectively and further assume a total to selective extinction ratio of 3.0 and an absolute

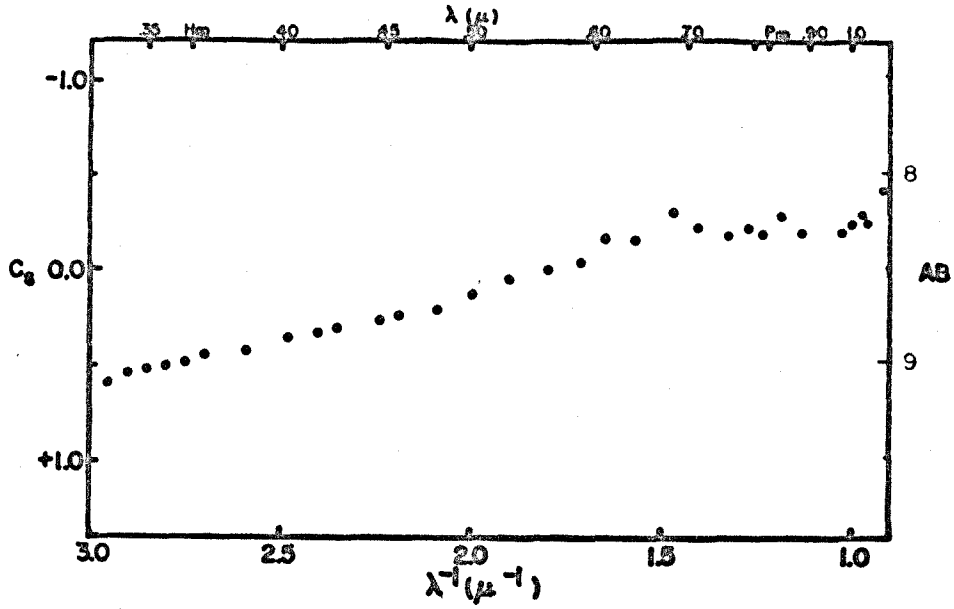

Fig. 38. Monochromatic colors, C_s, and magnitudes, AB, for HD 215835 in NGC 7380.

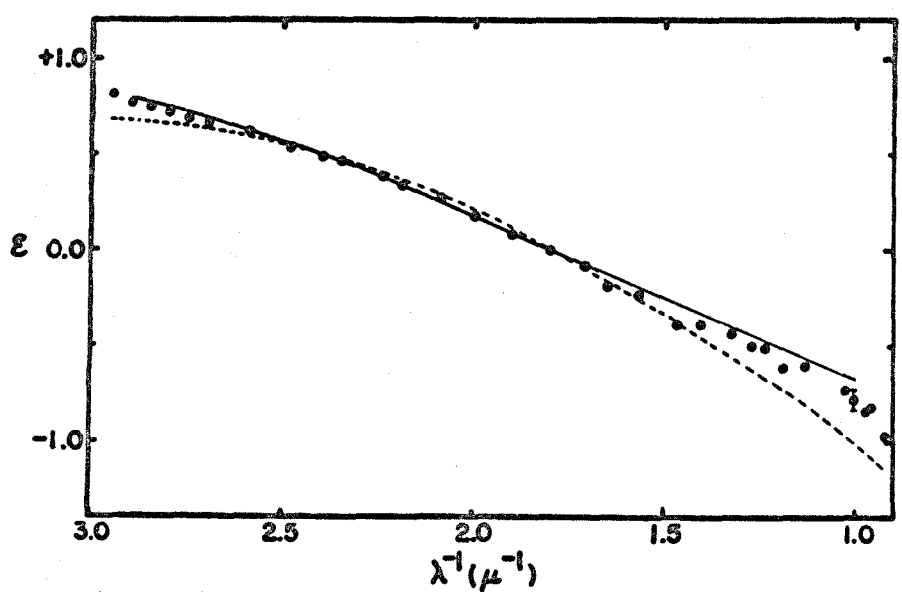

Fig. 39. The monochromatic reddening curve for HD 215835 in NGC 7380.

visual magnitude of -2.1 (Arp, 1958), we deduce a distance for this object of about 400 parsecs. The distance of the nebula, on the other hand, is given as 2000 parsecs by Pottasch (1965). Thus, this star is certainly a foreground object. Nevertheless the spectrophotometric data are displayed in Figure 40 and the resultant reddening curve in Figure 41. The normalized one-micron extinction is -0.73 ± 0.07 and the curve appears to be substantially similar to the field curve.

The star BD $+60^{\circ}2522$ was found to have a spectral type of O5 and considerations similar to those above place the star at a distance which is not inconsistent with the distance quoted in the Pottasch paper. The spectrophotometric data are shown in Figure 42 and the resultant reddening curve in Figure 43. The curve for this object also appears to be quite normal and this object has been assigned a normalized one-micron extinction of -0.74 ± 0.05.

III.4 Summary

The data which has been presented would tend to support the conclusion that the reddening anomaly which is observed for the stars in the Orion Nebula is a manifestation of a physical phenomenon which is intimately associated with H II regions. Indeed, the two nebulae which exhibit extinction curves most nearly like

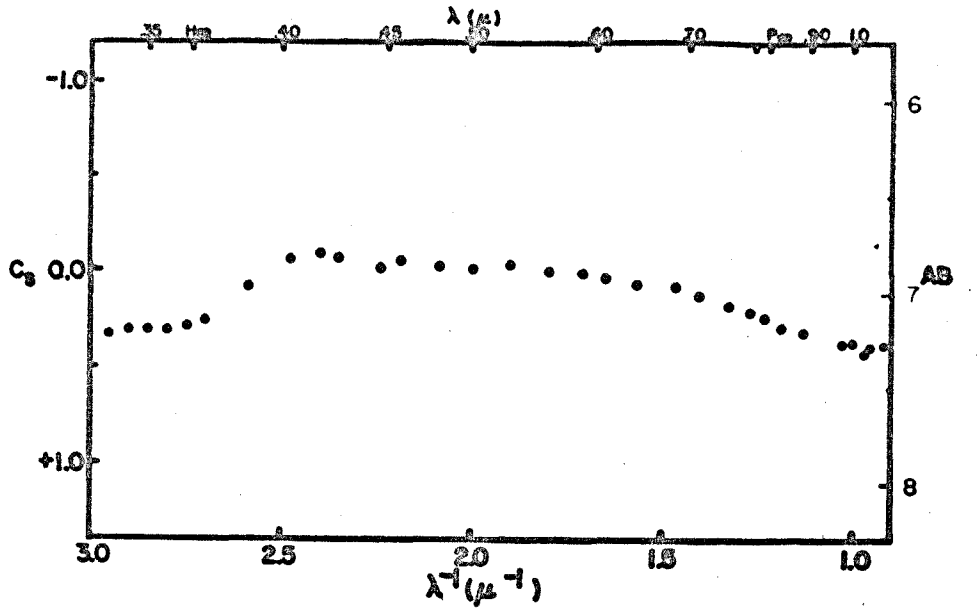

Fig. 40. Monochromatic colors, C_s, and magnitudes, AB, for HD 220057.

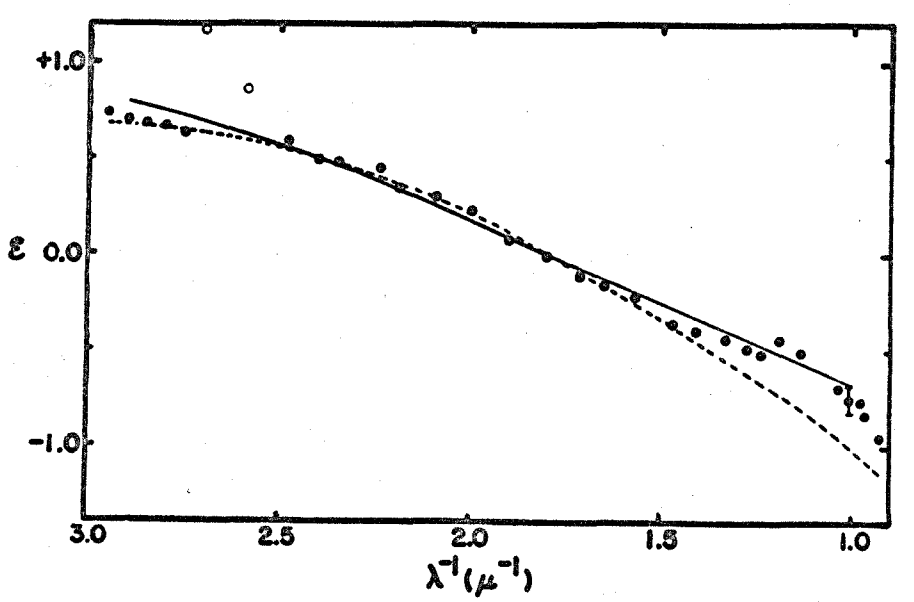

Fig. 41. The monochromatic reddening curve for HD 220057.

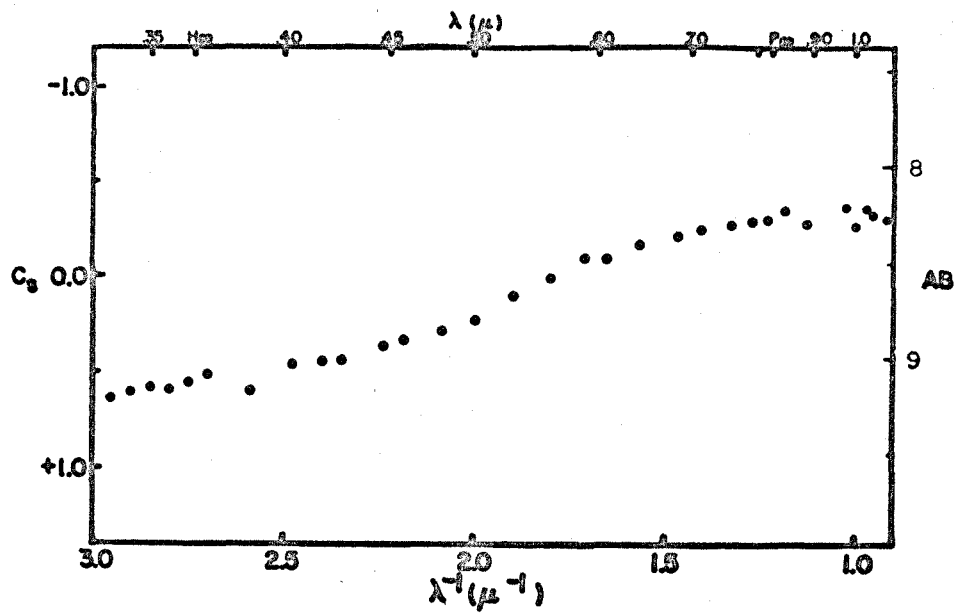

Fig. 42. Monochromatic colors, C_s, and magnitudes, AB, for BD +60° 2522 in NGC 7635.

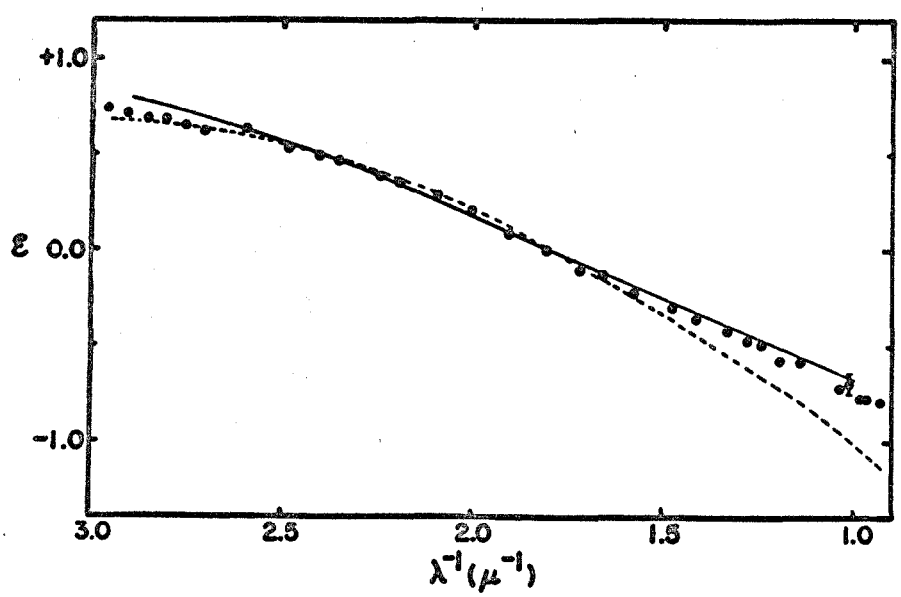

Fig. 43. The monochromatic reddening curve for BD +60° 2522 in NGC 7635.

that of the Orion Nebula are the two nebulae, NGC 6514 and NGC 6523, which have physical characteristics such as surface brightness, density, temperature and general structure most nearly like those of the Orion Nebula. Exhibiting weaker degress of reddening anomaly are HD 5005 in NGC 281, HD 15570 in IC 1805, HD 215835 in NGC 7380 and, perhaps, HD 200775 in NGC 7023. Finally, HD 15629 in IC 1805 as well as stars in IC 1848, NGC 2174, NGC 2244, NGC 6618, NGC 7635 appear to be substantially normal.

IV. DISCUSSION

IV. 1 The Radiation Pressure Mechanism

As previously mentioned, the usual explanation of the anomalous reddening curve of the stars in the Orion Nebula, as suggested first by Baade and Minkowski (1937) and further developed by Van de Hulst (1949), makes use of a grain size distribution which is deficient in the smaller sizes of grains. In this scheme, the small grain deficit is produced by the action of radiation pressure upon the grains. Since the acceleration of the grains due to radiation pressure alone will be inversely proportional to the grain size, the presence of a large ultraviolet radiation flux from the hot, young stars within the H II region will sweep the small grains from the nebula. This simple technique fails to take into account other forces upon the grains, the most important of which is viscous drag due to the gaseous component of the medium. Since the magnitudes of the forces due to radiation pressure and to drag will both be proportional to the grain area, it would be expected that the grains would reach a terminal velocity which would be independent of the size of the grains, and the small and large grains would not separate.

If, however, the time required to reach the terminal velocity is size dependent and large compared

to the time required for grains to traverse the nebula at such a velocity, separation might yet take place. In order to investigate this possibility we shall utilize a simple model. Consider the motion of a grain of radius a and density ρ in a gas of number density N of atoms of mass m. Let the grain be under the influence of a star which, for simplicity, will be taken to be a black body of temperature T and radius R at a distance d from the grain. The force on the grain due to radiation pressure is then:

$$F_{rp} = \frac{\pi a^2 \sigma T^4 R^2}{c\, d^2} \tag{8}$$

where σ is the Stefan-Boltzmann constant, c is the speed of light, and the efficiency factor for radiation has been set equal to unity. The viscous drag arises from the fact that the grain sweeps out a volume $\pi a^2 v$ per unit time and must impart a momentum mv to the $\pi a^2 vN$ gas atoms encountered per unit time. Most of the gas atoms which are swept up by the grain are either hydrogen or helium which immediately evaporate from the grain surface. For simplicity we shall assume here that all swept up atoms evaporate from the grain and that there is no preferential direction for the evaporation. Thus the mass of the grain is constant and there is no net contribution to the grain momentum from the recoil

of evaporating atoms. The drag force on the grain is then:

$$F_{vd} = \pi a^2 N m v^2 \quad . \tag{9}$$

If we neglect forces due to stellar gravitation (which will be unimportant throughout most of the nebula) and due to electrostatic interactions arising from the fact that the grains may be charged (Mathews, 1967), we obtain the equation of motion of the grain from (8) and (9):

$$\frac{dv}{dt} = \frac{3}{4a\rho}\left[\frac{\sigma T^4 R^2}{cd^2} - Nmv^2\right] \quad . \tag{10}$$

With the substitutions:

$$a^2 = \frac{3\sigma T^4 R^2}{4a\rho cd^2} \quad , \tag{11}$$

$$b^2 = \frac{3Nm}{4a\rho} \quad , \tag{12}$$

and

$$bv = x \tag{13}$$

equation (10) may be put in the form:

$$b\int dt = \int \frac{dx}{a^2 - x^2} \tag{14}$$

the integral of which is:

$$t = \frac{1}{ab} \operatorname{arctanh}\left(\frac{x}{a}\right) - \text{constant.} \qquad (15)$$

If we specify that at $t = 0$, $v = 0$, the constant in (15) is zero and we may solve for v as a function of t:

$$v = \frac{a}{b} \tanh(abt) \quad . \qquad (16)$$

Since for large argument the hyperbolic tangent approaches unity, we see that the quantity a/b is essentially the terminal velocity of the grains, thus from (11) and (12):

$$v_{max} = \left[\frac{\sigma T^4 R^2}{Nmcd^2} \right]^{1/2} \qquad (17)$$

which is, as anticipated, independent of the grain size. Equation (16) becomes upon substitution from (11) and (12):

$$v = v_{max} \tanh \left[\frac{3T^4 R}{4a\rho d} \sqrt{\frac{Nm}{c}}\ t \right]. \qquad (18)$$

From equation (15) we may define a time, τ_ξ , which is the time required to reach the fraction $\xi = v/v_{max}$ of the terminal velocity:

$$\tau_g = \left[\frac{4a\rho d}{3T^2 R} \sqrt{\frac{c}{Nm}} \right] \operatorname{arctanh} \xi \quad . \qquad (19)$$

As an example, consider a grain of radius a = 0.1 microns in a nebula of density $N = 10^2 cm.^{-3}$ which contains a star of temperature $T = 2 \times 10^4$ °K. Then for a dilution factor of $d^2/R^2 = 10^{12}$ we have from (17) a terminal velocity of 13.5 km sec^{-1} and a time to reach e^{-1} of the terminal velocity of 7.3×10^2 years. At velocities of the magnitude encountered here, it would take of the order of 10^5 years for a grain to travel a distance of one parsec. Since the grains attain their terminal velocities in the order of one percent of this time, it seems unlikely that such a process could result in a high degree of selective dilution in the nebula of one particular constituent.

The conclusion of this simple argument is confirmed by the more detailed work of Krishna Swamy and O'Dell (1967). These authors constructed a model nebula and utilized the same equation of motion as above except that they included a radiation pressure efficiency factor obtained from the Mie scattering theory. In spite of this modification, they found that the terminal velocity of the grains was "approximately independent of the particle size". Upon allowing the model nebula to evolve,

it was found that there was no significant alteration in the initial grain size distribution.

The equation of motion (10) which was used both in the present study and in that of Krishna Swamy and O'Dell is a highly simplified model of the dynamics of the grains. It has been shown (Spitzer 1941, and Mathews, 1967) that the grains will be charged. As pointed out by Krishna Swamy and O'Dell, this will have the effect of increasing the cross-sections of the grains and will thus slow the outward motion of the grains even more than the simple viscous drag of equation (9). Furthermore, outward moving grains will be decelerated by the Poynting-Robertson effect. This deceleration arises from the fact that thermal photons emitted by the grain in the forward direction will, in the frame of reference of the nebula, be blue shifted and will thus carry away more momentum than those photons emitted in the backward direction. These modifications tend to further inhibit the separation of grains of different sizes, and thus it would seem that the radiation pressure mechanism for the depletion of the small grain population must be abandoned.

IV.2 The Temperature of Interstellar Grains

As an alternative to the radiation pressure mechanism, Krishna Swamy and O'Dell argue that the

temperatures of the grains will depend upon the size of the grains such that smaller grains will be hotter and will thus evaporate. This situation is a result of the fact that the energy input to the grains is in the form of radiation of wavelengths which are of the same order as the size of the grains and the absorption is thus not strongly dependent upon the wavelength or grain size. However, due to the rather large dilution factors which obtain throughout most of the nebula, the black body equilibrium temperature at most points in the nebula will be of the order of tens or hundreds of degrees Kelvin. Under these circumstances the bulk of the radiation from the grains would be in the wavelength range of tens of microns, that is at wavelengths much larger than the grain sizes. In this regime the emissive efficiency of the grains does indeed depend upon the wavelength in the sense that the smaller the grain size to wavelength ratio, the smaller the efficiency. In order to compensate for lower emissive efficiency, the smaller grains will come to equilibrium at higher temperatures than will the larger grains. If the temperature of the small grains becomes high enough, these grains will evaporate, whereas the larger grains will not.

The energy absorbed by a grain of radius a is:

$$E_{in} = \pi a^2 \int_0^\infty \left[1 - A(a,\lambda)\right] F_\lambda \, d\lambda \qquad (20)$$

where $A(a,\lambda)$ is the albedo of the grain which may in general depend upon the grain size and on the wavelength of the light, λ, and F_λ is the monochromatic flux at the grain. In H II regions, the flux will be primarily in the ultraviolet at wavelengths of the same order as the size of the grains and thus, as in the case of the radiation pressure efficiency, it will be sufficiently accurate to assume that A does not depend upon the wavelength or grain size. With this simplification, equation (20) becomes:

$$E_{in} = \pi a^2 (1 - A) \mathcal{F} \qquad (21)$$

where $\mathcal{F}$ is now the integrated flux, which will be of the form:

$$\mathcal{F} = \sum_i \mathcal{F}_i (R^*/r)_i^2 + 4c \sum_j \mathcal{E}_j \ , \qquad (22)$$

where $\mathcal{F}_i$ and $(R^*/r)_i^2$ are the integrated flux and dilution factor for the i^{th} star respectively and $\mathcal{E}_j$ is the local energy density in the j^{th} spectral line (e.g. Lyman α). The total flux at a given point in the nebula is then the sum of the contributions from each star in the nebula plus the sum of the contributions of

each emission line.

The energy radiated by the grain may be written in the form:

$$E_{out} = 4\pi a^2 \int_o^\infty Q(a/\lambda)B(\lambda, T_g)\, d\lambda \qquad (23)$$

where $Q(a/\lambda)$ is the emission efficiency and $B(\lambda, T_g)$ is the Planck function for the grain temperature, T_g. The equation for the emissive efficiency which will be adopted here is that given by Van de Hulst (1949):

$$Q(a/\lambda) = \frac{2\pi a}{\lambda}\left[\mathrm{Im}\left(\frac{1 - m^2}{2 + m^2}\right)\right] = \frac{2\pi a}{\lambda} I \qquad (24)$$

where m is the complex index of refraction of the grain material. Substitution of (24) and the expression of the Planck function into (23) yields:

$$E_{out} = 8\pi^2 a^3 I \int_o^\infty \frac{2hc^2}{\lambda^6} \frac{1}{\exp(hc/kT_g\lambda) - 1}\, d\lambda \qquad (25)$$

where we have assumed that the wavelength dependence of the quantity I may be neglected. With the substitution $\lambda = x^{-1}$ (25) is transformed to a standard form, the integral of which gives:

$$E_{out} = 16\pi^2 a^3 hc^2 I \left[\frac{\Gamma(5)\,\zeta(5)}{(hc/kT_g)^6}\right]. \qquad (26)$$

The numerical value of the gamma function is 24 while that of the Riemann zeta function is $\zeta(5) = 1.036927$. Adopting the value for I according to Van de Hulst, we find:

$$E_{out} = 9.9545\ a^3 T_g^5 k^5\ \pi^2\ h^{-4} c^{-3} \quad . \tag{27}$$

Under conditions of equilibrium we require that:

$$E_{out} = E_{in} \tag{28}$$

which upon substitution from (21) and (27) leads to the expression:

$$T_g^5 = 0.1005\ h^4 c^3 k^{-5}\ \pi^{-1} (1 - A) \mathfrak{X}\ a^{-1} \tag{29}$$

or:

$$T_g = K a^{-1/5} \quad . \tag{30}$$

Utilizing the criteria outlined by Gaustad (1963), Krishna Swamy and O'Dell calculate evaporation temperatures for each of several possible interstellar grain constituents. Thus at each point in a nebula (i.e. at each value of $\mathfrak{X}$) there will be a minimum radius for grains of a specific composition. Krishna Swamy and O'Dell compute the minimum radius for grains of H_2O, NH_3 and CH_4 at representative

points in several H II regions, three of which were included in the present study. By the inclusion of the Lyman-α flux as deduced from observed $H\beta$ surface brightnesses and the emissivities given by Seaton (1960), they conclude that the presence of any dust at all in the regions rules out the very unstable CH_4 (evaporation temperature equal to 28°K) as a major component of the grains. They also find that small grains of ices as stable as H_2O (with an evaporation temperature of 105°K) will be significantly depleted in the Orion Nebula but not in either NGC 6514 or NGC 6523. This result is consistent with the dust content observations of O'Dell, Hubbard, and Peimbert (1966) but fails to predict the existence of the Orion-like reddening anomaly which is observed in NGC 6514 and NGC 6523. This discrepancy may arise if the physical anomaly in the grain population is localized in a highly concentrated central region of the nebula. Then the $H\beta$ surface brightness, observed at some distance from the star, may lead to a Lyman-α flux which is systematically low with respect to that relevant to the anomalous region. This in turn would cause an under estimate of the minimum grain radius. The influence of heavy obscuration patches, which are particularly noticeable in the immediate vicinity of Herschel 36, would also lead to low values for the

Lyman-α flux and thus of the minimum grain radius. Nevertheless, the existence of this discrepancy as well as the lack of a correlation between the reddening anomaly and the "gas to dust" ratio as defined by O'Dell *et al* motivates the following discussion of alternative explanations of the reddening anomaly.

IV.3 Intrinsic Colors and Grain Models

The above discussion is based upon the assumption that the anomalous colors of the stars in H II regions are a result of an interstellar grain population which is deficient in small grains relative to the general interstellar medium. There are, however, two possibilities which have yet to be completely ruled out. First, it is possible that the intrinsic colors which have been adopted for the stars are incorrect and that it is the stars rather than the grain population which are peculiar. It is also possible that the models of the grains which have thus far been used are incorrect and that chemical compositions, physical structures and grain size distributions which have heretofore been neglected might explain the observational data as well as or better than the presently accepted scheme.

If we assume that the reddening curve for the H II regions is the same as that for the field, what then would be the intrinsic spectrum required to produce

the observed colors? Consider the case of the star Herschel 36. If we assume that the spectrum in the blue is well represented by the model atmosphere with $\theta_e = 0.126$, i.e. that the color excess E(2.4) = 1.16 is correct, we may extract the reddening according to the field curve of Whiteoak from the observed colors and thus obtain the "intrinsic spectrum". The results of this procedure are illustrated in Figure 44. In the figure the predicted spectrum (solid dots) is compared with that of the $\theta_e = 0.126$ model atmosphere spectral energy distribution (solid line) and it is seen that the required anomaly in the spectrum of Herschel 36 would be an infrared excess which amounts to about 0.62 magnitudes at one micron and 0.38 magnitudes at the Paschen limit.

As a possible source of the excess infrared energy, we now consider the simple model of black body radiation. From the excesses at the Paschen limit and at one micron quoted above, and the physical fluxes of the high temperature model atmosphere spectra, we may predict the fluxes required to make up the excess. From these fluxes a color temperature and the ratio of the black body and model atmosphere surface areas may be calculated. The result of this process predicts as a best fit to the data of the present study, a black body with a temperature of 3700°K and a surface area

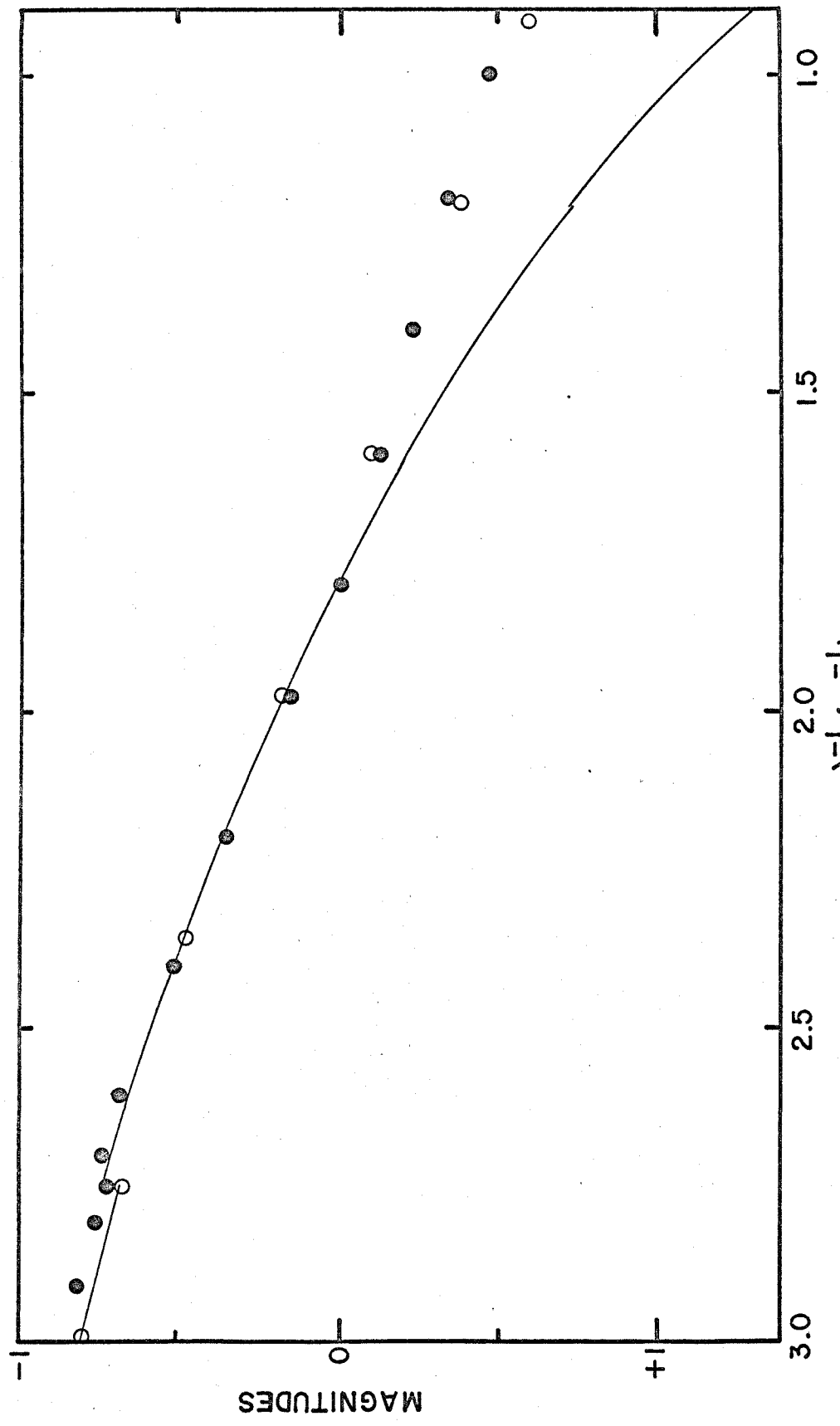

Fig. 44. The observed colors of Herschel 36 with extinction removed according to the field reddening curve of Whiteoak (filled circles) compared with a $\theta_e = 0.126$ model (line) and a composite model as described in the text (open circles).

2.28×10^2 times that of the hot star. The resultant composite model is given by the open circles in Figure 44.

If we now maintain the assumption that the reddening for Herschel 36 is "normal" such that $A_V/E_{B-V} = 3.0$, we deduce an absolute visual magnitude of -2.7 for the distance of the cluster NGC 6530 of 1100 psc. It should be noted that this is a rather low luminosity for a star of this spectral type. The bolometric correction for a star of $T = 4 \times 10^4$ °K is -3.9 (Allen, 1963) from which we may deduce the radius of the early type star:

$$M_{bol} = 4.72 - 2.5 \log (L/L_\odot) \tag{31}$$

so that:

$$\log (L/L_\odot) = 4.53 \tag{32}$$

then:

$$L/L_O = (R/R_\odot)^2 (T/T_\odot)^4 \tag{33}$$

which leads to a radius of $3.5\ R_\odot$, which would in turn imply a radius of $53\ R_\odot$ for the companion 3700°K black body. This temperature and radius is quite consistent with a giant or supergiant of late K spectral type. If this companion object is an evolved star, however, it

it should have originally been more massive than the existent, young, early-type star in order to have evolved in a time comparable to the life of such an early-type star. Utilizing a mass-luminosity relation coefficient of 3.3 we would deduce from (32) a mass for the early-type component of $23M_{\odot}$. The radius and effective temperature of the cool companion object imply a luminosity of $5.7 \times 10^2 L_{\odot}$. The evolutionary tracks of stars of $9M_{\odot}$ and $15M_{\odot}$ given by Iben (1966 a,b) do indeed reach temperatures as cool as 3700°K but do so at luminosities of about $7 \times 10^3 L_{\odot}$ and $7 \times 10^4 L_{\odot}$ respectively. The more massive star suggested by the present discussion should, presumably, be even more luminous than these two models and we thus see that the required companion object is severely underluminous. If Herschel 36 is actually more luminous, i.e. more distant but still normally reddened, the radius of the cool companion will be increased, but probably not unreasonably so, thus if the absolute visual magnitude of this star is -4.3 as suggested by Johnson (1967b), the black body radius becomes $109R_{\odot}$. Yet even these more liberal parameters would lead us to expect a companion object more massive than $37M_{\odot}$, and the radius and temperature would yield a luminosity of $2 \times 10^3 L_{\odot}$ which is still underluminous. If, on the

other hand, the cool companion is a pre main-sequence object, we see from the tracks of Iben (1965) that the temperature and luminosity may be obtained with objects of considerably lower mass.

If we extrapolate the composite model developed above to the 3.4 micron wavelength region, we find that the model fails to predict all of the infrared excess which is observed by Johnson (1967 a, b). These observations indicate an excess flux in the L magnitude ($\lambda^{-1} = .294\ \mu^{-1}$) of $1^{m}.41$ with respect to the K magnitude ($\lambda^{-1} = .455\ \mu^{-1}$) when the intrinsic spectrum of the object is represented by a black body with effective temperature appropriate to the 07 spectral type given by Johnson. The combination of objects with effective temperatures of 40,000°K and 3700°K and the aforementioned surface area ratio produces a K - L excess of $0^{m}.33$ with respect to the 40,000°K model. Lacking a detailed set of homogeneous spectrophotometric data, a detailed fit of black body models to these larger infrared excesses was not attempted. However, it was found that a black body of temperature 1500°K with an area 4.9×10^{3} times that of the combined 40,000°K and 3700°K black bodies would account for the excess energy at $\lambda^{-1} = .294\ \mu^{-1}$. This surface area would correspond to a radius of $1.08 \times 10^{3}\ R_{\odot}$ if the radiation were to come

from a single body.

Johnson (1967b) has suggested that the excess infrared radiation may come from a circumstellar shell. If we assume that this radiation comes from an optically thin cloud of refractory grains in the vicinity of the stars, the required surface area involved in emission can be obtained from 1.55×10^{38} grains of radius 6×10^{-6} cm. The grain size and the temperature of 1500°K were suggested by the work of Gaustad (1962). The temperature is the upper limit of grain evaporation and the radius is that suggested for iron grains. Extrapolation of Gaustad's data indicated an absorption cross-section at $\lambda^{-1} = 2.0\ \mu^{-1}$ of $1.1 \times 10^{-12} cm^2$. The dilution factor implied by the 1500°K grain temperature and the 40,000°K stellar temperature would correspond to several hundred solar radii, thus if the cloud of hot grains is confined to a sphere of radius $10^2\ R_\odot$ we deduce a grain density of $9 \times 10^{-2}\ cm^{-3}$. The optical depth implied by this density, N, the nebular dimension l, and the above quoted cross-section σ, is:

$$\tau = N \sigma l \qquad (34)$$

which has the numerical value of $\tau = 0.70$, which is quite reasonable in light of the known extinction of this object. Since the optical depth will be inversely proportional to the square of the nebular dimension, the size of the hot

grain cloud and the number of grains may be adjusted to give as much extinction as required by the observed properties of the star and remain well within the restrictions of dilution factor and total flux, (i.e. effective area) required. More detailed models of this general type have been computed by Stein (1966).

From the above discussion of Herschel 36, we may conclude that it is possible to account for the anomalous colors of the H II region stars by means of the superposition of one or more black body spectra upon the spectral energy distribution of the early type component. If the infrared excesses are the result of the presence of a late spectral type companion, high resolution spectral scans in the far infrared region where such a companion dominates the spectrum should reveal molecular band features of H_2O and other oxides known to be present in such stars from the Stratoscope II observations of Woolf, Schwarzschild and Rose (1964) and from the theoretical work of Auman (1967). If, on the other hand, the excess infrared light comes from circumstellar shell, it might be possible to detect the presence of the shell by interferometric techniques. Recently Wickramasinghe (1967) has suggested that the excess infrared radiation might come from emission bands in the lattices of circumstellar crystals. Such spectral features could also be

observed in high resolution spectral scans.

Although the above discussion would tend to indicate that the color anomalies which have been found for several stars involved in H II regions may be explained by the superposition of companion objects which would be undetectable in the visual region of the spectrum, we are left with the suspicious fact that the magnitude of the infrared excess in the individual stars is correlated with the blue color excess. This correlation is shown in Figure 45, in which stars which have been identified as having anomalous colors are indicated by filled circles, whereas stars of normal colors are shown by means of open circles. It is seen that the E(1.005) of the anomalous stars exceeds that for the normal stars by greater and greater amounts as the blue color excess, E(2.400), increases. This correlation would seem to indicate the direct association of the mechanism which produces the infrared color anomaly with the medium which produces the blue color excess. Furthermore if the color excess anomalies of the stars in the Trapezium are to be explained by the presence of either late-type companions or circumstellar shells, a most fortuitous set of companion or shell characteristics would be required in order to yield the same reddening curve for each of the three stars which were observed, since these objects display a

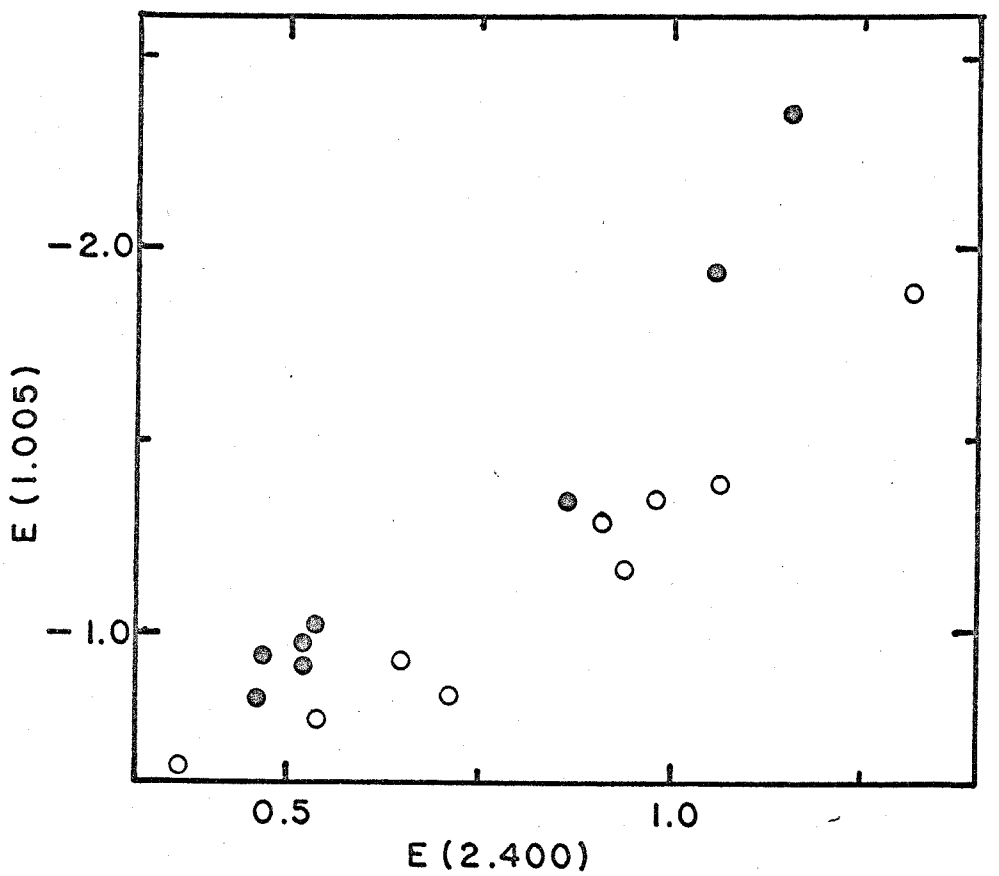

Fig. 45. The color excess near one micron, E (1.005), as a function of the blue color excess, E (2.400). Open circles indicate objects for which the reddening curve has been identified as normal, while filled circles represent stars for which the reddening curve is anomalous.

range of 1.6 magnitudes in AB(1.800). We shall thus return to a discussion of mechanisms which involve peculiar grain populations to explain the observed color anomalies.

As previously mentioned, it is quite possible that the grain models which have been used to explain the color anomaly of H II region stars are incorrect. The calculation of a set of extinction curves for various grain compositions, grain structures and grain size distributions is a rather involved task which is beyond the scope of the present work. The extinction curves which have been computed heretofore have involved a rather limited range of these characteristics. It is hoped that the application of modern computer techniques will lead to a more complete set of models of the extinction producing medium.

IV.4 Accretion and Erosion

Let us now return to a discussion of alternative mechanisms for the production of a grain size distribution which is deficient in small grains. It should first be noted that processes of grain growth by simple atom accretion and erosion by such processes as sputtering will not produce the desired effect. The rate at which the mass of a grain will change under accretion or erosion will be proportional to the surface area of the grain:

$$\frac{dm}{dt} = 4\pi a^2 Q \tag{35}$$

where Q is a function of the properties of the grain environment. For grains of density ρ the mass of the grains will be:

$$m = \frac{4}{3}\pi a^3 \rho \tag{36}$$

so that:

$$\frac{da}{dt} = Qa^0 \tag{37}$$

Thus accretion and erosion will not change the relative numbers of grains of different sizes and specifically will not purge the interstellar medium of the small grains. This does not rule out the possibility that grains of a composition and structure heretofore neglected, which have been affected by accretion or erosion, might explain the observed anomaly. This simple argument also does not exclude the possibility that complex physical and chemical processes will introduce additional grain size dependence which would result in the preferential depletion of small grains. As previously mentioned, however, the treatment of new grain models is beyond the scope of the present study.

IV.5 The Pre-H II Region Phase

All of the mechanisms which have been advanced to explain a small grain deficiency have dwelt upon the present conditions, i.e. high density, temperature and ultraviolet flux, within the H II regions. But these conditions have been shown to lead to the destruction of all of the grains in such a region (Zirin, 1952 and Wickramasinghe, 1965). It would thus seem to be profitable to examine other phases of the life of these regions for conditions which might lead to the anomalous grain population. In particular, two mechanisms, which might be operative in the high density but low temperature and ultraviolet flux conditions which will obtain immediately prior to the final contraction of the central star will be discussed.

Zirin suggested that condensation nuclei are required for the growth of grains even under the relatively high density conditions of H II regions. Once condensation nuclei are present, it is argued by Oort and Van de Hulst (1946) that grain growth will proceed at a rate which is proportional to a high power of the gas density. Thus in the dense nebulae, grain growth may proceed rapidly enough to exhaust the supply of condensation nuclei, in which case the proportion of small grains will decrease as the nuclei accrete material from the nebula and the supply of such nuclei is unreplenished or replenished at a much reduced rate.

The effectiveness of this mechanism will depend somewhat upon the source and nature of the condensation nuclei. The graphite core, ice mantle grain model proposed by Wickramasinghe, Dharmawardhana and Wyld (1966) have carbon grains as condensation nuclei. These nuclei have binding energies high enough to allow them to survive the hostile environment which periodically strips away the ice mantle. Thus in the context of the young nebulae the condensation muclei would be primordial and the very slow production of such grain nuclei would not make a significant contribution to the small grain population in the time scale suggested by the present model. If, on the other hand, the condensation nuclei are provided by fragmentation of large grains in non-central grain-grain collisions as suggested by Zirin (1952), rather severe limitations would be placed upon the motions of the grains in the cloud so that mutual encounters of grains would be infrequent but the grains would continue to accrete material from the nebular gas.

As a test of the plausability of this scheme, consider the Orion Nebula. Suppose that all of the carbon which would be expected in such a nebula were bound up in condensation nuclei of radius 0.05 μ and each such nucleus had an ice mantle of radius 0.4 μ. For simplicity we shall assume that the extinction efficiency of such a

grain is unity so that the cross-section will be $5 \times 10^{-9} cm^2$. From Allen (1963) we will assume the total mass of the nebula to be $700 M_\odot$, the radius of the nebula to be $6.2 \times 10^{16} cm$. and the ratio of hydrogen to carbon by mass to be 2.75×10^2. These conditions lead to a total of 10^{46} grains and thus a density of 10^{-11} grains cm^{-3}. With unity extinction efficiency, this then implies an optical depth of the nebula of 0.32 which is consistent with the observed extinction.

Another process which could lead to a deficiency of small grains is fusion. The influence upon the particle size distribution of mutual encounters was first discussed by Oort and Van de Hulst (1946). They assumed "somewhat arbitrarily" that fusion would take place if the energy in the center of mass coordinant system of the colliding grains was greater than or equal to, the energy required to raise the temperature of the entire mass to the melting point and to melt one-half of the mass but less than the energy required to vaporize the total mass. At energies below this range, inelastic collisions resulted while above it vaporization was the result. In this model, central collisions of pure H_2O ice grains of equal mass resulted in fusion if the collision velocity was greater than about 0.7 km sec^{-1} but less than about 2 km sec^{-1}. With this fusion criterion Oort and

Van de Hulst found that the grain size distribution was altered very little by grain-grain encounters. If, however, the fusion criterion used by these authors is modified by physical considerations, alteration of the grain size distribution might yet result.

Zirin (1952) has suggested that because of the low equilibrium temperatures of grains in interstellar space, very little rearrangement of atoms will occur after accretion. This will lead to rather open structure grains of low binding energy and low thermal conductivity. In such grains the most probable result of collision with other grains, even at energies considerably below that required for vaporization, will be mechanical disruption. Generalization of this argument suggests that if the rate at which thermal adjustments take place within the grain material is comparable to or more rapid than the rate of mechanical disruption, accomodation of the two grains might occur. In order to assess the effectiveness of thermal adjustment, let us consider a highly simplified model. The time and position dependence of the temperature within a grain will be governed by the thermal diffusion equation:

$$\nabla^2 T = \frac{C \rho}{K} \frac{\partial T}{\partial t} \qquad (38)$$

where C is the specific heat, K the thermal conductivity

and ρ the density of the material. The solution of (38) in one dimension is:

$$T(x,t) = \sqrt{\frac{C\rho}{4\pi Kt}} \quad \exp\left[-\frac{x^2}{4Kt/C\rho}\right] . \qquad (39)$$

This solution is in the form of a gaussian which has a width, r, of:

$$r = (4Kt/C\rho)^{1/2} . \qquad (40)$$

When equation (40) is solved for time, we have a characteristic interval, τ , for a thermal disturbance to reach a depth, r, of:

$$\tau = r^2 C\rho/4K. \qquad (41)$$

Then the characteristic velocity of a thermal disturbance, V_{td}, may be defined to be:

$$V_{td} = \frac{r}{\tau} \qquad (42)$$

or:

$$V_{td} = \frac{4K}{rC\rho} . \qquad (43)$$

As an example, consider grains of pure H_2O ice for which we will use a density of 1 gm cm^{-3}. From the Handbook of Chemistry and Physics (1960) we take values of the conductivity and specific heat of

$K = 4 \times 10^{-3}$ cal cm^{-1} sec^{-1} deg^{-1} and
$C = 2 \times 10^{-1}$ cal gm^{-1} deg^{-1} respectively. We then find a numerical value for (43) of:

$$V_{td} = 8 \times 10^{3}\ r^{-1}\ cm\ sec^{-1} \qquad (44)$$

where the dimension, r, is in units of 0.1 microns. Thus, in grains the dimensions of which are of the order of 0.01 microns, thermal disturbances will propogate at about one kilometer per second. Thus small grains, or grain fragments, which are of relatively consolidated structure might be capable of rapid thermal adjustment during a collision in which case fusion could occur. In order for this mechanism to be effective the internal motions of the cloud of grains should be of the order of a few kilometers per second. Wilson, Münch, Flather and Coffeen (1959) found that the difference between the observed line widths in the Orion Nebula and those expected from thermal motions amounted to 5 to 7 km sec^{-1} for the [OIII] line and about 2 km sec^{-1} more for hydrogen. These velocities apply to the present state of the nebula in which the internal motions are highly disturbed by ionization fronts, etc. It seems reasonable to suppose that prior to the ignition of the central stars, the internal motions were no greater than these presently observed and perhaps somewhat less.

Thus the velocities at which fusion could take place seem to be in reasonable agreement with the velocities within the nebula. However, at these velocities and at the density suggested above, 10^{-1}grains cm^{-3}, collisions between grains occur with a frequency of the order of $10^{-13}sec^{-1}$. If the contraction of the central stars takes of the order of 10^4 years, i.e. 3×10^{11} seconds, there will not be adequate time for a significant amount of fusion to occur. If the grains occured in condensations with densities of the order of 10^2 times the average or if the high density, low temperature condition persisted for somewhat longer than the stellar contraction time, this process could have some effect.

If the anomalous grain size distribution were the result of either of the processes suggested in the present section, we might expect to see a relaxation of the anomaly with time. Unfortunately the ages of H II regions are very poorly determined so that no attempt to correlate the extinction anomaly with age has been attempted. Furthermore, as the hostile environment of the H II region caused a relaxation of the grain size distribution anomaly, the total extinction caused by the H II region grains would decrease. This would result in a decrease with nebular age of the precision with which the extinction curve is determined, thus further

complicating the detection of an anomaly-age correlation.

IV.6 Conclusions and Desiderata

The data which has been presented indicates that a color anomaly very similar to that observed in the Orion Nebula is indeed present in several other H II regions. The data which is presently available does not completely rule out the possibility that the anomaly is the result of effects other than an abnormal grain size distribution. In particular, it is possible to fit the observed colors with a combination of early-type stellar models and one or more low temperature black body spectra. If the source of the low temperature component of such a composite spectrum were a late-type star, infrared spectra should reveal the presence of molecular bands. The pursuit of such an observational test is to be encouraged. The correlation between the infrared excess and the blue color excess argues in favor of the direct association of the source of the excess long wavelength energy with the dust, but might be explained either by radiation from a circumstellar dust shell or by anomalous extinction resulting from pecularities in the grain population. More extensive observations in the infrared, coupled with more detailed analysis might distinguish between these possibilities.

If the anomalous colors of the H II region stars

are the result of anomalous extinction, there are several possibilities. Although no work on the scattering of heretofore ignored grain models has been done in the present study, it seems to this author that additional, physically plausible grain population models might exist and investigation of such possibilities is desirable. If the small grain deficient particle size distribution is accepted as the correct explanation of the anomaly, we have seen that the dynamic action of radiation pressure, which has previously been utilized to establish the anomaly, will not, in fact, produce this effect. Of the alternative mechanisms which have been discussed, the size dependence of grain temperature and the possibility of rapid grain growth and condensation nucleus exhaustion seem more plausible. The opposite variation of the degree of the anomaly with time which is expected under the two processes, might admit of a test of these alternatives, if the derivation of dynamical ages of H II regions can be sufficiently refined to yield the required data.

Finally, it should be noted that the physical and chemical processes involved in the histories of interstellar grains are, at best, poorly understood. It is the opinion of the present author that a comprehensive theoretical and experimental study of the chemistry and physics of grain formation is one of the potentially most fruitful

fields of investigation at the present state of knowledge about the interstellar grains.

APPENDIX A

INCOMPLETED OBSERVATIONS

$C_s(\lambda^{-1})$

λ^{-1}	BD+20°1288 NGC 2174	HD164865 NGC 6530	Annon.B NGC 6618
2.950	+ .74	+2.12	
2.900	.69	2.09	+2.00
2.850	.72	2.17	1.94
2.800	.72	2.05	1.87
2.750	.68	2.02	1.85
2.700	.56	1.67	1.71
2.589	.42	1.36	1.57
2.480	.43	1.14	1.55
2.400	.42	1.06	1.28
2.350	.38	.98	1.29
2.240	.37	.82	1.07
2.190	.34	.73	.89
2.090	.25	.56	.80
2.000	.18	.32	.45
1.900	+ .11	+ .22	+ .24
1.800	0.00	0.00	0.00
1.712	+ .01	- .22	- .42
1.652		.31	
1.570		.35	
1.471		.62	
1.408		.49	
1.328		.80	
1.274		.95	
1.238		1.02	
1.190		1.08	
1.136		1.21	
1.031		1.35	
1.005		1.46	
0.976		1.40	
0.962		1.40	
0.926		1.48	
AB(1.8)	11.03	7.68	11.15

REFERENCES

Aitken, R. G. 1932, New General Catalogue of Double Stars Within 120° of the North Pole (Carnegie Institution of Washington).

Allen, C. W. 1963, Astrophysical Quantities (London, The Athlon Press).

Aller, L. H., Bowen, I. S., and Minkowski, R. 1955, Ap. J., 122, 62.

Arp, H. C. 1958, Handb. der Phys., 51, 75.

Auman, J., Jr. 1967, Ap. J. Suppl, XIV, 141.

Baade, W., and Minkowski, R. 1937, Ap. J., 86, 123.

Beers, Y. 1962, Introduction to the Theory of Errors (Addison Wesley Publishing Co., Inc.).

Borgmann, J. 1060, B.A.N., XV, 255.

Code, A. D., and Liller, W. C. 1962, "Direct Recording of Stellar Spectra", in Astronomical Techniques, ed. W. A. Hiltner (Chicago: University of Chicago Press).

Gaustad, J. E. 1962, Thesis, Princeton University.

-------. 1963, Ap. J., 138, 1050.

Greenstein, J. L. 1937, Harv. Circ., 422, 1.

-------. 1938, Ap. J., 87, 151.

Harris, D. L. III 1963, "The Stellar Temperature Scale and Bolometric Corrections", in Basic Astronomical Data, ed. K. Aa. Strand (Chicago: University of Chicago Press).

Herbig, G. H. 1958, P.A.S.P., 70, 468.

Hiltner, W. A. 1956, Ap. J. Suppl., II, 389.

Iben, I. 1965, Ap. J., 141, 993.

-------. 1966a, ibid., 143, 505.

-------. 1966b, ibid., 143, 516.

Johnson, H. L. 1965, Ap. J., 141, 923.

-------. 1966, Ann. Rev. of Astr. and Ap., Vol. 4, 193.

-------. 1967a, Ap. J., 147, 912.

-------. 1967b, ibid., 150, L 39.

Johnson, H. L. and Morgan, W. W. 1953, Ap. J., 117, 313.

Krishna Swamy, K. S. 1965, P.A.S.P., 77, 164.

Krishna Swamy, K. S., and O'Dell, C. R. 1967, Ap. J., 147, 529.

Mathews, W. G. 1967, Ap. J., 147, 965.

McCrea, W. H., and McNally, D. 1960, M.N.R.A.S., 121, 238.

Mihalas, D. 1965, Ap. J. Suppl., IX, 321.

-------. 1966, ibid., XIII, 1.

Moore, J. H., and Neubauer, F. J. 1958, Lick Obs. Bull., 20, 1.

Morgan, W. W., Code, A. D., and Whitford, A. E., 1955, Ap. J. Suppl., II, 41.

Morgan, W. W., Harris, D. L. III, and Johnson, H. L. 1953, Ap. J., 118, 92.

Morgan, W. W., Hiltner, W. A., Neff, J. S., Garrison, R., and Osterbrock, D. E. 1965, Ap. J., 142, 974.

Morgan, W. W., Keenan, P. C., and Kellman, E. 1943, An Atlas of Stellar Spectra, (Chicago: University of Chicago Press).

O'Dell, C. R., Hubbard, W. B., and Peimbert, M. 1966, Ap. J., 143, 743.

Oke, J. B. 1960, Ap. J., 131, 358.

-------. 1964, ibid., 140, 689.

-------. 1965, Ann. Rev. of Astr. and Ap., Vol. 3, 23.

Oort, J. H., and Van de Hulst, H. C. 1946, B.A.N., X, 187.

Pottasch, S. R. 1965, Vistas in Astronomy, Vol. 6, 149.

Schmidt-Kaler, Th. 1967, Ap. J., 149, 719.

Schoenberg, E., and Jung, B. 1933, A.N., 247, 413.

Schulte, D. H. 1956, Ap. J., 123, 250.

Seaton, M. J. 1960, Reports on Progress in Physics, 23, 313.

Sharpless, S. 1952, Ap. J., 116, 251.

-------. 1959, Ap. J. Suppl., IV, 257.

Spitzer, L. 1941, Ap. J., 93, 369.

Stebbins, J., and Kron, G. E. 1956, Ap. J., 123, 440.

Stebbins, J., and Whitford, A. E. 1943, Ap. J., 98, 20.

-------. 1945, ibid., 102, 318.

Stein, W. 1966, Ap. J., 145, 101.

Struve, O., and Titus, J. 1944, Ap. J., 99, 84.

Terzian, Y. 1965, Ap. J., 142, 135.

Trumpler, R. J. 1939, Lick Obs. Bull., 14, 154.

Van de Hulst, H. C. 1948, Harvard Obs. Mongr., 7, 73.

-------. 1949, Rech. Ast. de l'Obs. d'Utrecht, XI, (Part 2).

Walker, M. G. 1957, Ap. J., 125, 636.

Whiteoak, J. B. 1966, Ap. J., 144, 305.

Wickramasinghe, N. C. 1965, M. N. R. A. S., 131, 177.

-------. 1967, Nature, 216, 249.

Wickramasinghe, N. C., Dharmawardhana, M. W. C., and Wyld, C. 1966, M. N. R. A. S., 134, 25.

Wilson, O. C., Münch, G., Flather, E. M., and Coffeen, M. F. 1959, Ap. J. Suppl., IV, 199.

Woolf, N. J. 1961, P.A.S.P., 73, 206.

Woolf, N. J., Schwarzschild, M., and Rose, W. K. 1964, Ap. J., 140, 833.

Zirin, H. 1952, Harvard Obs. Bull., 921, 19